



Theoretical Study of Excitations in Interacting Bose and Fermi Systems

Thesis submitted in Partial Fulfillment of the
Degree of Doctor of Philosophy (Ph. D.)

by

Tarun Kanti Ghosh

The Institute of Mathematical Sciences

Chennai 600113, India

UNIVERSITY OF MADRAS

CHENNAI 600 005


JULY 2002

*dedicated to
my grandparents
late Nalini Ghosh
and
late Shaktipada Ghosh*

DECLARATION

I declare that the thesis entitled "Theoretical Study of Excitations in Interacting Bose and Fermi Systems" submitted by me for the Degree of Doctor of Philosophy is the record of research work carried out by me during the period from January 1999 to March 2002 under the guidance and supervision of Prof. G. Baskaran, and that this work has not formed the basis for the award of any degree, diploma, associateship, fellowship or other titles in this University or any other University or Institution of Higher Learning.

July 23, 2002



Tarun Kanti Ghosh
The Institute of Mathematical Sciences
Chennai 600 113
India

CERTIFICATE FROM THE SUPERVISOR

I certify that the thesis entitled "Theoretical Study of Excitations in Interacting Bose and Fermi Systems" submitted for the Degree of Philosophy by Mr. Tarun Kanti Ghosh is the record of bonafide research work carried out by him during the period from January 1999 to March 2002 under my guidance and supervision, and that this work has not formed the basis for the award of any degree, diploma, associateship, fellowship or other titles in this University or any other University or Institution of Higher Learning.

July 23, 2002



G. Baskaran
Senior Professor
The Institute of Mathematical Sciences
Chennai 600 113
India

Abstract

This Thesis is mainly devoted to theoretical study of various aspects of low-energy collective excitations in a trapped interacting alkali-metal atomic gases (Bose and Fermi) and of fractional quantum Hall systems. In the first chapter we review some of the basic properties of these quantum systems.

In the second chapter we derive an equation of motion for the velocity fluctuations of a two-dimensional deformed trapped Bose gas just above the critical temperature in the hydrodynamical regime. From this equation, we calculate the eigenfrequencies and the corresponding density fluctuations for a few low-lying excitation modes. Using the method of averages, we also derive a dispersion relation in a deformed trap at very high temperature that interpolates between the collisionless and hydrodynamic regimes. We make use of this dispersion relation to calculate the frequencies and the damping rates for monopole and quadrupole modes in both the regimes. We show that the time evolution of the wave packet width of a Bose gas in a time-independent as well as time-dependent trap can be obtained from the method of averages.

In the third chapter, using the time-dependent variational approach and *most general Gaussian variational ansatz* for the order parameter of the condensed state, we calculate analytical expressions for monopole and two quadrupole excitation frequencies of a two-dimensional anisotropic trapped interacting Bose gas at zero temperature. Within the energy weighted sum-rule approach, we derive a general dispersion relation of monopole and two quadrupole excitations of a two-dimensional deformed trapped interacting (contact interaction) quantum gas. Using this general dispersion relation, we also derive analytical expressions for monopole and two quadrupole mode frequencies of a two-dimensional unpolarized Fermi gas in an anisotropic trap.

In the fourth chapter we obtain a general condition for the universality of the monopole mode frequency and dynamics of width of a class of Gross-Pitaevskii

equation describing a trapped interacting Bose gas, at varying spatial dimensionality, order of the nonlinearity and the scaling exponent of the interaction potential. We also show that the dynamics of the width of this class of interacting Bose gas can be described *universally* by the same nonlinear singular Hill's equation. We give few examples which satisfy that particular condition and exhibit the universal nature of the monopole mode frequency and the dynamics of the width of a system.

In the fifth chapter we consider a Bose condensed state with gravity-like interatomic attractive interaction. Using the time-dependent variational approach we derive an analytical expressions for monopole and quadrupole mode frequencies of a Bose-Einstein condensate with gravity-like interatomic interaction. We estimate the superfluid coherence length and the critical angular frequencies to create a vortex around the z -axis. We also calculate the monopole mode frequency of the condensate in presence of a vortex.

In the sixth chapter cooperative ring-exchange is suggested as a mechanism of quantum melting of vortex lattices produced in a rapidly-rotating quasi two dimensional atomic Bose-Einstein condensates. A semiclassical path integral is used to estimate the condition for quantum melting instability by considering large-correlated ring exchanges in a two-dimensional Wigner crystal of vortices in a strong 'pseudomagnetic field' generated by the background superfluid Bose particles.

In the seventh chapter we model two-magnetoroton bound state problem at one-third filling fraction of quantum Hall systems. We show that a magnetoroton is an oriented dipole analogous to the description of a magnetic exciton. We obtain a *momentum dependent*, non-central effective potential between two magnetorotons by using the oriented character of the dipole moment and solve it variationally (analytically) to find a two-magnetoroton bound state.

Publications

This Thesis is based on the following publications:

1. Collective excitation frequencies and damping rates of a two dimensional deformed trapped Bose gas above the critical temperature.
Tarun Kanti Ghosh, Phys. Rev. A **63**, 013603 (2001).
2. Splitting between quadrupole modes of dilute quantum gas in a two dimensional anisotropic trap.
Tarun Kanti Ghosh and S. Sinha, Eur. Phys. J. D **19**, 371 (2002).
3. Universality of monopole mode and time evolution of a d -dimensional trapped interacting Bose gas.
Tarun Kanti Ghosh, Phys. Lett. A **285**, 222 (2001).
4. Collective excitation frequencies and vortices of a Bose-Einstein condensed state with gravity-like interatomic attraction.
Tarun Kanti Ghosh, Phys. Rev. A **65**, 053616 (2002).
5. Cooperative Ring Exchange and Quantum Melting of Vortex Lattices in Atomic Bose-Einstein Condensates.
Tarun Kanti Ghosh and G. Baskaran, cond-mat/0207484 (submitted to Phys. Rev. Lett.).
6. Modeling Two-Roton Bound State Formation in Fractional Quantum Hall System.
Tarun Kanti Ghosh and G. Baskaran, Phys. Rev. Lett. **87**, 186803 (2001).

Acknowledgments

First of all, I express my profound gratitude to my advisor Prof. G. Baskaran for his patience, advice, constant encouragement, and stimulating discussions during the course of this work, without which it would have been impossible for me to carry on. His quickness in getting to the essentials of any problems is something which I shall always envy. Moreover his good taste in the choice of problems and above all, treating the colleagues and students with kindness and respect are the qualities which I shall always fondly remember.

I would like to take this opportunity to express my sincere thanks to my elder brother Dr. Pijush K. Ghosh for his advice, constant encouragement and fruitful discussions not only during my research work, but throughout the whole of my academic career.

I am thankful to Dr. Sarbeswar Chowdhury and Prof. Asim Kumar Ray for constant encouragement during my college and university life. For encouragement, discussions and various helps I thank Profs. M. V. N. Murthy and R. Shankar.

I wish to thank my friends Rathin da, Swarnendu, Prakash, Subrata, Santosh, Shamindra, Arijit, Paramita, Rajesh, Manoj, Naveen, Golam, Soumen, Bobby for hours of fun and their co-operation during my work.

I thank all the academic and administrative members of IMSc and also I thank IMSc for providing me financial support during my Ph. D. work.

Last, but not least, my parents, sister-in-law, brothers and my nephew, Ritaman, are always with me even though they are thousands of kilometers away. I thank them all.

Tarun Kanti Ghosh

Contents

1	Introduction	1
1.1	Overview and purpose	1
1.1.1	Bose-Einstein condensation	1
1.1.2	Order parameter and mean-field theory	3
1.1.3	Collective excitations and their importance in quantum systems	5
1.1.4	Dynamics of a system	7
1.1.5	Trapped atomic Fermi gases	7
1.1.6	Low dimensional BEC	7
1.1.7	BEC with gravity-like attractive interaction	8
1.1.8	Condensed state with vortices	9
1.1.9	The quantum Hall effect	10
1.1.10	Inner structure of collective modes in FQHE	11
1.2	Organisation of this Thesis	12
2	Collective excitation frequencies and damping rates of a 2D de-	
	formed trapped Bose gas above the critical temperature	18
2.1	Introduction	18
2.2	Hydrodynamic equation of motion for the velocity fluctuations	20
2.3	Eigenfrequencies and the corresponding density fluctuations in the hydrodynamic regime	22
2.4	Method of averages	23
2.5	Summary and conclusions	27
3	Collective excitation frequencies of a quasi-2D deformed trapped	
	quantum gas at $T = 0$	30
3.1	Introduction	30
3.2	Modeling quasi two-dimensional trapped interacting Bose gas	31
3.3	Collective excitation frequencies of a quasi-2D deformed trapped Bose gas	33

3.4	Sum-rules and collective excitations	36
3.5	Collective excitation frequencies of a quasi-2D deformed trapped Fermi gas	40
3.6	Summary and conclusions	45
4	Universality of monopole mode frequency and dynamics of width of a class of an interacting Bose gas	49
4.1	Introduction	49
4.2	Universality of certain observables of a class of trapped interacting Bose gas	50
4.2.1	Universality of monopole mode	52
4.2.2	Universality of dynamics of width	53
4.3	Examples	55
4.3.1	Quasi-2D trapped Bose gas	55
4.3.2	One dimensional Tonk-Girardeau gas	55
4.3.3	Calogero model	57
4.4	Summary and conclusions	57
5	Collective excited states of a Bose-Einstein condensate with gravity-like interatomic attraction	61
5.1	Introduction	61
5.2	Collective excitation of Bose condensed state with gravity-like interatomic attractive interaction	62
5.2.1	TF-G regime	67
5.2.2	G regime	68
5.3	Vortex of a Bose condensed state with gravity-like interatomic interaction	69
5.3.1	TF-G regime	72
5.3.2	G regime	73
5.4	Summary and conclusions	73
A5	Appendix: Mean-field energy of the gravity-like potential	74
B5	Appendix: Exact forms of $F_{\alpha_1}[\alpha_{10}, \beta_{10}, \delta\alpha_1, \delta\beta_1]$ and $F_{\beta_1}[\alpha_{10}, \beta_{10}, \delta\alpha_1, \delta\beta_1]$	75
6	When the collective modes go unstable: Quantum melting of the vortex lattices in a rapidly rotating quasi-2D atomic Bose-Einstein	

condensate	79
6.1 Introduction	79
6.2 Hamiltonian of the vortices in a rapidly rotating quasi-2D BEC	81
6.3 Coherent state path integration	83
6.4 Cooperative ring exchange mechanism	86
6.5 Calculation of the tunneling coefficient	87
6.6 Summary and conclusions	89
A6 Appendix: Calculation of the parameters Q_x and Q_y	90
7 Inner structure of collective modes: Modeling two-magnetoroton bound state formation in fractional quantum Hall systems	94
7.1 Introduction	94
7.2 Dynamics of a magnetoroton	96
7.3 Hamiltonian of two magnetorotons	97
7.3.1 Kinetic energy operator	97
7.3.2 Two-body potential energy operator	98
7.3.3 Total Hamiltonian	99
7.4 Variational wave function for two-magnetoroton bound state	99
7.5 Binding energy of a two-magnetoroton bound state	100
7.6 Summary and conclusions	102
8 Conclusions	106
8.1 Summary of this Thesis	106
8.2 Outlook for future studies	109

List of Figures

3.1	Ratio of the widths of the condensate η vs the dimensionless effective interaction strength P for $\lambda = 3.0$	35
3.2	Monopole (solid line), quadrupole (dotted line) and scissors (dashed line) mode frequencies of an interacting Bose gas vs dimensionless effective strength P for $\lambda = 3.0$	39
3.3	Difference between the two quadrupole modes of an interacting Bose gas Δ_b/ω_0 vs the dimensionless effective strength P for $\lambda = 3.0$	41
3.4	Monopole (solid line), quadrupole (dotted line) and scissors (dashed line) mode frequencies of an interacting unpolarized Fermi gas vs the dimensionless parameter K_0 for $\lambda = 3.0$	43
3.5	Difference between the two quadrupole modes of an interacting unpolarized Fermi gas Δ_f/ω_0 vs the dimensionless parameter K_0 for $\lambda = 3.0$	44
5.1	Sound velocity c_s as a function of the dimensionless scattering parameter S	65
5.2	Monopole and quadrupole mode frequencies vs the scattering parameter S . The solid and dashed lines corresponds to the quadrupole and monopole mode frequencies, respectively.	67
5.3	Crossing between monopole (dashed line) and quadrupole (solid line) modes	68
5.4	Superfluid coherence length ξ as a function of the dimensionless scattering parameter S	71
5.5	Critical angular frequency Ω_1 as a function of the dimensionless scattering parameter S	72
6.1	A schematic diagram of cooperative ring exchange events on a ring and line	87

7.1	Schematic diagrams for (a) a single magnetoroton with momentum k_0 and (b) a two-magnetoroton bound state with total momentum $K = 0$	95
7.2	Annular region in k -space that contributes to $K = 0$ magnetoroton bound state.	100
7.3	Two-magnetoroton bound state wave function in momentum space for $\alpha l_0 = 0.41$ at which the energy is minimized.	101
7.4	Expected qualitative excitation spectrum of two-magnetoroton bound state compared with excitation spectrum of a single magnetoroton. . .	102

Chapter 1

Introduction

1.1 Overview and purpose

With the technological advancement it is now possible to make tunable finite size interacting quantum systems made up of bosons and/or fermions in the laboratory. Two most important examples are the trapped dilute interacting quantum gas of atoms at very low temperature and electrons in two dimensional plane subjected to strong magnetic field perpendicular to the plane which exhibit quantum Hall effect. Cold quantum gas clouds have many advantages for investigations of quantum phenomena. On the one hand, the trapped bosonic atoms at low temperature forms the Bose-Einstein condensed (BEC) state and on the other hand, the trapped fermionic alkali atoms at very low temperature is the most promising candidate for formation of Fermi sea and observing the atomic Cooper pairs.

1.1.1 Bose-Einstein condensation

The seminal work of S. N. Bose [1] led to prediction of BEC by A. Einstein [2]. According to quantum mechanical theory, all matter behaves like waves. The de Broglie wavelength, $\lambda_T = (2\pi\hbar^2/Mk_B T)^{1/2}$, of an object with reasonable mass M at room temperature T is extremely small. As the temperature of a system consisting of particles goes down, the de Broglie wavelength of the particles increases. Below a certain temperature (known as condensation transition temperature), the de Broglie wavelength exceeds the mean interparticle distance, and the wave packets of the particles start overlapping. Under this condition, it is favorable for bosons to fill the single lowest quantum state and lose their individual identities. This single quantum state represents a coherent macroscopic quantum system which is known

as Bose-Einstein condensation (BEC). The criterion for condensation of a free Bose gas in three dimensions is $\rho\lambda_T^3 = \zeta(3/2) = 2.612$, where ζ is the Riemann zeta function. The transition temperature is estimated at the critical point defined by $\rho\lambda_{T_c}^3 = 2.612$ and the condensate fraction is $(N_0/N) = 1 - \left(\frac{T}{T_c}\right)^{3/2}$ [3]. Evidence of this quantum phenomena has been found in liquid ^4He [4]. Because of the strong interatomic interaction among the helium atoms, only 10 percent of the helium atoms condense into the ground state even at very low temperature.

In the case of N bosons confined in a spherical harmonic potential $V_{\text{ext}} = \frac{1}{2}m\omega^2 r^2$, the proper thermodynamic limit is obtained by letting $N \rightarrow \infty$ and $\omega \rightarrow 0$, while keeping the product $N\omega^3$ constant. The critical temperature is given by [5]

$$k_B T_c = \hbar\omega \left(\frac{N}{\zeta(3)} \right)^{1/3}, \quad (1.1)$$

and the condensate fraction is $(N_0/N) = 1 - \left(\frac{T}{T_c}\right)^3$. In 1995, BEC was observed in a series of experiments with clouds of magnetically trapped weakly interacting alkali atoms at JILA [6], MIT [7] and RICE [8], and later in more than 25 laboratories all over the world. BEC is achieved by using the *evaporative cooling* method in which the more energetic atoms are removed from the trap, thereby cooling the remaining atoms. The system is dilute enough to produce 99 percent condensation of atoms at $T = 0$ K. The transition temperature was found to be very close to the value predicted by Eq. (1.1). The gaseous atomic condensed state exhibits very different properties from those in liquid helium. These systems have become the testing ground for the theoretical formalism of dilute condensates, and quantitative predictions can be made for comparison with experiments. Most relevant features of these trapped Bose gases are that they are inhomogeneous and finite-size systems with the number of atoms ranging from a few thousands to several millions. The size of the system is enlarged due to the effect of repulsive two-body forces and the trapped gases can become almost macroscopic objects whose properties are directly measurable using optical techniques. The inhomogeneity of these gases have several important consequences. The different temperature dependence exhibited by the condensate fraction compared to the uniform case is a consequence of the higher density of states characterizing the harmonic oscillator Hamiltonian. At $T = 0$ all particles are in the lowest eigenstate of the harmonic oscillator, namely, $\mu \rightarrow \epsilon_0 = \frac{3}{2}\hbar\omega$. Thus the particle density has the form of a Gaussian and the same is true for the momentum distribution. Unlikely the free gas, trapped BEC shows up in momentum space as well as in co-ordinate space. This provides novel methods for the investigation of measurable quantities, like the temperature dependence of

the condensate, density profile, interference phenomena, collective excitation frequencies and so on. Condensates in atomic gas can be manipulated and studied using the powerful techniques of atomic physics. Almost all the parameters can be controlled at will, including nature of the interaction strength (repulsive or attractive) a between the particles [9]. Since both liquid helium and dilute atomic gases are systems of interacting particles, a crucial question concerns the role played by the interaction, that is, whether and how much the interatomic forces modify the properties of BEC.

1.1.2 Order parameter and mean-field theory

The many body Hamiltonian describing N interacting bosons confined by an external potential V_{ext} is given by

$$H = \int d\mathbf{r} \Psi^\dagger(\mathbf{r}) \left[-\frac{\hbar^2}{2m} \nabla^2 + V_{ext}(\mathbf{r}) \right] \Psi(\mathbf{r}) + \frac{1}{2} \int d\mathbf{r} d\mathbf{r}' \Psi^\dagger(\mathbf{r}) \Psi^\dagger(\mathbf{r}') V(\mathbf{r} - \mathbf{r}') \Psi(\mathbf{r}') \Psi(\mathbf{r}), \quad (1.2)$$

where $\Psi^\dagger(\mathbf{r})$ and $\Psi(\mathbf{r})$ are the boson field operators that create and annihilate a particle at the position \mathbf{r} , respectively and $V(\mathbf{r} - \mathbf{r}')$ is the two-body interatomic potential. The ground state of the system as well as its thermodynamic properties can be directly calculated starting from the Hamiltonian. However, the calculation can be very hard or even impracticable for systems with much larger values of N . Mean-field approaches are commonly used for interacting systems in order to overcome the problem of solving exactly the full many-body Schroedinger equation. The basic idea for a mean-field description of a dilute Bose gas was formulated by Bogoliubov. The key point consists in separating out the condensate contribution to the bosonic field operator. In general, the field operator can be written as $\Psi(\mathbf{r}) = \sum_\alpha \Psi_\alpha(\mathbf{r}) a_\alpha$, where $\Psi_\alpha(\mathbf{r})$ are the single-particle wave functions and a_α are the corresponding annihilation operators. The bosonic creation and annihilation operators a_α^\dagger and a_α are defined in the Fock space:

$$a_\alpha^\dagger |n_\alpha\rangle = \sqrt{n_\alpha + 1} |n_{\alpha+1}\rangle, \quad (1.3)$$

$$a_\alpha |n_\alpha\rangle = \sqrt{n_\alpha} |n_{\alpha-1}\rangle, \quad (1.4)$$

where n_α are the eigenvalues of the number operators $n_\alpha = a_\alpha^\dagger a_\alpha$ giving the number of atoms in the single-particle α -state. BEC occurs when the number of atoms n_0 of a particular single-particle state becomes very large: $n_0 = N_0 \gg 1$ and the ratio N_0/N remains finite in the thermodynamic limit. In this limit the states with N_0 and $N_0 \pm 1 \sim N_0$ correspond to the same physical configuration and consequently, the

operators a_0 and a_0^\dagger can be treated as c-numbers: $a_0 = a_0^\dagger = \sqrt{N_0}$. For a uniform gas in a volume V , where BEC occurs in the single particle state, $\Psi_0 = 1/\sqrt{V}$ having zero momentum. Then the field operator $\Psi(\mathbf{r})$ can be decomposed in the form $\Psi(\mathbf{r}) = \sqrt{N_0/V} + \Psi'(\mathbf{r})$, where $\Psi'(\mathbf{r})$ is the field operator associated with the noncondensed particles. The generalization of the Bogoliubov prescription to the case of nonuniform and the time dependent configurations is given by

$$\Psi(\mathbf{r}, t) = \Phi(\mathbf{r}, t) + \Psi'(\mathbf{r}, t), \quad (1.5)$$

where we have used the Heisenberg representation for the field operators. $\Phi(\mathbf{r}, t)$ is a complex function defined as the expectation value of the field operator:

$$\Phi(\mathbf{r}, t) = \langle \Psi(\mathbf{r}, t) \rangle = |\Phi| e^{iS}. \quad (1.6)$$

Its modulus fixes the condensate density through $n_0(\mathbf{r}, t) = |\Phi(\mathbf{r}, t)|^2$ and the phase S is used to define a velocity field through $\mathbf{v} = \frac{\hbar}{m} \nabla S$. The function $\Phi(\mathbf{r}, t)$ is a classical field having the meaning of an order parameter and is often called macroscopic wave function of the condensate. It characterizes the off-diagonal long-range behavior of the one-particle density matrix $\rho_1(\mathbf{r}', \mathbf{r}, t) = \langle \Psi^\dagger(\mathbf{r}', t) \Psi(\mathbf{r}, t) \rangle$. The time evolution of the field operator $\Psi(\mathbf{r}, t)$ is

$$i\hbar \frac{\partial \Psi(\mathbf{r}, t)}{\partial t} = \left[-\frac{\hbar^2}{2m} \nabla^2 + V_{ext}(\mathbf{r}) + \int d\mathbf{r}' \Psi(\mathbf{r}', t) V(\mathbf{r} - \mathbf{r}') \Psi(\mathbf{r}', t) \right] \Psi(\mathbf{r}, t). \quad (1.7)$$

In a cold, dilute gas, only binary collisions at low energy are relevant and these collisions are characterized by a single parameter, namely the s -wave scattering length a . The effective two-body potential is then given by

$$V(\mathbf{r} - \mathbf{r}') = \frac{4\pi a \hbar^2}{m} \delta(\mathbf{r} - \mathbf{r}'). \quad (1.8)$$

Using the effective potential and replacing Ψ by Φ , we get the following closed equation for the order parameter:

$$i\hbar \frac{\partial \Phi(\mathbf{r}, t)}{\partial t} = \left[-\frac{\hbar^2}{2m} \nabla^2 + V_{ext}(\mathbf{r}) + \frac{4\pi a \hbar^2}{m} |\Phi(\mathbf{r}, t)|^2 \right] \Phi(\mathbf{r}, t). \quad (1.9)$$

This equation is known as Gross-Pitaevskii (GP) equation [10]. Its validity is based on the condition that the s -wave scattering length be much smaller than the average distance between atoms *i.e* the gas parameters should obey the condition: $n|a|^3 \ll 1$, where n is the mean particle density. The GP equation can be used at low temperature to explore the macroscopic behavior of the system, characterized

by variations of the order parameter over distances larger than the mean distance between atoms. In the available experiments on trapped atomic BEC, the total number of condensate atoms is $10^5 - 10^8$ in a trap with $\omega/2\pi \sim 100$ Hz. The width of the condensate can be several μm , upto the order of $100\mu m$. The scattering length a is of the order of a few nanometer. The central density is of the order of $10^{13} - 10^{15} cm^{-3}$, so that $n|a|^3$ is less than 10^{-3} , which ensures the applicability of GP theory. Despite the very dilute nature of these gases, the combination of BEC and the harmonic trapping enhances the effects of the atom-atom interactions on important measurable quantities. The ground state properties of the trapped ^{87}Rb system, including its geometry, momentum distribution, coherence length and critical angular velocity for vortex formation have been discussed by Baym and Pethick [11].

1.1.3 Collective excitations and their importance in quantum systems

The study of low-energy excitations is of primary importance in quantum many body theories. It plays a crucial role in understanding the quantum nature of the particles, two-body interactions and the effect of dimensionality. A peculiar feature of Bose superfluids is that their excitations at low energy correspond to collective modes, which can be described as fluctuations of the order parameter. This happens when their wavelength is larger than the healing length. For uniform and dilute gas, the spectrum of excitations is given by the Bogoliubov result, which are phononic at low momentum k and single-particle excitations at large momentum k . Low momentum excitations are phonons even in liquid helium, with sound velocity $c \sim 230$ m/s. However, since the superfluid helium is dense and highly correlated, the interpolation between the phononic and the single-particle regimes is more subtle. The phonon branch reaches a maximum at $k \sim 1\text{\AA}^{-1}$ and then forms a rather deep minimum at $k \sim 1.9\text{\AA}^{-1}$. The excitations near this minimum, whose dispersion is approximately parabolic, are called rotons. Their wavelength is of the order of the interatomic distances and slightly larger than the healing length, so that they still have collective character, but which are of the order of the atomic scale.

The excitation spectrum of a trapped alkali-metal atomic BEC is discrete due to the finite size of the system. The excited states are classified according to the number of radial nodes, n_r , the angular quantum number l and m , where m is the projection of l onto the symmetry axis. The discretization is particularly important for the lowest energy excitations, whose wavelength is comparable with system size

R , and corresponds to oscillations of the whole system.

An example of the collective mode is the state with $n_r = 1$ and $l = m = 0$, which is known as monopole or breathing mode in which the condensate alternately expands and contracts. By keeping $l = m = 0$ and increasing n_r , one finds density oscillations in the radial direction having wavelength smaller than R . If n_r is large, so that the wavelength becomes much smaller than R but still larger than healing length, these modes can be thought as stationary states of bulk excitations which propagate radially and reflect at the surface. For large R , these discretized states approach a continuum and the spectrum becomes closer and closer to the one of a uniform system, namely, the phononic dispersion in dilute gas and the phonon-roton branch in liquid helium.

Another interesting class of excitations is the one with $n_r = 0$ and $l \geq 2$. These modes correspond to shape oscillations, or surface oscillations, in which the spherically symmetric condensate distorts by alternately becoming prolate and oblate without changing its mean density. The lowest mode with $l = 2$ is called quadrupole mode.

The trapped Bose gas can be excited by applying small time-dependent perturbation to the trap potential. With this method, dipole, monopole, quadrupole modes have already been observed in three dimensional BEC [12]. The experimental results of these low-energy excitations [12] matches very well with the theoretical predictions based on the mean field approach [13, 14].

Similar to the monopole and quadrupole modes of trapped BEC, there is another mode called scissors mode. These scissors modes are rather special since they directly manifest the superfluid behavior of these atomic gases. A scissors mode in a BEC is associated with an irrotational flow with a velocity field of the form $\mathbf{v} = \alpha \nabla(xy)$, if the motion is taking place in the xy -plane. To excite a scissors mode in the xy -plane, one can rotate the x and y axes of the trap slightly around the z -axis. To such a perturbation the condensate will respond by oscillating around the equilibrium axes. On the other hand, if the axes change through a large angle this method excites the quadrupole mode. The study of the scissors mode in BEC of alkali atomic gas has been suggested by Guery-Odelin and S. Stringari [15] and experimental realization of their ideas has already been given by Margao *et al.* [16].

Phonon-like excitations with wavelength smaller than the condensate size can also be produced. For instance, one can suddenly switch-on a narrow laser beam, focused on the center of the trap. An optical dipole force acts on the atoms generating a wave packet of excitations which then moves throughout the condensate

as a sound wave. The velocity of this sound wave has been measured in [17], finding good agreement with the prediction of Bogoliubov theory. Phonon-like excitations have been also generated in light-scattering experiments [18].

1.1.4 Dynamics of a system

So far we have discussed the behavior of shape oscillations of a trapped Bose condensate. It is also interesting to study the dynamics of the expansion of the gas, following the switching-off the trap potential. The dynamics of the expansion is an important issue because much information on these Bose condensed gas is obtained experimentally from images of the expanded atomic cloud. This includes in particular the temperature of the gas, the release energy and the aspect ratio of the velocity distribution. The dynamics of the expansion of a Bose gas in cylindrical geometry have been studied theoretically [19]. The agreement between theory and experiment [20] is remarkable.

1.1.5 Trapped atomic Fermi gases

There is now renewed focus on the properties of trapped dilute gas of fermionic atoms at low temperature. Magneto-optical confinement of fermionic gases has been reported in [21]. It is also possible to cool down trapped Fermi gas to a regime where effects of the quantum statistics become noticeable [22]. The attractive interaction between ^6Li atoms holds promise of achieving Cooper pair states.

1.1.6 Low dimensional BEC

So far we have discussed the properties of the 3D BEC. The reduction in spatial dimension of a quantum system is also the subject of extensive study in trapped Bose systems as well as trapped Fermi systems. The statistical behavior of 2D and 1D Bose gases exhibits very peculiar features. In an uniform gas BEC can not occur in 2D and 1D at finite temperature because thermal fluctuations destabilize the condensate. It can be seen that, for an ideal gas in the presence of BEC, the chemical potential vanishes and the momentum distribution, $n(p) = [\exp(\beta p^2/2m) - 1]^{-1}$, exhibits an infrared $\frac{1}{p^2}$ divergence. In the thermodynamic limit, this yields a divergent contribution to the integral $\int dp n(p)$ in 2D and 1D, thereby violating the normalization condition. The absence of BEC in 1D and 2D can be also proven for interacting uniform systems, as shown by Hohenberg [23].

In the presence of harmonic trapping, the effects of thermal fluctuations

are strongly quenched due to the different behavior exhibited by the density of states $\rho(\epsilon)$. In fact while in the uniform gas $\rho(\epsilon)$ behaves as $\epsilon^{(d-2)/2}$, where d is the dimensionality of space, in presence of an harmonic potential one has instead the law $\rho(\epsilon) \sim \epsilon^{(d-1)}$, and consequently the integral converges also in 2D. The corresponding value of the critical temperature is given by [24]

$$k_B T_c = \hbar \omega_0 \left(\frac{N}{\zeta(2)} \right)^{1/2}, \quad (1.10)$$

where $\omega_0 = \sqrt{\omega_x \omega_y}$. In order to achieve quasi-two dimensional BEC, one should choose the frequency ω_z in the third direction large enough to satisfy the conditions $\hbar \omega_z \gg \mu \geq \hbar \omega_0$ and $k_B T < \hbar \omega_z$, where μ is the chemical potential of a quasi-2D trapped Bose gas. It is worth mentioning two important theoretical works, namely, the presence of conformal symmetry [25] and an explosion-implosion duality [26] in one and two dimensional BEC with or without a time-dependent harmonic trap. Recently, the lower dimensional (quasi-2D and quasi-1D) BEC has been realized at MIT [27]. The quasi-2D BEC has also been produced on a microchip [28, 29]. The collective excitations play an important role in probing microscopic interactions. It is interesting to study the various low-lying collective excitation frequencies of quasi-2D trapped Bose gas as well as Fermi gas [30, 31], which is given in the second and third chapters of this Thesis. The excitation frequencies of a harmonically trapped ideal Bose gas are simply multiples of the trap frequencies. However, for an interacting system, deviations from these frequencies are expected due to the effect of interaction. Interestingly, for an interaction potential with particular scaling property the monopole mode frequency does not depend on the interaction strength. Moreover, the dynamics of the width of the system with that particular potential can be solved exactly and explained by the same Hill's equation. This universal nature of monopole mode frequency and the dynamics of the width of a certain class of Bose gas which is described by the GP equation [32] is being addressed in the fourth chapter in this Thesis. These universal properties are due to the underlying $SO(2, 1)$ symmetry of the Hamiltonian [33, 25].

1.1.7 BEC with gravity-like attractive interaction

In the atomic BEC created so far, the atoms interact only at very short distances. Most of the properties of these dilute Bose gases can be explained by considering only two-body short-range interaction (Van der Waals interaction) which is characterized by the s -wave scattering length a . However, the BEC in the presence of

the dipole-dipole interactions has recently raised considerable interest [34]. If such dipole moment is sufficiently large, the resulting dipole-dipole forces may influence the properties of BEC. Novel physics is expected for dipolar BEC, since the dipole-dipole interactions are long-range, anisotropic, and partially attractive. A new kind of atomic BEC has been proposed by D. O'Dell *et al.* [35]. They have shown that the particular configuration of intense off-resonant laser beams gives rise to an effective gravity-like $\frac{1}{r}$ interatomic attraction between neutral atoms located well within the laser wavelength. This long range interaction potential is of the form, $U(r) = -\frac{u}{r}$, where $u = (11\pi/15)(I\alpha_0^2/c\epsilon_0^2\lambda_L^2)$ and I and λ_L are the total laser intensity and wave length respectively. α_0 is the atomic polarizability at the frequency $2\pi c/\lambda_L$. This suggests that it might be possible to simulate gravitational effects in the laboratory. Particularly interesting is the possibility of experimentally emulating boson stars: gravitationally bound condensed Bose systems of finite volume in which the zero point kinetic energy balances the gravitational attraction and thus stabilizes the system against collapse. The fifth chapter of this Thesis is devoted to the study of various low-energy excitation spectrum and the vortex state of a Bose condensed state with gravity-like interatomic attractive interaction [36].

1.1.8 Condensed state with vortices

Among the several questions that can be studied in quantum fluid is superfluidity. The vortex state plays an important role in characterizing the superfluid properties of an interacting quantum fluid systems. A small array of vortices has been observed in liquid ^4He [37]. With the achievement of atomic BEC, it is possible to study these phenomena in an extremely dilute quantum fluid. Vortex filament in the condensate can be generated by rotating the condensate above the certain angular frequency, known as critical frequency [11]. Many Vortices in the condensate can be nucleated by rotating the condensate with higher angular momentum. Recently, the ENS [38] and MIT groups [39] have observed the formation of triangular vortex lattices in rapidly-rotating atomic Bose condensed gas. These vortex lattices are produced by rotating the condensate around its long axis with the optical dipole force exerted by blue-detuned laser beams. These triangular lattices contained more than 130 vortices [39]. The vortex lattices are highly excited collective states of condensate states. It has been shown by Tin-Lun Ho that as the number of vortices increases, a BEC state will become quantum Hall like state [40]. It is interesting to study how and when the collective modes (vortex lattices) go unstable. In other words, what is the mechanism and condition for quantum melting of the vortex lattice structure?

It has been suggested that the vortex-lattice state of quasi-2D bosons melts due to quantum fluctuations when the boson filling factor ν_b , the ratio of boson density to the vortex density, is smaller than 6 and 8 based on the exact diagonalization study [41] and the microscopic calculation [42], respectively. In the sixth chapter of this Thesis, we [43] present how the vortex lattices can melt and attempt to estimate the condition for quantum melting instability by considering large correlated ring exchanges in a 2D Wigner crystal of vortices in a strong 'pseudomagnetic field' generated by the background superfluid Bose particles. The rotating BEC or the vortices in presence of the Bose superfluid is equivalent to the charged particle in a magnetic field. Can vortex liquid state exhibit the quantum Hall effect? This question has been addressed in [41] and predicted that the vortex liquid can be described as a Read-Rezayi parafermion states whose excitations obey non-Abelian statistics [44].

The field of ultracold trapped atomic gases is progressing very fast. For a detailed updated review on theoretical and experimental aspects of trapped alkali atomic gases, see the references [45].

1.1.9 The quantum Hall effect

The quantum Hall effect is one of the most remarkable phenomena in condensed matter physics. Under suitable conditions, electrons are effectively confined to two dimensions by an inversion layer. Inversion layers are formed at an interface of a semiconductor and an insulator or between two semiconductors. The basic experimental observation is the quantization of the Hall conductance, $\sigma_{xy} = \nu \frac{e^2}{h}$, of a system containing two-dimensional electron gas subjected to a strong magnetic field (B) perpendicular to the plane, where e is the electronic charge, h is the Planck's constant and ν is a quantum number. The Hall conductance is independent of specific material parameters. The diagonal conductivity vanishes, so that the state is dissipationless. The characteristic length scale for electrons in a magnetic field B is $l_0 = \sqrt{\frac{\hbar}{eB}}$. Typical range of l_0 is 50-100 Å and it is independent of material parameters. The electronic states are parameterized by Landau levels of energy $E_n = (n + \frac{1}{2})\hbar\omega_c$, where $\omega_c = \frac{eB}{m}$ is the cyclotron frequency. Each Landau level is highly degenerate and the number of states per unit area of one Landau level is $\rho_0 = \frac{B}{\phi_0}$, where $\phi_0 = \frac{e}{h}$ is the unit of flux quantum. So the degeneracy of one full Landau level is counted by the total number of flux quanta in the external magnetic field. The filling fraction ν is defined as the ratio of the electron density to the total number of states per unit area. The case $\nu = 1, 2, 3, \dots$ corresponding to the integer

quantum Hall effect was discovered by von Klitzing *et al.* [46]. The case $\nu = \frac{s}{(2ps+1)}$ and $p = 1, 2, \dots; s = 1, 2, \dots$ corresponding to the fractional quantum Hall effect (FQHE) was discovered by Tsui *et al.* [47]. The case $s = 1$ and $\nu = \frac{1}{(2p+1)} = \frac{1}{m}$ was explained by Laughlin with his famous wave function [48] which is,

$$\psi[z] = \prod_{i < j}^N (z_i - z_j)^m e^{-\sum_{i=1}^N \frac{|z_i|^2}{4l_0^2}}. \quad (1.11)$$

Here, z is the position of the electron in the complex plane, N is the total number of electrons. The Laughlin wave function is composed of single particle states in the lowest Landau level and is properly antisymmetric in accordance with fermionic statistics. Two main features of this wave function are the following: there is a zero on each electron and each electron sees other electrons as magnetic flux due to the accumulated phase when moving one electron around another. The more general case $s \geq 0, p \geq 1, \nu = \frac{p}{(2ps+1)}$ was explained by J. K. Jain using the idea of composite fermions [49]. The FQH liquid is isotropic and incompressible. Using the plasma analogy, Laughlin [48] has shown that the elementary charged excitations at filling fraction $\nu = \frac{1}{m}$ are quasiparticles and quasiholes with fractional charges $\pm \frac{e}{m}$. The quasiparticles and quasiholes also obey fractional statistics [50].

1.1.10 Inner structure of collective modes in FQHE

Despite the fact that the quantum Hall system is made up of fermions, the behavior is also reminiscent of superfluidity since the current is dissipationless. Indeed, within the 'composite boson picture', one views the FQHE ground state as a Bose condensate [51]. Using the single mode approximation, (like Feynmann used to calculate the excitation spectrum for liquid helium) Girvin, Macdonald and Platzman (GMP) analyzed the collective excitation spectrum of fractional quantum Hall systems [52]. This dispersion curve has finite gap at $k = 0$, quite different from the case of superfluid helium and trapped alkali atomic Bose gas in which mode is gapless. However like the case of the superfluid helium, it has a roton minimum, called 'magnetoroton' minimum at finite k . The collective excitation spectrum is different from the Fermi liquids. Girvin *et al.* [52] brought out non-trivial inner structure of neutral excitations of the FQH systems. This inner structure is very transparent for the magnetoroton, the minimum energy neutral excitations at finite wave vector $k_0 l_0 \sim 1.4$ for the $\nu = \frac{1}{3}$ quantum Hall state. They are approximated by a Laughlin quasihole and quasiparticle bound state, whereas the roton in liquid helium is considered as a localized highly excited state composed of few atoms. The

exact diagonalization studies by Haldane *et al.* [53] proved that the single mode approximation is extremely accurate. The excitation spectrum of fractional quantum Hall systems at $\nu = \frac{1}{3}$ has been measured by resonant inelastic light scattering experiment [54] which is in good agreement with the theoretical prediction. It was observed by GMP [52] that the zero momentum neutral excitation, as observed by numerical experiment [53] was in disagreement with their result. Since the numerically observed result was slightly less than sum of the two magnetoroton energy, they speculated that the minimum energy excitation could be a two-magnetoroton bound state. In the seventh chapter of this Thesis we will be concerned with the formation of two-magnetoroton bound state in fractional quantum Hall states at $\nu = \frac{1}{3}$. By focusing on the oriented dipole character of magnetoroton, we [55] model the two-magnetoroton bound state with binding energy which is in good agreement with the composite fermion [56] numerical results.

The quantum Hall systems are also interesting in the vicinity of even-denominator filling fractions. For example, the quantized Hall plateau does not occur at $\nu = \frac{1}{2}$ state [57] whereas the quantum Hall effect is observed at $\nu = \frac{5}{2}$ state [58]. The basic elementary excitations at $\nu = \frac{1}{2}$ are neutral, quite different from fractional charged excitations at odd-denominator filling fractions. The Chern-Simons theory [59] explained most of the properties at $\nu = \frac{1}{2}$ filling fraction. Attempts have been made to explain the $\nu = \frac{5}{2}$ state by considering *p*-wave pairing states known as Pfaffian states [60].

Theoretical understanding of the FQHE has progressed rapidly, but it is not yet complete. For an updated review and open problems in the quantum Hall effect, see the books and review articles [61].

1.2 Organisation of this Thesis

This Thesis is organised as follows. In the second chapter we derive the low-energy excitation frequencies and their damping rates of a 2D deformed trapped Bose gas above the critical temperature. In the third chapter we derive analytically the low-energy excitation spectra of a 2D deformed trapped interacting Bose gas as well as interacting Fermi gas at zero temperature. In the fourth chapter we show the universality of the monopole mode frequency and the time-evolution of a class of trapped interacting Bose gas. The fifth chapter is devoted to the study of various low-energy excitation spectra and the vortex state of a Bose condensate state with gravity-like interatomic attractive interaction. In the sixth chapter cooperative ring

exchange is suggested as a mechanism of quantum melting of vortex lattices produced in rapidly rotating quasi two dimensional BEC. We estimate the condition for quantum melting instability of vortex lattices. In the seventh chapter we model two-magnetoroton bound state formation in the fractional quantum Hall states at $\nu = \frac{1}{3}$ state. We present the summary and conclusions of this Thesis in the eighth chapter.

Bibliography

- [1] S. N. Bose, Z. Phys. **26**, 178 (1924).
- [2] A. Einstein, Sitzber. Kgl. Preuss. Akad. Wiss. 261 (1924).
- [3] K. Huang, *Statistical Mechanics*, 2nd edition (John Wiley and Sons, New York).
- [4] P. L. Kapitza, Nature **141**, 74, (1938);
J. F. Allen and A. D. Misener, Nature **140**, 62 (1938).
- [5] V. Baganato, D. E. Pritchard, and D. Kleppner, Phys. Rev. A **35**, 4354 (1987).
- [6] M. H. Anderson *et al.* Science **269**, 198 (1995).
- [7] K. B. Davis *et al.* Phys. Rev. Lett. **75**, 3969 (1995).
- [8] C. C. Bradley *et al.* Phys. Rev. Lett. **75**, 1687 (1995).
- [9] S. Inouye *et al.* Nature (London) **392**, 151 (1998);
J. Stenger *et al.* Phys. Rev. Lett. **82**, 2422 (1999).
- [10] E. P. Gross, Nuovo Cemento, A **20**, 454 (1961);
L. P. Pitaevskii, Sov. Phys. JETP **13**, 451 (1961).
- [11] G. Baym and C. J. Pethick, Phys. Rev. Lett. **76**, 6 (1996).
- [12] M. Edwards *et al.* Phys. Rev. Lett. **77**, 1671 (1996).
- [13] S. Stringari, Phys. Rev. Lett. **77**, 2360 (1996).
- [14] Victor M. Perez-Garcia *et al.* Phys. Rev. Lett. **77**, 5320 (1996).
- [15] D. Guery-Odelin and S. Stringari, Phys. Rev. Lett. **83**, 4452 (1999).
- [16] O. M. Margao *et al.* Phys. Rev. Lett. **84**, 2056 (2000).

- [17] M. R. Andrews *et al.* Phys. Rev. Lett. **79** 553 (1997) and Phys. Rev. Lett. **80** 2967 (1998).
- [18] D. M. Stamper-Kurn *et al.* Phys. Rev. Lett. **83** 2876 (1999).
- [19] Y. Castin and R. Dum, Phys. Rev. Lett. **77**, 5315 (1996);
Y. Kagan, E. L. Surkov and G. V. Shlyapnikov, Phys. Rev. A **54**, R1753 (1996);
F. Dalfovo, C. Minniti, L. Pitaevskii, and S. Stringari, Phys. Lett. A **227** 259 (1997).
- [20] U. Ernst *et al.* Europhys. Lett. **41**, 1 (1998); Appl. Phys. B **67**, 719 (1998).
- [21] W. I. McAlexander *et al.* Phys. Rev. A **51**, R871 (1995);
F. S. Cataliotti *et al.* Phys. Rev. A **57**, 1136 (1998).
- [22] B. De Marco and D. S. Jin, Science **285**, 1703 (1999).
- [23] P. C. Hohenberg, Phys. Rev. **158**, 383 (1967).
- [24] V. Baganato and D. Kleppner, Phys. Rev. A **44**, 7439 (1991).
- [25] Pijush K. Ghosh, Phys. Rev. A **65**, 012103 (2001).
- [26] Pijush K. Ghosh, cond-mat/0109073.
- [27] Gorlitz *et al.* Phys. Rev. Lett. **87**, 130402 (2001).
- [28] W. Hansel *et al.* Nature **413**, 498 (2001).
- [29] H. Ott *et al.* Phys. Rev. Lett. **87**, 230401 (2001).
- [30] Tarun Kanti Ghosh, Phys. Rev. A **63**, 013603 (2000).
- [31] Tarun Kanti Ghosh and S. Sinha, The Eur. Phys. J. D **19**, 371 (2002).
- [32] Tarun Kanti Ghosh, Phys. Lett. A **285**, 222 (2001).
- [33] L. P. Pitaevskii and A. Rosch, Phys. Rev. A **55**, R 853 (1997).
- [34] K. Goral and L. Santos, cond-mat/0203542.
- [35] D. O'Dell *et al.* Phys. Rev. Lett. **84**, 5687 (2000).
- [36] S. Giovanazzi *et al.* Europhys. Lett. **56**, 1 (2001);
Tarun Kanti Ghosh, Phys. Rev. A **65**, 053616 (2002).

- [37] E. J. Yarmchuk, M. J. V. Gordan, and R. E. Packard, Phys. Rev. Lett. **43**, 214 (1979).
- [38] K. W. Madison, Phys. Rev. Lett. **84**, 806 (2000).
- [39] J. R. Abo-Shaeer *et al.* Science **292**, 476 (2001).
- [40] Tin-Lun Ho, Phys. Rev. Lett. **87**, 060403 (2001).
- [41] N. R. Cooper *et al.* Phys. Rev. Lett. **87**, 120405 (2001).
- [42] J. Sinova, C. B. Hanna, and A. H. Macdonald, Phys. Rev. Lett. **89**, 030403 (2002).
- [43] Tarun Kanti Ghosh and G. Baskaran, cond-mat/0207484 (submitted to Phys. Rev. Lett.).
- [44] N. Read and E. H. Rezayi, Phys. Rev. B **59**, 8084 (1999).
- [45] F. Dalfovo *et al.* Rev. Mod. Phys. **71**, 463 (1999);
A. J. Leggett, Rev. Mod. Phys. **73**, 307 (2001);
C. J. Pethick and H. Smith, *Bose-Einstein condensation in dilute gases*, Cambridge University Press 2002.
- [46] K. von Klitzing *et al.* Phys. Rev. Lett. **45**, 494 (1980).
- [47] D. Tsui *et al.* Phys. Rev. Lett. **48**, 1599 (1982).
- [48] R. B. Laughlin, Phys. Rev. Lett. **50**, 1395 (1983).
- [49] J. K. Jain, Phys. Rev. Lett. **63**, 199 (1989).
- [50] D. Arovas, J. R. Schrieffer, and F. Wilczek, Phys. Rev. Lett. **53**, 145 (1984).
- [51] S. M. Girvin and A. H. Macdonald, Phys. Rev. Lett. **58**, 1252 (1987);
S. C. Zang, H. Hansson, and S. Kivelson, Phys. Rev. Lett. **62**, 82 (1989);
N. Read, Phys. Rev. Lett. **62**, 86 (1989).
- [52] S. M. Girvin, A. H. Macdonald, and M. P. Platzman, Phys. Rev. Lett. **54**, 581 (1985).
- [53] F. D. M. Haldane and E. H. Rezayi, Phys. Rev. Lett. **54**, 237 (1985).

- [54] A. Pinczuk *et al.* Phys. Rev. Lett. **70**, 3983 (1993);
H. D. M. Davies *et al.* Phys. Rev. Lett. **78**, 4095 (1997);
M. Kang *et al.* Phys. Rev. Lett. **84**, 546 (2000).
- [55] Tarun Kanti Ghosh and G. Baskaran, Phys. Rev. Lett. **87**, 186803 (2001).
- [56] K. Park and J. K. Jain, Phys. Rev. Lett. **84**, 5576, (2000).
- [57] R. L. Willet *et al.* Phys. Rev. Lett. **71**, 3846 (1993).
- [58] W. Pan *et al.* Phys. Rev. Lett. **83**, 3530 (1999).
- [59] B. I. Halperin *et al.* Phys. Rev. B **47**, 17312 (1993).
- [60] F. D. M. Haldane *et al.* Phys. Rev. Lett. **60**, 956 (1988); **60**, 1886 (1988).
- [61] R. E. Prange and S. M. Girvin, *The Quantum Hall Effect* (Springer-Verlag, NY, 1990);
S. Das Sarma and A. Pinczuk, *Perspective in Quantum Hall Effects*, (Wiley, New York, 1997);
S. M. Girvin, *The Quantum Hall Effect: Novel Excitations and Broken Symmetries*, Les Houches Summer School 1998.

Chapter 2

Collective excitation frequencies and damping rates of a 2D deformed trapped Bose gas above the critical temperature

2.1 Introduction

After the discovery of Bose-Einstein Condensation (BEC) in a trapped alkali atom, the influences of the dimension of a Bose systems has been a subject of extensive studies [1]. In our present technology one can freeze the motion of the trapped particles in one direction to create a quasi-two-dimensional Bose system. In the frozen direction the particles execute the zero point motion. To achieve this quasi-two dimensional system, the frequency (ω_z) in the frozen direction should be much larger than the frequency (ω_0) in the $x-y$ plane such that $k_B T \ll \hbar \omega_z$ and $\mu \geq \hbar \omega_0$. It has been shown by V. Baganato *et al.* [2] that for an ideal two-dimensional (2D) Bose gas under harmonic trap a macroscopic occupation of the ground state can exist at temperature $T < T_c = \sqrt{\frac{N}{\zeta(2)}} \frac{\hbar \omega_0}{k_B}$, where N is the total number of particles and $\zeta(2)$ is the Riemann ζ -function. Then the condition for creating a 2D trapped Bose gas above the critical temperature is $\sqrt{\frac{N}{\zeta(2)}} \hbar \omega_0 \ll k_B T \ll \hbar \omega_z$.

At very low temperature, when the whole system is Bose-Einstein condensed state, the motion is described by the hydrodynamic equations of superfluids. If the temperature is larger than the critical temperature for BEC the dynamical behaviour of a dilute gas is well described by the Boltzmann equation. Above the critical temperature (T_c), one can distinguish two regimes, the hydrodynamic(collisional)

one where collisions ensure the local thermal equilibrium and collisionless where the motion is described by the single particle Hamiltonian. In the hydrodynamic region, the characteristic mode frequency is small compared to the collision frequency ($\omega\tau \ll 1$). In the collisionless region ($\omega\tau \gg 1$), the collisions are not important. In the collisionless regime the system exhibits well defined oscillations which are driven by the external potential. The low-energy oscillation frequencies of a 3D trapped Bose gas above T_c have been measured in [3]. The low-lying collective mode frequencies of a 3D trapped Bose gas above T_c in the hydrodynamic region has been discussed by Griffin *et al.* [4] by using the kinetic theory. Damping of the hydrodynamic modes in a trapped Bose gas above the T_c is also discussed by Odell *et al.* [5] and Kavoulakis *et al.* [6]. These theoretical results are consistent with the experimental results.

It is well known that the excitation frequencies for monopole mode is $2\omega_0$ in a 2D isotropic trapped Bose gas. Using the approximation, $\omega_z \gg \omega_0$, the dispersion relation of the excitation frequencies for 3D trapped Bose gas above T_c obtained in [4, 5] does not produce the correct frequencies for monopole mode in a 2D trapped Bose system. The main aim of this chapter is to give analytic results for the dispersion law of low-lying collective modes of a 2D deformed trapped Bose gas above T_c and their damping rates in both regimes, hydrodynamic and collisionless.

This chapter is organised as follows. We derive in section [2.2] a closed equation of motion for the velocity fluctuations of a 2D deformed trapped Bose gas just above the critical temperature ($T > T_c$), using the kinetic theory. We make use of this equation in section [2.3] to calculate the excitation frequencies for a few low-lying collective modes and the corresponding density fluctuations. In section [2.4] we derive a dispersion relation of a 2D deformed trap Bose gas at very high temperature using the method of averages that interpolates between the collisionless and hydrodynamic regimes. From this dispersion relation, we calculate the eigenfrequencies and damping rates for monopole and quadrupole modes. We discuss the time evolution of the wave packet width of a Bose gas in a time-independent as well as time-dependent trap. In section [2.5] we present a summary and outlook of this chapter.

2.2 Hydrodynamic equation of motion for the velocity fluctuations

We shall discuss the collective modes of a 2D deformed trapped Bose gas in the hydrodynamic regime just above $T > T_c$, using the kinetic theory. In the low-energy excitations, we can use the semiclassical approximation for the dynamics of a Bose gas, using the following Boltzmann equation [7] for the phase-space distribution function $f(\mathbf{r}, \mathbf{p}, t)$:

$$\frac{\partial f}{\partial t} + \mathbf{v} \cdot \nabla_{\mathbf{r}} f + \frac{\mathbf{F}}{m} \cdot \nabla_{\mathbf{v}} f = I_{coll}(f), \quad (2.1)$$

where I_{coll} is the collisional integral, and $\mathbf{F} = -\nabla U_0(\mathbf{r})$. The trap potential is $U_0(r) = \frac{1}{2}m(\omega_x^2 x^2 + \omega_y^2 y^2)$. In the hydrodynamic regime, collisions ensures the local thermodynamic equilibrium. To the lowest order, the perturbed distribution function produced by a slowly varying external potential is the equilibrium Bose distribution function:

$$f(\mathbf{r}, \mathbf{p}, t) = [\exp(\beta(\mathbf{r}, t)\eta(\mathbf{r}, t) - 1)]^{-1}, \quad (2.2)$$

$$\eta(\mathbf{r}, t) = \frac{[\mathbf{p} - m\mathbf{v}(\mathbf{r}, t)]^2}{2m} - \mu(\mathbf{r}, t). \quad (2.3)$$

$\mu(\mathbf{r}, t)$ is the chemical potential. The inverse temperature is $\beta(\mathbf{r}, t) = \frac{1}{k_B T(\mathbf{r}, t)}$. The local density $n(\mathbf{r}, t)$, the local velocity $\mathbf{v}(\mathbf{r}, t)$ and the local energy $E(\mathbf{r}, t)$ are defined as

$$n(\mathbf{r}, t) = \int \frac{d^2 p}{(2\pi)^2} f(\mathbf{r}, \mathbf{p}, t), \quad (2.4)$$

$$\mathbf{v}(\mathbf{r}, t) = \int \frac{d^2 p}{(2\pi)^2} \frac{\mathbf{p}}{m} f(\mathbf{r}, \mathbf{p}, t), \quad (2.5)$$

$$E(\mathbf{r}, t) = \int \frac{d^2 p}{(2\pi)^2} \frac{p^2}{2m} f(\mathbf{r}, \mathbf{p}, t). \quad (2.6)$$

The conservation laws are [8]

$$\frac{\partial n(\mathbf{r}, t)}{\partial t} + \nabla \cdot [n(\mathbf{r}, t)\mathbf{v}(\mathbf{r}, t)] = 0, \quad (2.7)$$

$$mn(\mathbf{r}, t) \frac{\partial \mathbf{v}}{\partial t} = -[\nabla P(\mathbf{r}, t) + n(\mathbf{r}, t)\nabla U_0(\mathbf{r})], \quad (2.8)$$

$$\frac{\partial E(\mathbf{r}, t)}{\partial t} = -\nabla \cdot [(P(\mathbf{r}, t) + E(\mathbf{r}, t))\mathbf{v}(\mathbf{r}, t)] - n(\mathbf{r}, t)\mathbf{v}(\mathbf{r}, t) \cdot \nabla U_0(\mathbf{r}). \quad (2.9)$$

These conservation laws are obtained from Eq.(2.1) by multiplying 1, \mathbf{p} , $\frac{\mathbf{p}^2}{2m}$, and integrating the resulting equation over \mathbf{p} . During collisions, the total number of

particles N , momentum \mathbf{p} , and energy $\frac{\mathbf{p}^2}{2m}$ are conserved, so the collisional term vanishes. We are only interested in a small perturbations around the equilibrium states. We linearize the density, velocity and pressure as follows. $n(\mathbf{r}, t) = n_0(\mathbf{r}) + \delta n(\mathbf{r}, t)$, $\mathbf{v}(\mathbf{r}, t) = \delta \mathbf{v}(\mathbf{r}, t)$ and $P(\mathbf{r}, t) = P_0(\mathbf{r}) + \delta P(\mathbf{r}, t)$ with $n_0(\mathbf{r})$ and $P_0(\mathbf{r})$ being the equilibrium density and pressure, respectively. The linearized conservation laws are

$$\frac{\partial n_0(\mathbf{r}, t)}{\partial t} + \nabla \cdot [n_0(\mathbf{r}) \delta \mathbf{v}(\mathbf{r}, t)] = 0, \quad (2.10)$$

$$m n_0(\mathbf{r}) \frac{\partial \delta \mathbf{v}}{\partial t} = -[\nabla P_0(\mathbf{r}, t) + n_0(\mathbf{r}, t) \nabla U_0(\mathbf{r})], \quad (2.11)$$

$$\frac{\partial E(\mathbf{r}, t)}{\partial t} = -\nabla \cdot [(P_0(\mathbf{r}) + E(\mathbf{r})) \delta \mathbf{v}] - n_0 \delta \mathbf{v} \cdot \nabla U_0(\mathbf{r}). \quad (2.12)$$

Using the quantum-statistical mechanics, the pressure and density can be written as

$$\frac{P}{k_B T} = \frac{g_2(z)}{\Lambda^2}, \quad (2.13)$$

$$n = \frac{g_1(z)}{\Lambda^2}, \quad (2.14)$$

where $g_n(z) = \sum_{i=1}^{\infty} (\frac{z^i}{i^n})$ are the Bose-Einstein functions. $z(\mathbf{r}, t) = e^{\beta(\mathbf{r}, t)\mu(\mathbf{r}, t)}$ is the local thermodynamic fugacity, which is always less than one. $\Lambda = \sqrt{\frac{2\pi\hbar^2}{mk_B T}}$ is the thermal de Broglie wave length.

One can easily get the relation

$$P(\mathbf{r}, t) = E(\mathbf{r}, t) \quad (2.15)$$

in 2D. The static local equilibrium values of the thermodynamic functions which are given in the above can be obtained by setting $\delta \mathbf{v}(\mathbf{r}, t) = 0$, $T(\mathbf{r}, t) = T_0$ and $z = z_0 = e^{\frac{\mu_0(\mathbf{r})}{k_B T_0}}$, where $\mu_0(\mathbf{r}) = \mu - U_0(\mathbf{r})$ and μ is the chemical potential. Using Eq.(2.15), Eq.(2.12) can be written as

$$\frac{\partial P_0(\mathbf{r}, t)}{\partial t} = -2\nabla \cdot [(P_0(\mathbf{r}) \delta \mathbf{v}(\mathbf{r}, t)] - n_0 \delta \mathbf{v}(\mathbf{r}, t) \cdot \nabla U_0(\mathbf{r}). \quad (2.16)$$

Taking the time derivative of Eq. (2.11) and using Eqs. (2.10) and (2.16), we obtain

$$m \frac{\partial^2 \delta \mathbf{v}}{\partial t^2} = 2 \frac{P_0(\mathbf{r})}{n_0(\mathbf{r})} \nabla [\nabla \cdot \delta \mathbf{v}] - [\nabla \cdot \delta \mathbf{v}] \nabla U_0(\mathbf{r}) - \nabla [\delta \mathbf{v} \cdot \nabla U_0(\mathbf{r})]. \quad (2.17)$$

The term $\frac{P_0(\mathbf{r})}{n_0(\mathbf{r})}$ of (2.17) is associated with the Bose statistics.

Without any external potential, $U_0 = 0$, Eq. (2.17) becomes

$$m \frac{\partial^2 \delta \mathbf{v}}{\partial t^2} = 2 \frac{P_0(\mathbf{r})}{n_0(\mathbf{r})} \nabla [\nabla \cdot \delta \mathbf{v}]. \quad (2.18)$$

It has the plane-wave solution with the dispersion relation $\omega^2 = c^2 k^2$. The sound velocity is

$$c^2 = \frac{2P_0(\mathbf{r})}{mn_0(\mathbf{r})} = \frac{2k_B T_0}{m} \frac{g_2(z_0)}{g_1(z_0)}, \quad (2.19)$$

where $z_0 = e^{\frac{\mu}{k_B T_0}}$. At high temperature ($z \ll 1$), the sound velocity becomes $c^2 = \frac{2k_B T_0}{m}$. This sound velocity exactly matches with known result.

From the continuity Eq.(2.10), we have

$$\frac{\partial \delta n(\mathbf{r}, t)}{\partial t} = -(\nabla \cdot \delta \mathbf{v}) n_0(\mathbf{r}) - \delta \mathbf{v}(\mathbf{r}, t) \cdot \nabla n_0(\mathbf{r}, t). \quad (2.20)$$

The density fluctuation is given by $\delta n(\mathbf{r}, t) = \delta n(\mathbf{r}) e^{-i\omega t}$. In classical limit, the static density profile is $n_0(\mathbf{r}) = n_0(\mathbf{r} = 0) e^{-\frac{m(\omega_x^2 x^2 + \omega_y^2 y^2)}{2\theta}}$, where $\theta = k_B T$.

2.3 Eigenfrequencies and the corresponding density fluctuations in the hydrodynamic regime

The different eigenmodes may be summarised as follows:

1) The normal-mode solution of (2.17) is $\delta \mathbf{v}(\mathbf{r}) = \nabla(z^l)$, where $z = (x + iy)$ and $l > 0$. The excitation frequencies and the associated density fluctuations are $\omega^2 = l\omega_x^2$, $\delta n_x \sim \omega_x^2 x z^{(l-1)} n_0(\mathbf{r})$ and $\omega^2 = \omega_x^2 + (l-1)\omega_y^2$, $\delta n_y \sim \omega_y^2 y z^{(l-1)} n_0(\mathbf{r})$. For an isotropic trap, the frequency is $\omega = \omega_0 \sqrt{l}$. The corresponding density fluctuation is $\delta n(\mathbf{r}) \sim n_0(\mathbf{r}) r^l e^{il\theta}$. At $r = 0$, there is no density fluctuation. There is a maximum density fluctuation at $r = \sqrt{\frac{l\theta}{m\omega_0^2}}$.

2) The other solution of Eq. (2.17) is $\delta \mathbf{v}(\mathbf{r}) = \nabla[\alpha x^2 \pm \beta y^2]$. The positive sign is for the monopole mode, and the negative sign is for quadrupole mode. In a deformed trap, the excitation frequencies are

$$\omega_{\pm}^2 = \frac{1}{2} \left[3(\omega_x^2 + \omega_y^2) \pm \sqrt{9(\omega_x^2 + \omega_y^2)^2 - 32\omega_x^2 \omega_y^2} \right]. \quad (2.21)$$

For an isotropic trap, it becomes $\omega_+ = 2\omega_0$ or $\omega_- = \sqrt{2}\omega_0$. Hence, in the anisotropic trap, the monopole mode is coupled to the quadrupole mode. If $\omega_x \ll \omega_y$, the lowest excitation frequency is $\omega = \sqrt{\frac{8}{3}}\omega_x$. If $\omega_x \gg \omega_y$, the lowest excitation frequency is $\omega = \sqrt{\frac{8}{3}}\omega_y$. The density fluctuation for the monopole mode is

$$\delta n(\mathbf{r}) \sim \left[2 - \frac{m(\omega_x^2 x^2 + \omega_y^2 y^2)}{\theta} \right] n_0(\mathbf{r}), \quad (2.22)$$

where as the density fluctuation for quadrupole mode is $\delta n(\mathbf{r}) \sim (\omega_y^2 y^2 - \omega_x^2 x^2) n_0(\mathbf{r})$.

3) There is another quadrupole mode which has velocity field $\delta \mathbf{v}(\mathbf{r}) = \nabla(xy)$. This is also called the scissors mode [11]. The excitation frequency is $\omega^2 = \omega_x^2 + \omega_y^2$ and the corresponding density fluctuation is $\delta n(\mathbf{r}) \sim (\omega_x^2 + \omega_y^2) xy n_0(\mathbf{r})$. In an isotropic trap, $\omega^2 = 2\omega_0^2$, which agrees with that for the scissors mode in hydrodynamic regime above T_c [11]. The quadrupole and scissors mode frequencies are degenerate in an isotropic trap. This degeneracy is lifted up due to the trap deformation.

2.4 Method of averages

At very high temperature, the dynamical behaviour of a dilute gas is described by the Boltzmann transport equation. Here we include the collisional term in the Boltzmann transport equation, and study the eigenfrequencies for monopole and quadrupole mode using the method of averages [5]. These two modes are coupled in a deformed trap.

From Eq. (2.1), one can obtain the equations for the average of a dynamical quantity $\chi(\mathbf{r}, \mathbf{v})$ is [7, 9]

$$\frac{d\langle\chi\rangle}{dt} - \langle\mathbf{v} \cdot \nabla_{\mathbf{r}} \chi\rangle - \left\langle \frac{\mathbf{F}}{m} \cdot \nabla_{\mathbf{v}} \chi \right\rangle = \langle I_{coll} \chi \rangle, \quad (2.23)$$

where the average is taken in phase space, and $\langle \chi \rangle$ can be written as

$$\langle \chi \rangle = \frac{1}{N} \int d^2 r d^2 v f(\mathbf{r}, \mathbf{v}, t) \chi(\mathbf{r}, \mathbf{v}). \quad (2.24)$$

$\langle \chi I_{coll} \rangle$ can be defined as

$$\langle \chi I_{coll} \rangle = \frac{1}{4N} \int d^2 r d^2 v [\chi_1 + \chi_2 - \chi'_1 - \chi'_2] I_{coll}(f). \quad (2.25)$$

If $\chi = a(\mathbf{r}) + \mathbf{b}(\mathbf{r}) \cdot \mathbf{v} + c(\mathbf{r}) v^2$, for elastic collision the collisional term is zero [5, 7]. a , b , and c are arbitrary functions of the position.

Now we define the following quantities:

$$\chi_1 = x^2 + y^2, \quad (2.26)$$

$$\chi_2 = y^2 - x^2, \quad (2.27)$$

$$\chi_3 = xv_x + yv_y, \quad (2.28)$$

$$\chi_4 = yv_y - xv_x, \quad (2.29)$$

$$\chi_5 = v_x^2 + v_y^2, \quad (2.30)$$

$$\chi_6 = v_y^2 - v_x^2. \quad (2.31)$$

Using the Boltzmann kinetic equation (2.23), we obtain the following closed set of equations:

$$\langle \ddot{\chi}_1 \rangle = 2\langle \chi_5 \rangle - t\langle \chi_1 \rangle + \epsilon\langle \chi_2 \rangle, \quad (2.32)$$

$$\langle \ddot{\chi}_2 \rangle = 2\langle \chi_6 \rangle - t\langle \chi_2 \rangle + \epsilon\langle \chi_1 \rangle, \quad (2.33)$$

$$\langle \ddot{\chi}_3 \rangle = 2\epsilon\langle \chi_4 \rangle - 2t\langle \chi_3 \rangle, \quad (2.34)$$

$$\langle \ddot{\chi}_4 \rangle = 2\epsilon\langle \chi_3 \rangle - 2t\langle \chi_4 \rangle - \frac{\langle \chi_6 \rangle}{\tau}, \quad (2.35)$$

$$\langle \ddot{\chi}_5 \rangle = \epsilon\langle \chi_6 \rangle - t\langle \chi_5 \rangle - \epsilon t\langle \chi_2 \rangle + \frac{\epsilon^2 + t^2}{2}\langle \chi_1 \rangle, \quad (2.36)$$

$$\langle \ddot{\chi}_6 \rangle = -\epsilon t\langle \chi_1 \rangle + \frac{\epsilon^2 + t^2}{2}\langle \chi_2 \rangle + \epsilon\langle \chi_5 \rangle - \frac{\langle \dot{\chi}_6 \rangle}{\tau} - t\langle \chi_6 \rangle, \quad (2.37)$$

where double dot indicates the double derivative with respect to time. $t = \omega_x^2 + \omega_y^2$ and $\epsilon = \omega_x^2 - \omega_y^2$. χ_6 is not a conserved quantity, so the collisional contribution comes only through the χ_6 term. We have used the fact that $\langle \chi_6 I_{coll} \rangle = -\frac{\chi_6}{\tau}$, where τ is the relaxation time. This relaxation time τ can be computed by a Gaussian ansatz for the distribution function. The relaxation time τ is order of the inverse of the collision rate $\gamma_{coll} \sim n(0)v_{th}\sigma_0$, where $v_{th} = \sqrt{\frac{\pi k_B T}{2m}}$ is the mean thermal velocity, and $n(0) = \frac{Nm\omega_0^2\lambda}{2\pi k_B T a_z}$ is the central density for a quasi-2D system. a_z is the oscillator length in the z direction. Hence $\tau \sim \frac{4a_z}{N\sigma_0\omega_0^2\lambda} \sqrt{\frac{2\pi k_B T}{m}}$. $\sigma_0 = 8\pi a^2$ is the 3-D scattering cross-section. It can be written in terms of T_c as

$$\tau \sim \frac{1}{\omega_0} \sqrt{\frac{2}{\pi\sqrt{\zeta(2)}(N\lambda)^{\frac{3}{2}}}} \left(\frac{a_z a_0}{a^2} \right) \sqrt{\frac{T}{T_c}}, \quad (2.38)$$

where $a_0 = \sqrt{\frac{\hbar}{m\omega_0}}$ is the oscillator length. The relaxation time τ varies as \sqrt{T} in a quasi-2D system, where as in a 3D system it varies as T [6]. Now we are looking for a solutions of Eqs. (2.32)-(2.37) as $e^{-i\omega t}$. We have the following dispersion relation:

$$(\omega^2 - 4\omega_x^2)(\omega^2 - 4\omega_y^2) + \frac{i}{\omega\tau} [\omega^4 - 3\omega^2(\omega_x^2 + \omega_y^2) + 8\omega_x^2\omega_y^2] = 0. \quad (2.39)$$

This dispersion relation interpolates between the collisionless and hydrodynamic regimes. In the hydrodynamical regime ($\omega\tau \rightarrow 0$), the first term does not contribute. It gives $\omega^2 = \frac{1}{2} [3(\omega_x^2 + \omega_y^2) \pm \sqrt{9(\omega_x^2 + \omega_y^2)^2 - 32\omega_x^2\omega_y^2}]$. This eigenfrequency exactly match with Eq. (2.21), a result we found using the equation of motion for the velocity fluctuations even in a deformed trap. We have considered a

few low-energy excitation modes for which $\nabla \cdot \delta \mathbf{v}$ is constant. The first term of the right-hand side of Eq. (2.17) does not contribute in the excitation spectrum. That's why the frequencies of these normal modes are the same for a Bose gas just above T_c and at very high temperature. In pure collisionless regime ($\omega\tau \rightarrow \infty$), it gives $\omega_C = 2\omega_x$ and $\omega_C = 2\omega_y$.

We can write phenomenological interpolation formula for the frequency and the damping rate of the modes in the following form [5, 6]:

$$\omega^2 = \omega_C^2 + \frac{\omega_H^2 - \omega_C^2}{1 - i\omega\tau}. \quad (2.40)$$

The imaginary part of the above equation for the damping rate gives

$$\Gamma = \frac{\tau}{2} \frac{d}{1 + (\omega\tau)^2}, \quad (2.41)$$

where $d = (\omega_C^2 - \omega_H^2)$. In the hydrodynamic limit ($\omega\tau \rightarrow 0$), the damping rate is

$$\Gamma_{HD} = \frac{\tau}{2} d, \quad (2.42)$$

where as in the collisionless region ($\omega\tau \rightarrow \infty$),

$$\Gamma_{CL} = \frac{d}{2\omega_C^2\tau}. \quad (2.43)$$

The damping rate depends on the difference between the square of the frequencies in the collisional and hydrodynamical regimes. The damping rates can be calculated for different values of temperature, and number of trapped atoms as well as of the trapping parameters and scattering length through the relaxation time τ (2.38). For a monopole mode in an isotropic trap, the difference d is zero. Thus there is no damping in the monopole mode in a 2D isotropic trapped Bose system when the temperature is very high. This was first shown by Boltzmann [9] and later by Guery-Odelin *et al.* [5], in 3D trapped Bose system at very high temperature.

For an isotropic harmonic trap, Eqs. (2.32) - (2.37) decouple into two subsystems, one for the monopole mode and the other for the quadrupole mode. The closed set of equations for monopole mode are

$$\langle \ddot{\chi}_1 \rangle = 2\langle \chi_5 \rangle - 2\omega_0^2 \langle \chi_1 \rangle, \quad (2.44)$$

$$\langle \ddot{\chi}_3 \rangle = -4\omega_0^2 \langle \chi_3 \rangle, \quad (2.45)$$

$$\langle \ddot{\chi}_5 \rangle = 2\omega_0^4 \langle \chi_1 \rangle + 2\omega_0^2 \langle \chi_3 \rangle. \quad (2.46)$$

There is no collisional term in the above equations. Thus there is no damping for the monopole mode of a classical dilute gas confined in an isotropic trap. We are looking for solutions of Eqs. (2.44) - (2.46) like $e^{-i\omega t}$, we obtain $\omega = 2\omega_0$.

Equations (2.44) - (2.46) can be rewritten as

$$\ddot{\langle\chi_1\rangle} - \frac{\langle\dot{\chi}_1\rangle^2}{2\langle\chi_1\rangle} + 2\omega_0^2\langle\chi_1\rangle = \frac{Q}{\langle\chi_1\rangle}, \quad (2.47)$$

where $Q = 2(\langle\chi_1\rangle\langle\chi_5\rangle - \langle\chi_3\rangle^2)$ is an invariant quantity under time evolution. We define $X(t) = \sqrt{\langle\chi_1\rangle}$, which is the wave-packet width and substituting it into Eq. (2.47) gives

$$\ddot{X} + \omega_0^2 X = \frac{Q}{X^3}. \quad (2.48)$$

This is a nonlinear singular Hill equation. The same equation was obtained at $T = 0$ in 2D by Garcia Ripoll *et al.* [10]. At equilibrium, $X_0^4 = \frac{Q}{\omega_0^2}$. We linearized Eq. (2.48) around the equilibrium point X_0 , we obtained

$$\delta\ddot{X} + 4\omega_0^2\delta X = 0. \quad (2.49)$$

One obtains that the oscillation frequency of the gas is $\omega = 2\omega_0$, corresponding to the frequency of a single-particle excitation in the gas.

For a time-dependent trap, the equation of motion for the width of the wave-packet is

$$\ddot{X} + \omega_0^2(t)X = \frac{Q}{X^3}. \quad (2.50)$$

The general solution [12] is $X(t) = \sqrt{u^2(t) + \frac{Q}{W^2}v^2(t)}$ where $u(t)$ and $v(t)$ are two linearly independent solutions of the equation $\ddot{p} + \omega_0^2(t)p = 0$ which satisfy $u(t_0) = X(t_0)$, $\dot{u}(t_0) = X'(t_0)$, $v(t_0) = 0$, $v'(t_0) \neq 0$. W is the Wronskian. The time-dependent Hill equation (2.50) can be solved explicitly only for a particular choice of $\omega_0(t)$.

The closed set of equations for a quadrupole mode in an isotropic trap are

$$\ddot{\langle\chi_2\rangle} = 2\langle\chi_6\rangle - 2\omega_0^2\langle\chi_2\rangle, \quad (2.51)$$

$$\ddot{\langle\chi_4\rangle} = -4\omega_0^2\langle\chi_4\rangle - \frac{\langle\chi_6\rangle}{\tau}, \quad (2.52)$$

$$\ddot{\langle\chi_6\rangle} = 2\omega_0^4\langle\chi_2\rangle - \frac{\dot{\langle\chi_6\rangle}}{\tau} - 2\omega_0^2\langle\chi_6\rangle. \quad (2.53)$$

Solving this set of equations, we obtain the damped quadrupole mode,

$$(\omega^2 - 4\omega_0^2) + \frac{i}{\omega\tau}(\omega^2 - 2\omega_0^2) = 0. \quad (2.54)$$

In the hydrodynamic regime, the oscillation frequency is $\omega^2 = 2\omega_0^2$, whereas in the collisionless region the frequency is just a single-particle oscillator frequency. The damping rate can be calculated by using Eqs. (2.42) and (2.43).

2.5 Summary and conclusions

In this chapter, we derived the equations of motion for velocity fluctuations of a Bose gas in a 2D deformed trap potential just above the critical temperature. Without any external trap potential ($U_0 = 0$), this becomes a wave equation, from which we found the exact sound velocity at high temperature. We have also computed the frequency of the scissors mode in a hydrodynamic regime above T_c which agrees with the result obtained by Guery-Odelin and Stringari [11]. We have also calculated the frequencies for monopole and quadrupole modes and the corresponding density fluctuations in a deformed trap above T_c .

Using the method of averages, we obtained a dispersion relation that interpolates between the collisionless and hydrodynamic regimes at very high temperature. In a deformed trap as well as an isotropic trap, we have found frequencies and damping rates (in terms of the relaxation time) for monopole and quadrupole modes in both the regimes. In the hydrodynamical regime, the excitation frequencies for monopole and quadrupole modes exactly match with the previous result that we found from Eq. (2.17). We have also shown that the relaxation time τ varies as \sqrt{T} in a quasi-2D Bose gas whereas in 3D τ varies as T .

We have shown that there is no damping for monopole mode in a 2D isotropic trapped Bose gas when the temperature is very high. This is also true for 3D isotropic trapped Bose gas above the critical temperature which was first shown by Boltzmann [9], and later by Guery-Odelin *et al.* [5].

We have also shown that the time evolution of the wave packet width of a Bose gas in a time-independent as well as time-dependent isotropic trap can be obtained from the method of averages. This can be described by the solution of the Hill's equation.

The objective for future work would be to develop the method of averages by taking into account the effect of particle interactions. The contribution from the mean field interaction energy in Boltzmann transport equation is also known as the Vlasov contribution. One can derive the low-energy excitation spectra and the dynamics of the width of a 2D trapped interacting Bose gas above the critical temperature from the method of averages by including Vlasov term in the Boltzmann

transport equation. We believe that the monopole mode frequency will be independent of the interaction strength and the dynamics of the width can be described by the same nonlinear singular Hill's equation.

Bibliography

- [1] L. P. Pitaevskii and A. Rosch, Phys. Rev. A **55**, R853 (1997);
Tin-Lun Ho and Michael Ma, J. Low Temp. Phys. **115**, 61 (1999);
D. S. Petrov, M. Holzmann and G. V. Shlyapnikov, Phys. Rev. Lett. **84**, 2551 (2000).
- [2] V. Baganato and D. Kleppner, Phys. Rev. A **44**, 7439 (1991).
- [3] M-O Mewes *et al.* Phys. Rev. Lett. **77**, 416 (1996);
D. S. Jin *et al.* Phys. Rev. Lett. **77**, 420 (1996);
D. M. Stamper-Kurn *et al.* Phys. Rev. Lett. **81**, 500 (1998).
- [4] A. Griffin, Wen-Chin Wu and S. Stringari, Phys. Rev. Lett. **78**, 1838 (1997).
- [5] David Guery-Odelin, F. Zambelli, J. Dalibard, S. Stringari, Phys. Rev. A **60**, 4851, (1999).
- [6] G. M. Kavoulakis, C. J. Pethick and H. Smith, Phys. Rev. A **57**, R2938 (1998).
- [7] K. Haug, *Statistical Mechanics*, (Wiley Eastern Limited, 1986), 2nd reprint.
- [8] L. P. Kadanoff and G. Baym, *Quantum Statistical Mechanics*. (Addison-Wesley).
- [9] G. E. Uhlenbeck and G. W. Ford, *Lectures in Statistical Mechanics*, (American Mathematical Society, Providence, R. I. 1963).
- [10] Juan. J. Garcia-Ripoll and Victor M. Perez-Garcia, Phys. Rev. Lett. **83**, 1715 (1999).
- [11] Guery-Odelin and S. Stringari, Phys. Rev. Lett. **83**, 4452 (1999).
- [12] W. Magnus and S. Winklen, *Hill's equation*, (Dover Publications, N.Y, 1966);
F. M. Arscott, *Periodic differential equations*, (Pergamen Press, Oxford (1964)).

Chapter 3

Collective excitation frequencies of a quasi-2D deformed trapped quantum gas at $T = 0$

3.1 Introduction

In the previous chapter we have derived the low-energy excitation frequencies and their damping rates of a two-dimensional (2D) deformed trapped Bose gas above the critical temperature. In this chapter we will discuss the low-energy excitation frequencies of a 2D deformed trapped alkali-metal atomic Bose and Fermi gases at zero temperature.

The low-energy collective excitation spectra of a three dimensional (3D) trapped Bose condensed state has been discussed analytically by Stringari [1], using the sum-rule approach. A few low-lying excitations have also been calculated analytically by using time-dependent variational approach [2]. The low-energy excitation spectra obtained in sum-rule approach coincides with the spectra obtained by using time-dependent Gaussian variational ansatz in the limit of large particle number. Also a similar type of scaling ansatz has been used to describe the excitation frequencies and the time evolution of the condensate in the large N limit [3, 4, 5]. Experimentally the low-lying collective excitation frequencies of a 3D condensate have been measured at zero temperature [6]. These observed values of the collective oscillation frequencies are in excellent agreement with the theoretical results at zero temperature.

The reduction in spatial dimensions of a quantum system is the subject of extensive study in trapped Bose systems [7, 8, 9, 10, 11] as well as in trapped Fermi

systems [12]. Recently, quasi-2D dimensional Bose-Einstein condensation (BEC) has also been realized at MIT [13]. So it is interesting to study the monopole, quadrupole and scissors mode frequencies of quasi-2D BEC. The main purpose of this chapter is to give an explicit, analytic description of monopole, quadrupole and scissors mode frequencies of a 2D deformed trapped quantum gas (Bose and Fermi) at zero temperature and to calculate the splitting between the quadrupole modes for an arbitrary deformation of the trap.

This chapter is organised as follows. In section [3.2] we model quasi-two dimensional trapped Bose system at zero temperature. Using the time-dependent variational method we calculate the monopole and quadrupole excitation frequencies of a two dimensional deformed trapped interacting Bose gas. In section [3.3], using the sum-rule approach we derive a general dispersion relation for the monopole and quadrupole excitation frequencies of a two-dimensional trapped quantum system interacting through Fermi pseudo-potential. This relation is valid for both Fermi and Bose statistics. We apply this general dispersion relation to calculate the same excitation frequencies of a trapped interacting Bose system. We show that the monopole and quadrupole excitation frequencies obtained from both methods are exactly the same. In section [3.4] we consider trapped unpolarized interacting fermions and apply the dispersion relation obtained from sum-rule approach to calculate the frequencies of monopole and quadrupole modes. In section [3.5] we present the summary and conclusions of our work.

3.2 Modeling quasi two-dimensional trapped interacting Bose gas

In BEC experiments, the trap potential can be approximated by an effective three-dimensional harmonic oscillator potential, with tunable trap frequencies ω_z in the axial (z) direction and ω_x, ω_y in the transverse ($x-y$) plane. The alkali-metal vapors used in experiment are very dilute and the interparticle interaction is well described by the short-range pseudopotential and the interaction strength is determined by s-wave scattering length a . Here we consider the case when the interparticle interaction is strongly repulsive. The Gross-Pitaevskii (GP) [14] energy functional of the trapped boson of mass m is given by,

$$E[\psi] = \int d^2r dz \left[\frac{\hbar^2}{2m} |\nabla \psi(\mathbf{r}, z)|^2 + \frac{m}{2} (\omega_x^2 x^2 + \omega_y^2 y^2 + \omega_z^2 z^2) |\psi(\mathbf{r}, z)|^2 + \frac{g}{2} \int d^2r' dz' \delta^2(\mathbf{r} - \mathbf{r}') \delta(z - z') |\psi(\mathbf{r}', z')|^2 |\psi(\mathbf{r}, z)|^2 \right], \quad (3.1)$$

where $g = \frac{4\pi a\hbar^2}{m}$ is the interaction strength determined by the s -wave scattering length a , \mathbf{r} is the position vector in $x - y$ plane and $\psi(\mathbf{r}, z)$ is the condensate wave function.

It has been shown by Baganato *et al.* [15] that for an ideal two-dimensional Bose gas under harmonic trap, a macroscopic occupation of the ground state can exist at temperature $T < T_c = \sqrt{\frac{N}{\zeta(2)}} \frac{\hbar\omega_0}{k_B}$. To achieve this quasi-two-dimensional system, the frequency in the frozen direction should be much larger than the frequency in the $x - y$ plane and the mean interactions between the particles. Alternatively, the trap frequencies are such that $\hbar\omega_z \gg \mu > \hbar\omega_0$ and $k_B T \ll \hbar\omega_z$, where μ is the chemical potential of the two-dimensional trapped Bose gas.

For a quasi-two-dimensional system we may assume that the wave function in the z direction is separable and is given by,

$$\psi(z) = \frac{1}{(\sqrt{\pi}a_z)^{1/2}} e^{-\frac{z^2}{2a_z^2}}, \quad (3.2)$$

where $a_z = \sqrt{\frac{\hbar}{m\omega_z}}$ is the oscillator length in the z -direction. Now we integrate out the z -component in the three dimensional GP energy functional, then we get the effective energy functional in two dimensions:

$$E - \frac{N\hbar\omega_z}{2} = \int d^2r \left[\frac{\hbar^2}{2m} |\nabla\psi(\mathbf{r})|^2 + \frac{m}{2} (\omega_x^2 x^2 + \omega_y^2 y^2) |\psi(\mathbf{r})|^2 + \frac{g_2}{2} \int d^2r' \delta^2(\mathbf{r} - \mathbf{r}') |\psi(\mathbf{r}')|^2 |\psi(\mathbf{r})|^2 \right], \quad (3.3)$$

where $g_2 = 2\sqrt{2\pi}\hbar\omega_z a_z a$ is the effective coupling strength in two dimensions, a is the s -wave scattering length in three dimensions and N is the total number of particles in the condensate. The same effective coupling constant is obtained in Ref.[8]. The effective interaction in two dimensions is given by

$$V_I = g_2 \delta^2(\mathbf{r} - \mathbf{r}'). \quad (3.4)$$

Recently, the two-dimensional Bose condensed state has been realized at MIT [13]. In this experimental set up, they have loaded the number of condensate sodium atoms between 3×10^4 and 2×10^6 in a trap with trap frequencies $\omega_z = 2\pi \times 790$ Hz, $\omega_x = 2\pi \times 30$ Hz and $\omega_y = 2\pi \times 10$ Hz. The scattering length for sodium atom is $a = 2.75$ nm. The chemical potential of a quasi-two-dimensional Bose condensed state is $\mu = \hbar\omega_0 \sqrt{\sqrt{2\pi} \frac{Na}{a_z}} = \mu \sim 0.19\hbar\omega_0 \sqrt{N}$, where $\omega_0 = 2\pi \times \sqrt{\omega_x \omega_y} \sim 2\pi \times 18$ Hz is the average trap frequency. It is clear that the chemical potential and the trap

potential energy satisfy the condition for quasi-two dimensional Bose state. To show the monopole and two quadrupole mode frequencies graphically we will use the above mentioned parameter which we have taken from the MIT experiment [13]

3.3 Collective excitation frequencies of a quasi-2D deformed trapped Bose gas

In two dimensions, the equation of motion of the condensate wave function is described by the following Gross-Pitaevskii equation:

$$i\hbar \frac{\partial \psi(\mathbf{r})}{\partial t} = \left[-\frac{\hbar^2}{2m} \nabla^2 + V(\mathbf{r}) + g_2 |\psi(\mathbf{r})|^2 \right] \psi(\mathbf{r}), \quad (3.5)$$

where $V(\mathbf{r}) = \frac{1}{2}m(\omega_x^2 x^2 + \omega_y^2 y^2)$ is the deformed trap potential in two dimensions. The normalization condition for ψ is $\int d^2r |\psi|^2 = N$. One can write down the Lagrangian density corresponding to this system as follows:

$$\mathcal{L} = \frac{i\hbar}{2} \left(\psi \frac{\partial \psi^*}{\partial t} - \psi^* \frac{\partial \psi}{\partial t} \right) + \left(\frac{\hbar^2}{2m} |\nabla \psi|^2 + V(\mathbf{r}) |\psi|^2 + \frac{g_2}{2} |\psi|^4 \right), \quad (3.6)$$

where asterisk denotes the complex conjugation. One can get the nonlinear Schroedinger equation (3.5) by minimizing the action related to the above Lagrangian density (3.6). In order to obtain the evolution of the condensate we assume the *most general Gaussian wave function*,

$$\psi(X, Y, t) = C(t) e^{-\frac{1}{2} [\alpha(t)X^2 + \beta(t)Y^2 + \gamma(t)XY]}, \quad (3.7)$$

where $C(t)$ is the normalization constant. X and Y are the dimensionless variables, $X = \frac{x}{a_0}$, $Y = \frac{y}{a_0}$, where $a_0 = \sqrt{\frac{\hbar}{m\omega_0}}$ is the oscillator length and $\omega_0 = \sqrt{\omega_x \omega_y}$ is the mean frequency. Further, $\alpha = \alpha_1 + i\alpha_2$, $\beta = \beta_1 + i\beta_2$ and $\gamma = \gamma_1 + i\gamma_2$ are the time-dependent dimensionless complex variational parameters. The α_1 and β_1 are inverse square of the condensate widths in x and y direction, respectively. The square of the normalization constant is $|C(t)|^2 = \frac{N\sqrt{D}}{\pi a_0^2}$, where $D = \alpha_1\beta_1 - \gamma_1^2$. The Gaussian ansatz (eq. (3.7)) for the order parameter can also be generalized to three dimensional anisotropic trapped Bose system to study various scissors modes.

The Gaussian variational ansatz becomes an exact ground state in the non interacting limit and in the presence of repulsive interaction it gives rise to spreading of the condensate wave function. To describe the quadrupoles and monopole oscillation, we consider the most general time-dependent quadratic exponent of the variational ansatz.

We obtain the effective Lagrangian L by substituting Eq. (3.7) into Eq. (3.6) and integrating the Lagrangian density over the space coordinates;

$$\frac{L}{N\hbar\omega_0} = \frac{1}{4D} \left[-(\beta_1\dot{\alpha}_2 + \alpha_1\dot{\beta}_2 - 2\gamma_1\dot{\gamma}_2) + (\alpha_1 + \beta_1)D + (\alpha_2^2 + \gamma_2^2)\beta_1 + (\beta_2^2 + \gamma_2^2)\alpha_1 - 2(\alpha_2 + \beta_2)\gamma_1\gamma_2 + \lambda\beta_1 + \frac{\alpha_1}{\lambda} + PD^{3/2} \right], \quad (3.8)$$

where λ is the asymmetric ratio, $\lambda = \frac{\omega_x}{\omega_y}$ and $P = \sqrt{\frac{2}{\pi}} 2N \frac{a}{a_z}$. In the MIT experiment [13] $\lambda = 3.0$. The equilibrium energy of the static condensate is given in terms of the equilibrium values of the inverse square width of the condensate along the x and y directions,

$$\frac{E}{N\hbar\omega_0} = \frac{1}{4} \left[(\alpha_{10} + \beta_{10}) + \left(\frac{\lambda}{\alpha_{10}} + \frac{1}{\lambda\beta_{10}} \right) + P\sqrt{\alpha_{10}\beta_{10}} \right]. \quad (3.9)$$

One can obtain the equilibrium value of the variational parameters, α_{10} and β_{10} by minimizing the energy with respect to the variational parameters

$$\alpha_{10}^2 = \lambda - \frac{P}{2}\alpha_{10}\sqrt{\alpha_{10}\beta_{10}}, \quad (3.10)$$

$$\beta_{10}^2 = \frac{1}{\lambda} - \frac{P}{2}\beta_{10}\sqrt{\beta_{10}\alpha_{10}}. \quad (3.11)$$

From the above two relations, we obtain

$$\eta^4 + \frac{P\eta^3}{2} - \frac{P\eta}{2\lambda^2} - \frac{1}{\lambda^2} = 0, \quad (3.12)$$

where η is the ratio of the condensate widths in the x and y direction, $\eta = \sqrt{\frac{\beta_{10}}{\alpha_{10}}}$. From Eq. (3.12) one can see how η changes with the number of atoms N and the coupling constant g_2 . The variation of η with the dimensionless effective interaction strength P is shown in figure 3.1.

The ratio between the widths of the condensate η varies from $\frac{1}{\sqrt{\lambda}}$ to $\frac{1}{\lambda}$, as the interaction strength increases from zero to large value (Thomas-Fermi limit). In the Thomas-Fermi limit, the equilibrium values of the parameters α_1 and β_1 are

$$\alpha_{10} = \lambda\sqrt{\frac{2}{P}}, \quad \beta_{10} = \frac{1}{\lambda}\sqrt{\frac{2}{P}}. \quad (3.13)$$

In this limit, the energy per particle is $\frac{E}{N} = \hbar\omega_0\sqrt{\frac{P}{2}}$. In the non-interacting limit, $\alpha_{10}^2 = \lambda$ and $\beta_{10}^2 = \frac{1}{\lambda}$. The energy per particle is $\frac{E}{N} = \frac{\hbar\omega_0}{2}(\sqrt{\lambda} + \sqrt{\frac{1}{\lambda}})$.

We are interested in the low-energy excitations of a Bose system. The low-energy excitations of the condensate correspond to the small oscillations of

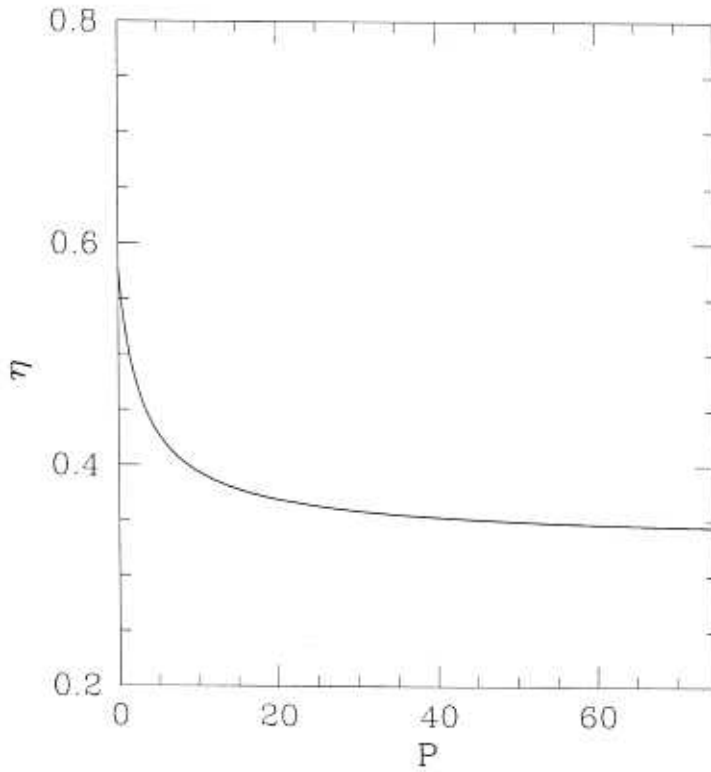


Figure 3.1: Ratio of the widths of the condensate η vs the dimensionless effective interaction strength P for $\lambda = 3.0$

the cloud around the equilibrium configuration. Therefore, we expand the time-dependent variational parameters around the equilibrium points in the following way: $\alpha_1 = \alpha_{10} + \delta\alpha_1$, $\beta_1 = \beta_{10} + \delta\beta_1$ and $\alpha_2 = \delta\alpha_2$, $\beta_2 = \delta\beta_2$, $\gamma_1 = \delta\gamma_1$, $\gamma_{10} = 0$ and $\gamma_2 = \delta\gamma_2$.

Using the Euler-Lagrange equation, the time evolution of the inverse square of the width around the equilibrium points are given by

$$\delta\ddot{\alpha}_1 + \lambda \frac{(8 + 3P\eta)}{(2 + P\eta)} \delta\alpha_1 + \frac{P\lambda\eta}{(2 + P\eta)} \delta\beta_1 = 0, \quad (3.14)$$

$$\delta\ddot{\beta}_1 + \frac{P}{\lambda(2\eta + P)} \delta\alpha_1 + \frac{(8\eta + 3P)}{\lambda(P + 2\eta)} \delta\beta_1 = 0, \quad (3.15)$$

$$\delta\ddot{\gamma}_1 + \left[\frac{4\lambda\eta^2}{(2 + P\eta)} + \left(\lambda + \frac{1}{\lambda} \right) \right] \delta\gamma_1 = 0. \quad (3.16)$$

From the above equations we can see that the modes corresponding to the fluctuations of the average of x^2 and y^2 are coupled, but the mode associated with the fluctuation of the average value of xy is decoupled. Eqs. (3.14) and (3.15) are

coupled equations of the modes α_1 and β_1 , where the mode xy is decoupled. This is due to the fact that the Hamiltonian is invariant under reflection, $x \rightarrow -x$ and $y \rightarrow y$ or $x \rightarrow x$ and $y \rightarrow -y$, and the modes which are odd or even under this parity operation separate out.

Now we look for time-dependent solutions of $e^{i\omega t}$ type, we obtain from Eqs. (3.14) and (3.15),

$$\frac{\omega_{\pm}^2}{\omega_0^2} = \frac{\lambda(8+3P\eta)}{2(2+P\eta)} + \frac{1}{2\lambda} \frac{(8\eta+3P)}{(2\eta+P)} \pm \sqrt{\left[\frac{\lambda(8+3P\eta)}{2(2+P\eta)} - \frac{(8\eta+3P)}{2\lambda(2\eta+P)} \right]^2 + \left(\frac{P\lambda\eta^2}{2+P\eta} \right)^2}. \quad (3.17)$$

For an isotropic trap,

$$\omega_+ = 2\omega_0, \quad (3.18)$$

$$\omega_- = \omega_0 \sqrt{\frac{(8+2P)}{(2+P)}}. \quad (3.19)$$

For large N limit, $\omega_- = \sqrt{2}\omega_0$. So ω_+ and ω_- may be identified as the monopole mode frequency and quadrupole mode frequency respectively. The monopole mode is coupled with the quadrupole mode in an anisotropic trap. However, the monopole mode frequency in an isotropic trap is independent of the interaction strength of the two-body potential and the number of particles in the condensate state. This is due to the underlying $SO(2,1)$ symmetry in the Hamiltonian [9], [10].

From Eq.(3.16) we obtain,

$$\frac{\omega_s^2}{\omega_0^2} = \frac{4\lambda\eta^2}{(2+P\eta)} + \left(\lambda + \frac{1}{\lambda} \right). \quad (3.20)$$

In an isotropic trap, $\omega_s = \omega_-$ and the quadrupole and scissors modes are degenerate states. In the non-interacting limit, $\omega_s = \omega_x + \omega_y$. In the Thomas-Fermi limit, Eq. (3.20) reduces to $\omega_s = \sqrt{\omega_x^2 + \omega_y^2}$. In an isotropic trap this mode corresponds to the quadrupole excitation. This excitation is also known as scissors mode [16], and this oscillation has been observed experimentally [17].

3.4 Sum-rules and collective excitations

In this section, we study the quadrupole excitations of a two dimensional deformed trapped quantum gas at zero temperature within the sum rule approach. In the collisionless regime the collective excitation frequencies of a confined gas are well described by the sum-rule method. The collective excitation of any system is usually probed by applying external fields. Given an excitation operator F , many

useful quantities of the excited system can be calculated from the so-called strength function [18],

$$S_{\pm}(E) = \sum_n |\langle n|F_{\pm}|0\rangle|^2 \delta(E - E_n), \quad (3.21)$$

where E_n and $|n\rangle$ are the excitation energy and the excited state respectively, and $F_+ = F$, $F_- = F^\dagger$. Various energy weighted sum rules are derived from the moments of the strength distribution function,

$$m_k^{\pm} = \frac{1}{2} \int E^k (S_+(E) \pm S_-(E)) dE. \quad (3.22)$$

It is easy to see that, for a given k , the moments may be expressed in terms of the commutators of the excitation operator F with the many body Hamiltonian H . We give below some of the useful energy weighted sum rules,

$$m_0^- = \frac{1}{2} \langle 0 | [F^\dagger, F] | 0 \rangle, \quad (3.23)$$

$$m_1^+ = \frac{1}{2} \langle 0 | [F^\dagger, [H, F]] | 0 \rangle, \quad (3.24)$$

$$m_2^- = \frac{1}{2} \langle 0 | [J^\dagger, J] | 0 \rangle, \quad (3.25)$$

$$m_3^+ = \frac{1}{2} \langle 0 | [[F^\dagger, H], [H, [H, F]]] | 0 \rangle, \quad J = [H, F], \quad (3.26)$$

where $[,]$ denotes the commutator between corresponding operators. Near the collective excitation frequency the strength distribution becomes sharply peaked, and the collective excitation energy is described by the moments of the strength distribution,

$$\hbar\omega = \sqrt{\frac{m_3^+}{m_1^+}}. \quad (3.27)$$

Following Ref.[19], one can derive the above form of collective excitation energy by using the variational principle. Given the many body ground state it is possible to find out the collective excitation energy and the excited state, if one is able to find an operator O^\dagger , which satisfies the following equation of motion :

$$[\hat{H}, O^\dagger] = \hbar\omega_c O^\dagger. \quad (3.28)$$

The excitation energy is then given by the following expression,

$$\hbar\omega_c = \frac{\langle 0 | [O, [\hat{H}, O^\dagger]] | 0 \rangle}{\langle 0 | O, O^\dagger | 0 \rangle}. \quad (3.29)$$

We may now take the variational ansatz for O^\dagger as, $O^\dagger = F + bJ$ with the variational parameter b . By minimizing the energy with respect to the variational parameter, we obtain the collective excitation energy as $E_c = \sqrt{\frac{m_3^+}{m_1^+}}$, which is same as eq.(3.27).

Similarly, we construct the most general excitation operator $F = x^2 + by^2$ when monopole and quadrupole modes are coupled. b is a variational parameter. In a symmetric trap potential, if $b = 1$, F is monopole mode and if $b = -1$, F is the quadrupole mode. In the same way we can calculate the lowest energy excitation in this particular sector of excitations variationally. The lowest energy mode turns out to be the quadrupole mode.

Calculating the moments m_1 and m_3 by taking the excitation operator with the Hamiltonian, we obtain,

$$E_{\text{coll}}^2 = \frac{4\hbar^2}{m} \frac{E_x}{\langle x^2 \rangle} \frac{(1 + Ab^2 + Bb)}{(1 + Cb^2)}, \quad (3.30)$$

where $A = \frac{E_y}{E_x}$, $B = \frac{E_{\text{int}}}{2E_x}$, $C = \frac{\langle y^2 \rangle}{\langle x^2 \rangle}$ and $E_x = \langle T_x \rangle + \langle V_x \rangle + \frac{1}{4}\langle E_{\text{int}} \rangle$, $E_y = \langle T_y \rangle + \langle V_y \rangle + \frac{1}{4}\langle E_{\text{int}} \rangle$. Here $\langle \rangle$ denotes the expectation value of the corresponding operators in the ground state and T_x , V_x and T_y , V_y represents the kinetic energy and potential energy along x and y coordinates respectively. The interaction energy is given by $E_{\text{int}} = \frac{g_2}{2} \int |\psi|^4 d^2r$. Now we minimize this collective energy with respect to the variational parameter β . The value of β for which the collective energy is minimum, is given by

$$b_0 = \frac{-2(C - A) \pm \sqrt{4(C - A)^2 + 4B^2C}}{2BC}. \quad (3.31)$$

It can be easily shown that for an isotropic trap, $b_0 = \pm 1$. So we have identified that the monopole mode can be excited by the operator $F = x^2 + b_0 y^2$ and quadrupole mode can be generated by $F = x^2 - b_0 y^2$. Inserting b_0 into Eq. (3.30), we obtain the following collective oscillation frequencies:

$$\omega_{\pm}^2 = \frac{2}{m} \left[\left(\frac{E_y}{\langle y^2 \rangle} + \frac{E_x}{\langle x^2 \rangle} \right) \pm \sqrt{\left(\frac{E_y}{\langle y^2 \rangle} - \frac{E_x}{\langle x^2 \rangle} \right)^2 + \frac{E_{\text{int}}^2}{4\langle x^2 \rangle \langle y^2 \rangle}} \right]. \quad (3.32)$$

Using the variational wave function of the ground state in deformed trap, one can easily obtain the excitation frequencies. The lowest energy excitation frequency in this sector is

$$\frac{\omega_-^2}{\omega_0^2} = \frac{\lambda(8 + 3P\eta)}{2(2 + P\eta)} + \frac{1}{2\lambda} \frac{(8\eta + 3P)}{(2\eta + P)} - \sqrt{\left[\frac{\lambda(8 + 3P\eta)}{2(2 + P\eta)} - \frac{(8\eta + 3P)}{2\lambda(2\eta + P)} \right]^2 + \left(\frac{P\lambda\eta^2}{2 + P\eta} \right)^2}. \quad (3.33)$$

It can be identified as quadrupole mode since in an isotropic trap, its excitation frequency exactly matches with the quadrupole mode frequency. The above expression for the excitation frequency Eq. (3.33) is exactly same as the mode frequency ω_- in Eq. (3.17).

The higher energy excitation exactly matches within the monopole mode, although it is not the local minimum of the energy, Eq. (3.30). The dispersion relation for this monopole mode frequency is:

$$\frac{\omega_+^2}{\omega_0^2} = \frac{\lambda(8+3P\eta)}{2(2+P\eta)} + \frac{1}{2\lambda} \frac{(8\eta+3P)}{(2\eta+P)} + \sqrt{\left[\frac{\lambda(8+3P\eta)}{2(2+P\eta)} - \frac{(8\eta+3P)}{2\lambda(2\eta+P)} \right]^2 + \left(\frac{P\lambda\eta^2}{2+P\eta} \right)^2} \quad (3.34)$$

Monopole, quadrupole and scissors modes vs P are shown in figure 3.2 for $\lambda = 3$.

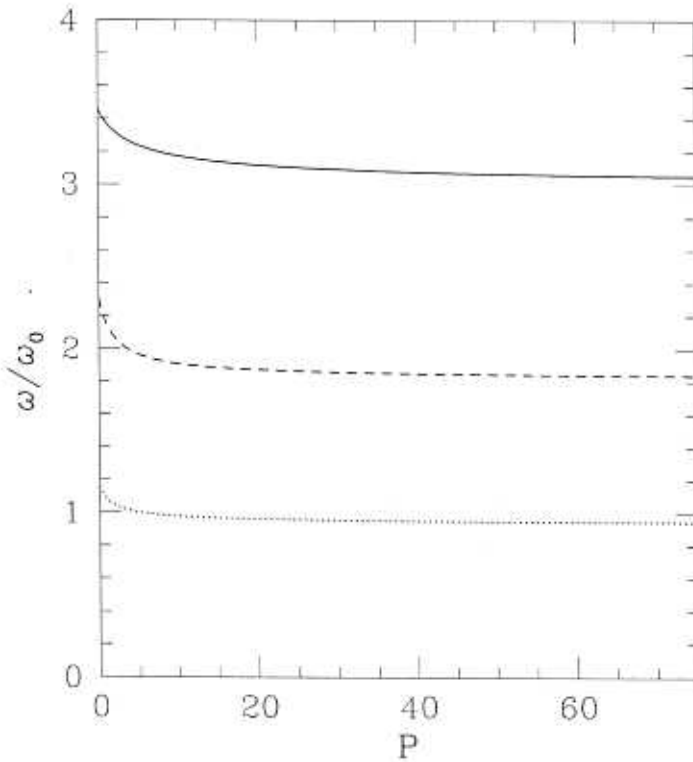


Figure 3.2: Monopole (solid line), quadrupole (dotted line) and scissors (dashed line) mode frequencies of an interacting Bose gas vs dimensionless effective strength P for $\lambda = 3.0$

For another quadrupole mode, the excitation operator is $F = xy$. Using

the commutation relation, we obtain,

$$m_1 = \frac{\hbar^2}{2m} \langle (x^2 + y^2) \rangle, \quad (3.35)$$

$$m_3 = m_3(T) + m_3(V) + m_3(ee), \quad (3.36)$$

where,

$$m_3(T) = \frac{\hbar^4}{m^3} \langle (p_x^2 + p_y^2) \rangle, \quad (3.37)$$

$$m_3(V) = \frac{\hbar^4}{2m} (\omega_x^2 + \omega_y^2) \langle (x^2 + y^2) \rangle, \quad (3.38)$$

$$m_3(ee) = \frac{g_2 \hbar^4}{2m^2} \left[\int d^2r \rho(r) \left(y \frac{\partial}{\partial x} + x \frac{\partial}{\partial y} \right)^2 \rho(r) + \int d^2r \left(x \frac{\partial \rho}{\partial y} + y \frac{\partial \rho}{\partial x} \right)^2 \right]. \quad (3.39)$$

Using the variational wave function, we can obtain all these moments. In this case $m_3(ee)$ exactly vanishes. So the frequency for the quadrupole mode is

$$\frac{\omega_s^2}{\omega_0^2} = \frac{4\lambda\eta^2}{(2 + P\eta)} + \left(\lambda + \frac{1}{\lambda} \right). \quad (3.40)$$

This expression for the quadrupole mode frequency is also the same as Eq.(3.20). So ω_- in Eq. (3.33) and ω_s in Eq.(3.40) shows the splitting occurs between two quadrupole modes in a two dimensional deformed trapped Bose gas and the dependence of the splitting on the interaction strength and trap anisotropy can be analyzed from the analytical expressions. For an isotropic trap, the two quadrupole modes are degenerate. The variation of the splitting between two quadrupole modes $\Delta_s = \omega_s - \omega_-$, of a trapped interacting Bose gas, with the dimensionless interaction parameter P is shown in figure 3.3.

We have checked that the sum-rule method gives correct results for the excitation frequencies of the two quadrupole modes for a system of interacting bosons in an anisotropic trap. Now we apply this method to calculate the excitation energies of the quadrupole modes of a system of interacting fermions in a deformed trap.

3.5 Collective excitation frequencies of a quasi-2D deformed trapped Fermi gas

After the discovery of BEC in alkali atomic gas, the behaviour of trapped Fermi gas is also in focus. It is also possible to trap the fermionic atoms at very low temperature, where the quantum effects can be observed. There has been experimental progress towards cooling a Fermi gas into the degenerate regime ($T < T_F$) [20]. Several

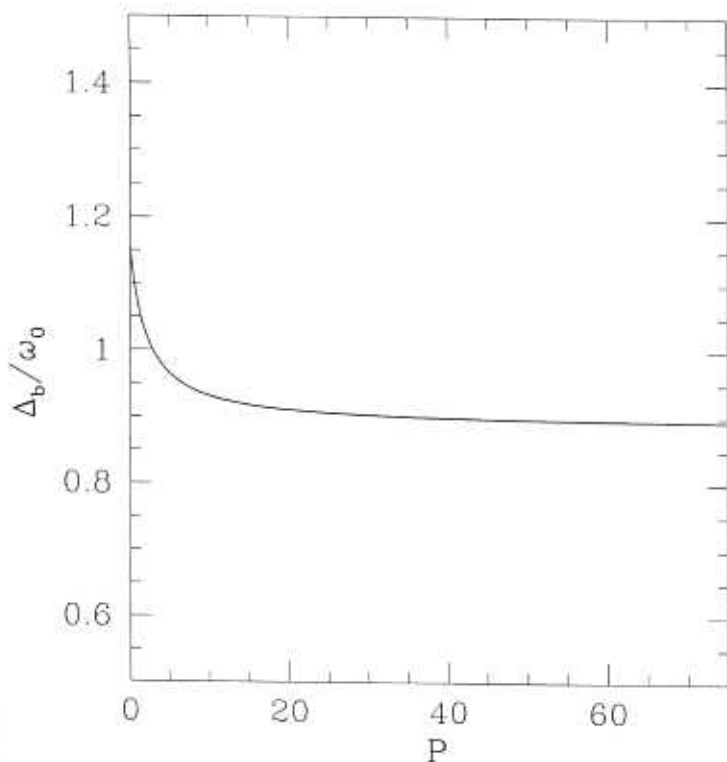


Figure 3.3: Difference between the two quadrupole modes of an interacting Bose gas Δ_b/ω_0 vs the dimensionless effective strength P for $\lambda = 3.0$

authors have studied the thermodynamic properties [21, 22], collective excitation frequencies in the normal phase [23, 24, 25] as well as in the superfluid phase [26, 27] of a three dimensional trapped Fermi gas.

In the previous section we derived the general form of the monopole and quadrupole mode frequencies of a two-dimensional quantum gas with the short-range interaction potential between the particles by using the sum-rule approach. In this chapter we apply those general form of the excitation frequencies and discuss the collective oscillation of a two dimensional deformed trapped unpolarized Fermi gas at zero temperature within the sum-rule approach. Using this approach, the collective excitations have been studied in other finite fermionic systems like atomic nuclei, metal clusters [28] and quantum dots [29]. This sum-rule method allows us to calculate the monopole mode and the quadrupole modes of a Fermi system in a deformed trap where the equation of motion technique does not hold. These modes can be observed in nano structures like quantum dots. When the two-body interaction is long-ranged, the sum-rule method can be generalised.

We consider a two dimensional deformed trapped unpolarized fermionic atoms at very low temperature. The two-body interaction of the dilute gas can be described by the short-range pseudopotential $V(\mathbf{r} - \mathbf{r}') = g_2 \delta^2(\mathbf{r} - \mathbf{r}')$, where g_2 is the coupling constant and its form is given in the section [3.2]. The Hamiltonian of the trapped fermionic atoms is given by,

$$H = \sum_i \left(\frac{p_i^2}{2m} + V_{\text{ext}}(\mathbf{r}_i) \right) + g_2 \sum_{i < j} \delta^2(\mathbf{r}_i - \mathbf{r}_j), \quad (3.41)$$

where the confining potential is

$$V_{\text{ext}}(\mathbf{r}) = \frac{1}{2} m \omega_0^2 \left(\lambda x^2 + \frac{y^2}{\lambda} \right). \quad (3.42)$$

The Thomas-Fermi energy functional of this trapped interacting Fermi system is given by,

$$E[\rho(r)] = \int d^2r \left[\frac{\hbar^2 \pi}{2m} \rho^2(r) + V_{\text{ext}} \rho(r) + \frac{\tilde{g}_2}{2} \rho^2(r) \right], \quad (3.43)$$

where $\tilde{g}_2 = g_2/2$. Here we assume the density of two spin components are same, $\rho_\uparrow = \rho_\downarrow$. The interaction energy density $g_2 \rho_\uparrow \rho_\downarrow$, can be written as $\frac{g_2}{4} \rho^2$, where ρ is the total density. By minimizing the energy functional with respect to the density, we obtain

$$\rho(r) = \frac{R_F^2}{2K_0 \pi a_0^4} \left[1 - \frac{r^2}{R_F^2} \right], r \leq R_F, \quad (3.44)$$

where $R_F = (4NK_0)^{1/4} a_0$ is the radius of the atomic gas which is determined from the condition $\int d^2r \rho(r) = N$ and $K_0 = 1 + \frac{g_2 m}{\pi \hbar^2} = 1 + \sqrt{\frac{2}{\pi}} \frac{a}{a_s}$ is a dimensionless constant. At very low temperature, collisions are suppressed due to Fermi statistics and system is in the collisionless regime. We study the collective excitation frequencies in this regime by sum-rule approach.

In Sec.III we have derived the expressions for quadrupole excitation frequencies within sum-rule approach. We can use expression Eq.(3.32), to calculate one of the quadrupole mode frequencies for Fermi gas also.

We evaluate all the expectation values of the corresponding operators by using the Thomas-Fermi density (3.44),

$$\frac{E_x}{\langle x^2 \rangle} \pm \frac{E_y}{\langle y^2 \rangle} = \frac{m \omega_0^2}{2} \frac{(3K_0 + 1)}{2K_0} \left(\lambda \pm \frac{1}{\lambda} \right). \quad (3.45)$$

Using Eqs. (3.32) and (3.45), we obtain,

$$\frac{\omega_{\pm}^2}{\omega_0^2} = \frac{(3K_0 + 1)}{2K_0} \left(\lambda + \frac{1}{\lambda} \right) \pm \sqrt{\left[\frac{(3K_0 + 1)}{2K_0} \left(\lambda - \frac{1}{\lambda} \right) \right]^2 + \left(1 - \frac{1}{K_0} \right)^2}. \quad (3.46)$$

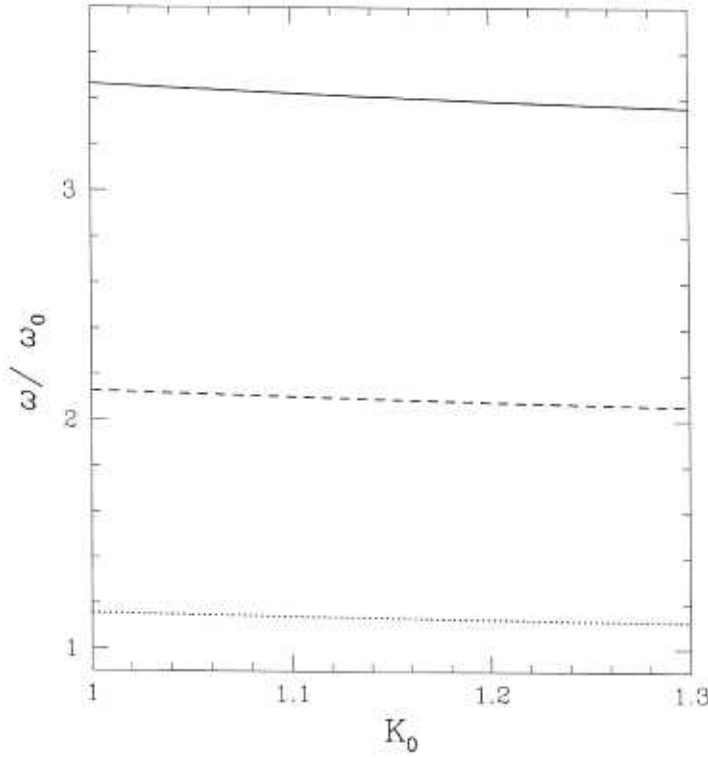


Figure 3.4: Monopole (solid line), quadrupole (dotted line) and scissors (dashed line) mode frequencies of an interacting unpolarized Fermi gas vs the dimensionless parameter K_0 for $\lambda = 3.0$

For an isotropic trap, the monopole mode frequency becomes $\omega_+ = 2\omega_0$.

There is another quadrupole mode for which the excitation operator is $F = xy$. Using the density for the trapped interacting Fermi gas at $T = 0$, we get the following moments:

$$m_1 = \frac{\hbar^3 R_F^6}{48m^2 a_0^6 \omega_0 K_0} \left(\lambda + \frac{1}{\lambda} \right), \quad (3.47)$$

$$m_3 = \frac{\hbar^5 \omega_0 R_F^6}{12K_0 m^2 a_0^6} \left[\frac{1}{K_0} + \frac{(\lambda + \frac{1}{\lambda})^2}{4} \right]. \quad (3.48)$$

In this case also, $m_3(ee)$ exactly vanishes. The quadrupole oscillation frequency is given by,

$$\frac{\omega_s}{\omega_0} = \sqrt{\left[\left(\lambda + \frac{1}{\lambda} \right) + \frac{4}{K_0 \left(\lambda + \frac{1}{\lambda} \right)} \right]}. \quad (3.49)$$

The monopole, quadrupole and scissors mode frequencies of an unpolarized trapped interacting Fermi gases vs the K_0 is shown in figure 3.4.

For an isotropic trap, ω_- in Eq. (3.46) and Eq. (3.49) becomes

$$\omega_- = \omega_s = \sqrt{2}\omega_0 \sqrt{\frac{(1 + K_0)}{K_0}}. \quad (3.50)$$

In Eq.(3.46) and Eq.(3.49), ω_- exhibits the splitting of the quadrupole modes of a two dimensional deformed trapped Fermi gas. The scissors mode is also discussed in Ref. [26] for superfluid Fermi gas.

The monopole mode frequency of an isotropic trapped interacting Fermi system is $2\omega_0$, which is independent of the interaction strength of the two-body potential and the number of particles. This is because of the presence of $SO(2, 1)$ symmetry in the Hamiltonian (Eq.(3.41)) as discussed in the previous section.

The splitting between two quadrupole modes, $\Delta_f = \omega_s - \omega_-$, of a deformed trapped interacting Fermi gas is shown in figure 3.5. The frequencies of these two modes and the splitting between them are independent of the particle number for two dimensional fermions within Thomas-Fermi approximation. This splitting decreases almost linearly with increasing interaction strength.

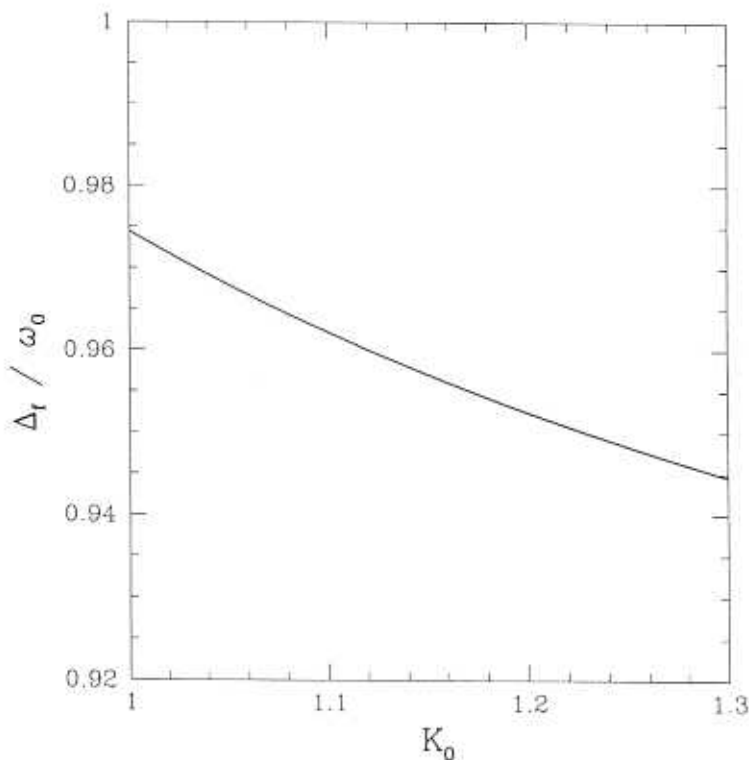


Figure 3.5: Difference between the two quadrupole modes of an interacting unpolarized Fermi gas Δ_f/ω_0 vs the dimensionless parameter K_0 for $\lambda = 3.0$.

3.6 Summary and conclusions

In this chapter, we have mainly considered monopole mode and two non-degenerate quadrupole modes of a quantum gas in an anisotropic harmonic oscillator potential. We investigated the effect of interaction on the monopole mode, the two quadrupole modes and the splitting between these quadrupole modes for an arbitrary trap deformation.

First, we have calculated a few low-lying collective excitation frequencies of a two dimensional trapped Bose gas in an anisotropic trap, by using time-dependent variational method with the *most general Gaussian ansatz* for the order parameter. We found that one quadrupole mode is coupled with the monopole mode in presence of the trap deformation. Another quadrupole mode associated with the fluctuation of the average value of xy (which is also known as scissors mode) is decoupled.

Using the energy weighted sum-rule approach we derived the general dispersion relation of the monopole mode and two quadrupole excitations. Using the same variational wave function for bosons we checked that the collective frequencies obtained from the sum-rule approach are exactly the same as those obtained from the variational method. The main advantage of the sum-rule method is that it can be applied to both trapped bosons and fermions to calculate the excitation frequencies in the collisionless regime. This method can be applied for any number of confined particles and also it can be generalised for long-range interactions. This energy weighted sum-rule method can be extended for Coulomb interaction to study the quadrupole excitations in a deformed electronic nanostructure like an elliptic quantum dots. The splitting between the quadrupole modes obtained from this method is non-perturbative in the trap anisotropy parameter.

We considered a system of two dimensional spin unpolarised interacting fermions in an anisotropic harmonic oscillator potential within Thomas-Fermi approximation. Applying the sum-rule technique to this deformed Fermi gas, we obtained the monopole, quadrupole and scissors excitation frequencies and the splitting between the quadrupole and scissors modes analytically. For both statistics, the amount of splitting between the quadrupole and scissors modes decreases with increasing interaction strength. For a two dimensional Fermi system the frequencies and the splitting are independent of the particle number within the Thomas-Fermi approach.

For an isotropic trap, the monopole mode frequency of a Bose gas as well as Fermi gas is $2\omega_0$. This monopole mode frequency is independent of the strength

of the two-body interaction potential and the number of particles. This is due to the underlying $SO(2, 1)$ symmetry in the Hamiltonian.

Recent experimental progress at MIT [13] on quasi two dimensional Bose condensed state shows the possibilities of verification of our results. The above mentioned quadrupole modes are excited in the two dimensional plane and for simplicity we consider only the two dimensional trapped quantum gas. This method and the *most general Gaussian ansatz* for the order parameter can also be extended to three dimensional anisotropic systems to study the various quadrupole modes. The splitting in these two quadrupole modes may be used to find trap anisotropy. It will be interesting to study the splitting between the quadrupole modes of an anisotropic quantum system in presence of terms having definite chirality, like magnetic field or rotation.

Bibliography

- [1] S. Stringari, *Phy. Rev. Lett.* **77**, 2360 (1996).
- [2] Victor M. Perez-Garcia, H. Michinel, J. I. Cirac, M. Lewenstein, and P. Zoller, *Phys. Rev. Lett.* **77**, 5320 (1996).
- [3] Y. Castin and R. Dum, *Phys. Rev. Lett.* **77**, 5315 (1996).
- [4] Y. Kagan, E. L. Surokov and G. Shlyapnikov, *Phys. Rev. A* **54**, R1753 (1996).
- [5] Pippa Storey and M. Olshanii, *Phys. Rev. A* **62**, 033604 (2000).
- [6] D. S. Jin, J. R. Ensher, M. R. Matthews, C. E. Wiemann, and E. A. Cornell, *Phys. Rev. Lett.* **77**, 420 (1996);
M. O. Mewes, M. R. Andrews, N. J. van Druten, D. M. Kurn, D. S. Drfee, C. G. Townsend, and W. Ketterle. *Phys. Rev. Lett.* **77**, 988 (1996).
- [7] T. Haugset and H. Haugerud, *Phys. Rev. A* **57**, 3809 (1998);
Sadhan K. Adhikari, *Phys. Rev. E* **62**, 2937 (2000);
Tarun K. Ghosh. *Phys. Rev. A* **63**, 013603 (2001).
- [8] Tin-Lun Ho and Michael Ma, *J. Low Temp. Phys.* **115**, 61 (1999).
- [9] L. P. Pitaevskii and A. Rosch, *Phys. Rev. A* **55**, R853, (1997);
Pijush K. Ghosh, *Phys. Rev. A* **65**, 012103 (2002).
- [10] Tarun K. Ghosh, *Phys. Lett. A* **285**, 222 (2001).
- [11] Pijush K. Ghosh, cond-mat/0109073.
- [12] Tin-Lin Ho, C. V. Ciobanu. *Phys. Rev. Lett.* **85**, 4648 (2000);
S. Ghosh, M. V. N. Murthy and S. Sinha. *Phys. Rev. A* **64**, 053603 (2001).
- [13] A. Gorlitz *et al.*, *Phys. Rev. Lett.* **87**, 130402 (2001).

- [14] E. P. Gross, *Nuovo Cimento A* **20**, 454 (1961);
L. P. Pitaevskii, *Pis'ma Zh. Eksp. Teor. Fiz.* **77**, 988 (1961) [*Sov. Phys. JETP* **13**, 451 (1961)].
- [15] V. Baganato and D. Kleppner, *Phys. Rev. A* **44**, 7439 (1991).
- [16] D. Guery-Odelin and S. Stringari, *Phys. Rev. Lett.* **83**, 4452 (1999).
- [17] O. M. Marago, S. A. Hopkins, J. Arlt, E. Hodby, G. Hechenblaikner and C. J. Foot, *Phys. Rev. Lett.* **84**, 2056 (2000).
- [18] O. Bohigas, A. M. Lane, J. Martorell, *Phys. Rep.* **51**, 267 (1979);
E. Lipparini and S. Stringari, *Phys. Rep.* **175**, 102 (1989).
- [19] E. Lipparini, N. Barberan, M. Barranco, M. Pi, and L. Serra, *Phys. Rev. B* **56**, 12375 (1997).
- [20] B. DeMacro and D. S. Jin, *Science* **285**, 1703 (1999);
M. O. Mewes, G. Ferrari, F. Schreck, A. Sinatra and C. Salomon, *Phys. Rev. A* **61**, 011403(R) (2000).
- [21] D. A. Butts and D. S. Rokhsar, *Phys. Rev. A* **55**, 4346 (1997).
- [22] L. Salasnich, B. Pozz, A. Parola and L. Reatto, *J. Phys. B* **33**, 3943 (2000).
- [23] M. Amoruso, I. Meccoli, A. Minguzzi and M. P. Tosi, *Eur. Phys. J. D* **7**, 441 (1999).
- [24] L. Vichi and S. Stringari, *Phys. Rev. A* **60**, 4734 (1999).
- [25] Georg M. Brunn and Charles W. Clark, *Phys. Rev. Lett.* **83**, 5415 (2000).
- [26] A. Minguzzi and M. P. Tosi, *Phys. Rev. A* **63**, 023609 (2001).
- [27] M. A. Baranov and D. S. Petrov, *Phys. Rev. A* **62**, 041601 (2000).
- [28] W. de Heer, *Rev. Mod. Phys.* **65**, 611 (1993);
M. Brack, *Rev. Mod. Phys.* **65**, 677 (1993).
- [29] S. Sinha, *Physica E* **8**, 24 (2000).

Chapter 4

Universality of monopole mode frequency and dynamics of width of a class of an interacting Bose gas

4.1 Introduction

It is known that the excitation frequencies of an ideal Bose gas under the harmonic trap potential are simply multiples of the trap frequencies. However, for an interacting system, deviations from these frequencies are expected due to the effect of the interaction. Similarly, the dynamics of a trapped ideal Bose system can be solved exactly and described by the Hill's equation. But, for an interacting system, it is expected that the dynamics of the system can not be described by the Hill's equation. Interestingly, for an interaction potential with particular scaling property the monopole mode frequency does not depend on the interaction strength and the dynamics of the system can be solved exactly which is explained by the same Hill's equation. In the previous chapter we have already seen that the monopole mode frequency of the two-dimensional (2D) isotropic harmonic trapped interacting Bose gas is independent of the two-body interaction strength. This peculiar nature of the monopole mode frequency of a 2D trapped interacting Bose gas have been found in Refs. [1, 2, 3]. This peculiar behavior of monopole mode frequency depends on the scaling property of the interaction potential. Without trap potential, the 2D Gross-Pitaevskii (GP) equation is scale invariant. Introduction of harmonic potential breaks the scale invariance. Pitaevskii and Rosch [1] have pointed out that due

to the special property of the harmonic potential, $SO(2,1)$ symmetry still exists. They have shown the universal nature of the monopole mode frequency only for 2D GP equation by constructing the generators of the $SO(2,1)$ symmetry [1].

The main purpose of this chapter is to show the presence of the universal nature of the monopole mode frequency and also the universal nature of the dynamics of the width for a class of an interacting Bose system. In this chapter we obtain a condition for having the universality of the monopole mode frequency and the dynamics of width of a class of GP equation describing the trapped interacting Bose system, at varying spatial dimensionality, order of the nonlinearity and the scaling exponent of the interaction potential. Interestingly, the dynamics of the width of a class of GP equation can be described by the same Hill's equation if the Bose system satisfy that particular combination or shows the universal monopole mode frequency.

This chapter is organised as follows. In section [4.2], using the time-dependent variational analysis we show that for a particular combination of n , k and d the generalised GP equation describing the d -dimensional harmonic trapped Bose gas exhibits the universal monopole oscillation frequency $2\omega_0$. We also derive the time-evolution of the width of the d -dimensional trapped Bose system which satisfies that particular combination which can be described universally by the same Hill's equation. We also discuss the condition for exact self-similar solutions of the GP equation. In section [4.3] we give three examples which show the universal nature of the monopole mode frequency and the dynamics of the width. Two examples are in the context of current Bose-Einstein condensate (BEC) experiment. In section [4.4] we present the summary and conclusions of our work.

4.2 Universality of certain observables of a class of trapped interacting Bose gas

To show the universality of the monopole mode frequency and the dynamics of the width of a class of GP equation (also known as nonlinear Schrödinger equation (NLSE)), we use the time-dependent variational method. This variational method has been extensively and successfully used to explain many properties in BEC and other nonlinear systems. Using this method, Garcia *et al.* [4] derived a general dispersion relation for the low-energy excitations of a three dimensional deformed trapped Bose gas which exactly coincides with the results obtained by Stringari [5] for a large number of particles.

Consider a system of Bose particles in d -dimensional ($d \leq 3$) harmonic trapped potential $V_t(\mathbf{r}) = \frac{1}{2}M\omega_0^2 r^2$ at zero temperature and interacting with a translationally invariant interaction potential $V_I = g_d V(\mathbf{r} - \mathbf{r}')$, where $r^2 = \sum_{i=1}^d x_i^2$ and g_d is the coupling constant in d dimension. M is the atomic mass and \mathbf{r} is a d -dimensional vector. Under the scale transformation, $\mathbf{r} \rightarrow \lambda \mathbf{r}$, we assume $V_I(\lambda \mathbf{r}) = \lambda^n V_I(\mathbf{r})$, where n is the scaling exponent of the interaction potential.

We are considering a generalized d -dimensional GP equation [6] describing a d -dimensional harmonic trapped weakly interacting Bose gas with a nonlinearity of order $(2k+1)$ and scaling exponent n of an arbitrary interaction potential $V_I = g_d V(\mathbf{r} - \mathbf{r}')$ is

$$i\hbar \frac{\partial \psi(\mathbf{r})}{\partial t} = \left[-\frac{\hbar^2}{2M} \nabla^2 + V_t(r) + g_d \int d^m r' \psi^*(\mathbf{r}') V(\mathbf{r} - \mathbf{r}') \psi(\mathbf{r}') |\psi(\mathbf{r})|^{2(k-1)} \right] \psi(\mathbf{r}), \quad (4.1)$$

where ∇^2 is the d -dimensional Laplacian operator and asterisk denotes the complex conjugation. The generalised d -dimensional energy functional is

$$E[\psi] = \int d^d r \left[\frac{\hbar^2}{2M} |\nabla \psi(\mathbf{r})|^2 + \frac{M\omega_0^2 r^2}{2} |\psi(\mathbf{r})|^2 + \frac{g_d}{k+1} \int d^m r' \psi^*(\mathbf{r}) \psi^*(\mathbf{r}') V(\mathbf{r} - \mathbf{r}') \psi(\mathbf{r}') |\psi(\mathbf{r})|^{2(k-1)} \psi(\mathbf{r}) \right]. \quad (4.2)$$

If $m = d =$ arbitrary dimension and $V(\mathbf{r} - \mathbf{r}')$ is a d -dimensional delta function potential, the above equation gives the nonlinear term of order $(2k+2)$. If $k = 1$ and $m = d \geq 1$, Eq. (4.1) becomes *ordinary* GP equation and if $k = 2$ and $m = d = 1$, Eq. (4.1) gives the 1D *modified* GP equation in which the $|\psi|^6$ interaction term is present [7, 8, 9].

One can write down the generalised Lagrangian density corresponding to this system which is

$$L = \frac{i\hbar}{2} \left(\psi \frac{\partial \psi^*}{\partial t} - \psi^* \frac{\partial \psi}{\partial t} \right) + \left[\frac{\hbar^2}{2M} |\nabla \psi|^2 + V_t(r) |\psi(\mathbf{r})|^2 + \frac{g_d}{(k+1)} \int d^m r' \psi^*(\mathbf{r}) \psi^*(\mathbf{r}') V(\mathbf{r} - \mathbf{r}') \psi(\mathbf{r}') |\psi(\mathbf{r})|^{2(k-1)} \psi(\mathbf{r}) \right]. \quad (4.3)$$

Without the interaction potential, Eq. (4.1) reduces to the linear Schrödinger equation which has the Gaussian wave function for the ground state. In order to get the evolution of the square of the radius, we assume the following Gaussian wave

function:

$$\psi(r) = C(t)e^{-\frac{r^2}{2\alpha(t)}[1 + i\beta(t)]}, \quad (4.4)$$

where $C(t)$ is the normalization constant which can be determined by the normalization condition $\int |\psi|^2 d^d r = N$ and $a_0 = \sqrt{\frac{\hbar}{M\omega_0}}$ is the oscillator length. N is the total number of particles in the system. $\alpha(t)$ and $\beta(t)$ are the time-dependent dimensionless variational parameters. $\alpha(t)$ is the square of the radius of the system. In order to describe the dynamics of the variational parameter $\alpha(t)$, the phase factor $i\beta(t)r^2$ is required [4]. Note that the same kind of phase factor is also present in Eq. (4) of Ref. [3] to get the dynamics of the width of a system. We obtain the effective Lagrangian $L_{\text{eff}}(\alpha, \beta)$ by substituting Eq. (4.4) into Eq. (4.3) and integrating the Lagrangian density over the space coordinates

$$L_{\text{eff}} = \frac{N\hbar\omega_0}{4} \left[-\alpha\dot{\beta}d + \frac{d}{\alpha} + \alpha d(1 + \beta^2) + G_d \alpha^{\frac{(n+m-kd)}{2}} \right], \quad (4.5)$$

where

$$G_d = \left(\frac{g_d N^k a_0^{(n+m-kd)}}{(k+1)\hbar\omega_0} \right) \left(\frac{2^{\frac{(d+m+n+4)}{2}}}{\pi^{\frac{(k+1)d}{2}}} \right) \int d^d R d^m R' e^{-(R^2 + R'^2)} V(\mathbf{R} - \mathbf{R}') e^{-(R'^2 + R^2(2k-1))}. \quad (4.6)$$

Using the Lagrange equation of motion, we get the equation of motion for the variational parameter $\alpha(t)$. The time evolution of the variational parameter $\alpha(t)$ is

$$\ddot{\alpha} = 2\alpha\dot{\beta}^2 + \frac{2}{\alpha} - 2\alpha - \frac{(n+m-kd)}{d} G_d \alpha^{\frac{(n+m-kd)}{2}}. \quad (4.7)$$

This “.” represents the derivative with respect to the dimensionless variable $\tau = \omega_0 t$. The total energy of the system is

$$\tilde{E} = \frac{4E}{N\hbar\omega_0} = \alpha\dot{\beta}^2 d + \frac{d}{\alpha} + \alpha d + G_d \alpha^{\frac{(n+m-kd)}{2}}. \quad (4.8)$$

At equilibrium, $\beta = 0$ and $\frac{\partial E}{\partial \alpha}|_{\alpha=\alpha_0} = 0$. The equilibrium point α_0 satisfies the following relation in d -dimensions

$$\alpha_0^2 + \frac{(n+m-kd)}{2d} G_d \alpha_0^{(n+m-kd+1)} = 1. \quad (4.9)$$

4.2.1 Universality of monopole mode

To show the universality of monopole mode of a certain class of interacting Bose gas we choose n , m , k and d such that they satisfy the following relation:

$$n + m - kd + 2 = 0. \quad (4.10)$$

If n , m , k , and d satisfy the above relation, Eq. (4.7) can be written as

$$\ddot{\alpha} + 4\alpha = 2\tilde{E}(\alpha). \quad (4.11)$$

We define $I(t) = \int d^d r |\psi(\mathbf{r}, t)|^2 r^2$ which is the expectation value of the square of the radius. The above equation can be rewritten as

$$\ddot{I} + 4\omega_0^2 I = \frac{4E_0}{M}. \quad (4.12)$$

From now onwards “.” indicates derivative with respect to time t . For monopole excitation, the average value of the collective coordinate r^2 oscillates around its equilibrium value. We expand $I(t)$ around its equilibrium point I_0 as $I(t) = I_0 + \delta I(t)$ and we get,

$$\delta \ddot{I} + 4\omega_0^2 \delta I = \frac{4E_0}{M}, \quad (4.13)$$

where $E_0 = d \left(\frac{1}{\alpha_0} + \alpha_0 + \frac{G_d}{d} \right)$ is the equilibrium energy of the system. This equation is identical with the classical equation (1) of Ref. [1] which was derived using the virial theorem. The solution of this equation is

$$I(t) = A \cos(2\omega_0 t + \theta) + \frac{E_0}{M\omega_0^2}. \quad (4.14)$$

A and θ are constants which can be determined from the initial conditions on ψ . Thus the square of the system radius oscillates with a frequency $2\omega_0$ in any dimension if $n + m - kd + 2 = 0$. This monopole frequency $2\omega_0$ is universal because it is independent of nature (long-range, short-range, local, non-local) of the interatomic interaction, dimensionality of the trap, order of the nonlinearity and the total number of atoms N . For *ordinary* GP equation in $d(=m)$ dimensions, $k=1$, then the monopole mode frequency of an *ordinary* d -dimensional GP equation is the universal frequency $2\omega_0$ if $n = -2$. Eqs.(4.7) and (4.10) explicitly shows how the scaling exponent of the interaction potential gives the universal monopole mode frequency.

4.2.2 Universality of dynamics of width

To show the universality of the time-evolution of a class of interacting Bose gas, we choose n , m , d and k such that they satisfy Eq.(4.10). Then Eq.(4.7) can be rewritten for time-independent trap as well as for time-dependent trap as

$$\ddot{I}(t) - \frac{\dot{I}^2(t)}{2I(t)} + 2\omega^2(t)I(t) = \frac{Q_d}{I(t)}, \quad (4.15)$$

where $Q_d = (\frac{N\hbar d}{2M})^2(1 + G_d)$ is the positive invariants under time evolution. Let $X(t) = \sqrt{I(t)}$ is the condensate width. The above equation can be written as

$$\ddot{X}(t) + \omega_0^2(t)X(t) = \frac{Q_d}{X^3(t)}. \quad (4.16)$$

This is a nonlinear singular Hill's equation in d dimensions. This is an interesting result because the time evolution of the width can be described by the same Hill's equation in any dimensions if $n + m - kd + 2 = 0$. The dynamics of the width is universal because the time evolution of the width can be described universally by the same nonlinear singular Hill's equation in any dimensions. Moreover, this Hill's equation can be solved analytically and exactly. Eq.(4.16) can be viewed as the classical motion of a fictitious particle in an effective d -dimensional potential

$$V_{\text{eff}} = \frac{\omega_0^2(t)X^2}{2} + \frac{Q_d}{2X^2}. \quad (4.17)$$

The general solution of Eq.(4.16) is $X(t) = \sqrt{u^2(t) + \frac{Q_d}{W^2}v^2(t)}$ where $u(t)$ and $v(t)$ are two linearly independent solutions of the equation $\ddot{p} + \omega^2(t)p = 0$ which satisfy the initial conditions $u(t_0) = X(t_0)$, $\dot{u}(t_0) = X'(t_0)$, $v(t_0) = 0$ and $v'(t_0) \neq 0$. W is the Wronskian. This time-dependent Hill's equation can be solved explicitly only for particular choices of $\omega_0(t)$. For time-dependent periodic trap potential, the equation is known as Mathieu equation which is well studied. In most of the BEC experiment, the trap potential is time-independent. For time-independent trap potential, a solution of this equation is

$$X(t) = \sqrt{\cos^2(2\omega_0 t) + \frac{Q_d}{4\omega_0^2} \sin^2(2\omega_0 t)}. \quad (4.18)$$

To discuss the free expansion of the atomic cloud we suddenly switch-off the external potential and the system starts expanding. This corresponds to solving the equation (4.16) with the second term set equal to zero:

$$\ddot{X}(t) - \frac{Q_d}{X^3(t)} = 0. \quad (4.19)$$

This reduced system of a particle in an inverse-square potential is a well-studied problem and the solution of this equation is given by [10]

$$X^2 = 1 + Q_d t^2. \quad (4.20)$$

From Eq.(4.10), we get $kd = 2$ for 1D *modified* GP equation, and 2D *ordinary* GP equation with $n = -2$. This is the condition for self-similar solution of a nonlinear GP equation discussed in by Rybin *et al.* [7], and Kolomeisky *et al.* [8]. There is no self-similar solution in 1D *ordinary* GP equation since it does not obey Eq.(4.10).

4.3 Examples

We now discuss few systems which satisfy Eq.(4.10) and shows the universal monopole mode frequency and the dynamics of the width of the system that can be described by Eq.(4.18).

4.3.1 Quasi-2D trapped Bose gas

In the previous chapter we have modeled the quasi-2D interacting Bose gas at zero temperature. The effective interaction potential between atoms is $V_I = g_2 \delta^2(\mathbf{r} - \mathbf{r}')$ [11], where $g_2 = 2\sqrt{2\pi}\hbar\omega_z a a_z$ is the effective coupling strength in quasi-2D Bose system and a is the s -wave scattering length in 3D. This quasi-2D BEC state can be described by the *ordinary* GP equation which is valid only when $a < a_z$ [12]. The same effective coupling constant is obtained in [13]. Under the scale transformation, $\mathbf{r} \rightarrow \lambda \mathbf{r}$, $V_I(\lambda \mathbf{r}) = \frac{1}{\lambda^2} V_I(\mathbf{r})$. So this interaction potential has the scaling exponent $n = -2$. In this system, $m = d = 2$ and $k = 1$ which satisfy Eq. (4.10) and the monopole mode frequency is $2\omega_0$.

The time-evolution of this system is

$$\ddot{X} + \omega_0^2 X = \frac{Q_2}{X^3}, \quad (4.21)$$

where $Q_2 = \frac{N^2 \hbar^2}{M^2} \left(1 + \sqrt{\frac{2}{\pi}} N \frac{a}{a_z}\right)$. The same equation is obtained by using different method at zero temperature [3, 14]. Here, we have identified the value of Q_2 at $T = 0$. So the dynamics of the width can be described by the Eq. (4.18). At equilibrium, $X_0^4 = \frac{Q_2}{\omega_0^2}$. When we linearize Eq. (4.21) around the equilibrium point X_0 , we get

$$\delta \ddot{X} + 4\omega_0^2 \delta X = 0. \quad (4.22)$$

Once again we obtain the universal oscillation frequency of the condensate width to be $\omega = 2\omega_0$, corresponding to the frequency of a single-particle excitation in the condensate state.

4.3.2 One dimensional Tonk-Girardeau gas

It has been shown by Petrov *et al.* [15] that in 1D trapped Bose gases the quantum fluctuations suppresses due to the trap potential but do not destroy the condensate at very low temperature. We consider a dilute gas of N bosons confined in a very elongated harmonic trap with radial and axial frequencies ω_0 and ω_z ($\omega_z \ll \omega_0$). If the temperature and the interaction energy per particle do not exceed the transverse

level spacing $\hbar\omega_0$, the system becomes effectively one-dimensional. The bosons in a cigar shape trap are in two regimes, Tonk-Girardeau (TG) regime and Thomas-Fermi (TF) regime, depending on the gas parameter [9]. A one-dimensional gas of impenetrable bosons referred to as a Tonk-Girardeau gas. When the gas parameter is small, the system is in the TG regime which can be described by the quartic interaction in the non-linear Schroedinger equation (NLSE). On the other hand, when the gas parameter is large, the system is in the TF regime which can be described by the quadratic interaction in the NLSE. The gas parameter is defined as the product of the density (n) with the effective scattering length $|a_{1D}|$ [16], i.e $n|a_{1D}|$. The interaction energy per particle is given below for two limiting cases [17],

$$\epsilon(n) = \frac{1}{2}(2\hbar\omega_0 a)n, \quad n|a_{1D}| \rightarrow \infty, \quad (4.23)$$

$$\epsilon(n) = \frac{1}{3} \frac{\pi^2 \hbar^2}{2M} n^2, \quad n|a_{1D}| \rightarrow 0. \quad (4.24)$$

The energy functional of 1D TG gas which can be described by the *modified* GP equation is

$$E = \int dz \left[\frac{\hbar^2}{2M} \left| \frac{d\psi}{dz} \right|^2 + \frac{M\omega_z^2 z^2}{2} |\psi|^2 + \frac{\hbar^2 \pi^2}{6M} |\psi|^6 \right]. \quad (4.25)$$

In this system, $d = m = 1$, $k = 2$ which satisfy Eq. (4.10) and $g_1 = \frac{\hbar^2 \pi^2}{2M}$. The time-evolution of the system is

$$\ddot{X} + \omega_0^2 X = \frac{Q_1}{X^3}, \quad (4.26)$$

where $Q_1 = \frac{N^2 \hbar^2}{4M^2} \left[1 + \frac{4\pi N^2}{3\sqrt{3}} \right]$. The same equation is obtained in [7, 8] by using different method. But here we have identified the value of constant Q_1 . This 1D *modified* GP equation also exhibits an universal monopole mode frequency $2\omega_z$ and satisfy the self-similar condition. The dynamics can be described by the Hill's equation which is exactly solvable.

For 1D ordinary GP equation which describe 1D TF Bose gas, $m = d = k = 1$, which does not satisfy the relation (4.10). The monopole mode frequency is $\sqrt{2}\omega_z$ for a large number of particles. Thus the monopole mode frequency is modified by the interatomic strength and the time-evolution of the system can not be described by nonlinear singular Hill's equation. By measuring the monopole mode frequency one can distinguish between two regimes of 1D trapped Bose gas. Recently, the monopole mode frequency of 1D TF and TG Bose gas is obtained by using the sum-rule approach which is same with our results [18].

4.3.3 Calogero model

A system of trapped particles interacting through pair potential $\frac{1}{r^2}$ is well known as the Calogero-Sutherland model [19]. Only an inverse square pair potential, $\frac{1}{r^2}$, has the scaling, $n = -2$, in any dimensions and it satisfies Eq. (4.10) for $k = 1$ in arbitrary d . For $m = k = 0$ and $n = -2$, we get Calogero model [19] in arbitrary d which gives the same universal monopole mode frequency $2\omega_0$. In this system the dynamics of the width can be described universally by the same Eq. (4.18). In fact, Benjamin *et al.* [20] have shown that the energy spectrum of a system of harmonic trapped particles interacting with $\frac{1}{r^2}$ potential is divided into sets of equidistant levels with separation $2\omega_0$ in any dimensions. Also, B. Sutherland [21] considered a one-dimensional system of particles interacting by an inverse square pair potential and shown that the monopole mode frequency is the universal frequency $2\omega_0$.

Apart from these two potentials, there are some other model potentials which have the scaling exponent $n = -2$. For example, the derivative delta function potential in 1D, the double delta function potential in 1D, and the $\frac{1}{x} \times$ delta function potential in 1D. For all these model potentials, one can get the universal monopole mode frequency and the dynamics of the width.

4.4 Summary and conclusions

In this chapter, using the time-dependent variational analysis, we have obtained the condition, $n + m - kd + 2 = 0$, for which a class of NLSE exhibits the universal monopole oscillation frequency $2\omega_0$. We have also shown the universality of time evolution of the width in a time-independent trap as well as a time-dependent trap for a class of GP equation. Interestingly, this dynamics of the width can be described by the same Hill's equation (4.16) if the Bose system satisfy the condition, $n + m - kd + 2 = 0$. This Hill's equation is analytically and exactly solvable. This monopole mode frequency and the time-evolution of the system is universal because it does not depend on the strength and nature (short-range, long-range, local, non-local) of the interaction potential, order of the nonlinearity and the total number of atoms N . Using the time-dependent variational analysis, we have also obtained the condition for self-similar solutions, $kd = 2$, of a class of nonlinear GP equation.

As an example, we have shown that the quasi-2D trapped Bose gas described by the *ordinary* GP equation, 1D Tonk-Girardeau Bose gas described by the *modified* GP equation and a system described by the Calogero model shows the universal nature of the monopole mode frequency and the dynamics of the width of

the system.

These important results, the universality of monopole mode and the dynamics of the width of a trapped interacting Bose system, are not an artifacts of the Gaussian approximation, but also hold for an exact calculation using a set of time-dependent transformations [22]. Note that the phase factor in the variational ansatz of the wave function (Eq.(4)) is required to get the correct dynamics of the width [4]. Similarly, the phase factor is also present in equation of the time dependent transformations in [22]. In Ref.[22], using those time-dependent transformations, the universality of the monopole mode and the dynamics of the width is obtained for a class of NLSE. Our results obtained from the variational approach are identical to the exact results of [22]. This is because of the similarity in the phase factor of the variational ansatz for the wave function and the transformation equations (Eq.(2)) in Ref. [22].

Our result is also valid for $SO(2,1)$ invariant multicomponent NLSE describing an interacting Bose system [24]. These universal properties are also true for Fermi systems and at any temperature. Recently, quasi-2D and quasi-1D BEC have been observed at MIT [23]. Experimentally it is also possible to check the validity of the two-body potential in quasi-2D BEC state [1] and the order of the nonlinearity in quasi-1D BEC state by measuring the universal monopole mode frequency and the dynamics of the width of the Bose system.

Bibliography

- [1] L. P. Pitaevskii and A. Rosch, Phys. Rev. A **55**, R853 (1997).
- [2] L. P. Pitaevskii, Phys. Lett. A **221**, 14 (1996).
- [3] Yu. Kagan, E. L. Sukrov, and G. V. Shlyapnikov, Phys. Rev. A **54**, R1753 (1996).
- [4] Victor M. Perez-Garcia, H. Michinel, J. I. Cirac, M. Lewenstein, and P. Zoller, Phys. Rev. Lett. **77**, 5320 (1996).
- [5] S. Stringari, Phys. Rev. Lett. **77**, 2360 (1996).
- [6] E. P. Gross, Nuovo Cimento A **20**, 454 (1961);
L. P. Pitaevskii, Pis'ma Zh. Eksp. Teor. Fiz. **77**, 988 (1961) [Sov. Phys. JETP. **13**, 451 (1961)].
- [7] A. Rybin, G. Varzugin, M. Lindberg, J. Timonen, and R. K. Bullough, Phys. Rev. E **62**, 6224 (2000).
- [8] E. B. Kolomeisky, T. J. Newman, Joseph, Joseph P. Straley, and Xiaoya Qi, Phys. Rev. Lett. **85**, 1146 (2000).
- [9] Vanja Dunjko, Vincent Lorent, and Maxim Olshanii, Phys. Rev. Lett. **86**, 5413 (2001).
- [10] V. de Alfaro, S. Fubini and G. Furlan, Nuvo Cimento A **34**, 569 (1976);
R. Jackiw, Ann. Phys. (N.Y) **129**, 183 (1980); **201**, 83 (1990).
- [11] Tarun Kanti Ghosh and S. Sinha, Eur. Phys. J. D **19**, 371 (2002).
- [12] D. S. Petrov, M. Holzmann, and G. V. Shlyapnikov, Phys. Rev. Lett. **84**, 2551 (2000).
- [13] Tin-Lun Ho and Michael Ma, J. Low Temp. Phys. **115**, 61 (1999).

- [14] Juan J. Garcia-Ripoll and Victor M. Perez-Garcia, Phys. Rev. Lett. **83**, 1715 (1999).
- [15] D. S. Petrov, G. V. Shlyapnikov, and J.T. M. Walraven, Phys. Rev. Lett. **85**, 3745 (2000).
- [16] Maxim Olshanii, Phys. Rev. Lett. **81**, 938 (1998).
- [17] E. H. Lieb and W. Liniger, Phys. Rev. **130**, 1605 (1963).
- [18] C. Menotti and S. Stringari, cond-mat/0201158.
- [19] F. Calogero, J. Math. Phys. (N. Y.) **10**, 2191 (1969); **10**, 2197 (1969);
B. Sutherland, J. Math. Phys. (N. Y.) **12**, 246 (1971); **12**, 251 (1971).
- [20] S. C. Benjamin, L. Quiroga, and N. F. Johnson, Phys. Rev. A **54**, 4309 (1996).
- [21] B. Sutherland, Phys. Rev. Lett. **80**, 3678 (1998).
- [22] Pijush Kanti Ghosh, Phys. Rev. A **65**, 012103 (2002).
- [23] A. Gorlitz *et al.* Phys. Rev. Lett. **87**, 130402 (2001).
- [24] Pijush Kanti Ghosh, Phys. Rev. A **65**, 053601 (2002).

Chapter 5

Collective excited states of a Bose-Einstein condensate with gravity-like interatomic attraction

5.1 Introduction

The discovery of Bose-Einstein condensation (BEC) in a dilute alkali-metal atomic gas opens up a new perspective in the field of many-body physics [1, 2]. Most of the properties of these dilute gases can be explained by considering only a two-body short-range interaction which is characterized by the s -wave scattering length a [2, 3]. However, the BEC in presence of the dipole-dipole interactions has recently evoked considerable interest. Novel physics is expected for dipolar BEC, since the dipole-dipole interactions are long-range, anisotropic, and partially attractive. The non-trivial task of achieving and controlling dipolar BECs is thus particularly challenging.

Recently, a new kind of atomic BEC has been proposed by D. O'Dell *et al.* [4]. They have shown that the particular configuration of intense off-resonant laser beams gives rise to an effective gravity-like $\frac{1}{r}$ interatomic attraction between neutral atoms located well within the laser wavelength. This long range interaction potential is of the form $U(r) = -\frac{u}{r}$, where $u = (11\pi/15)(I\alpha_0^2/c\epsilon_0^2\lambda_L^2)$. I and λ_L are the total laser intensity and wave length respectively. α_0 is the atomic polarizability at the frequency $2\pi c/\lambda_L$. In this system, the gravity-like $\frac{1}{r}$ attraction balances the pressure due to the zero point kinetic energy and the short-range interaction potential. For a strong induced gravity-like potential, the BEC becomes stable even without the external trap potential [5]. There is a competition between the

gravity-like potential either with the kinetic energy (G) or the two-body short-range interatomic interaction potential characterized by the s -wave scattering length a (TF-G), which gives two new regimes for new atomic BEC. These two regimes are obtained based on the Gaussian variational ansatz for the ground state wave function [4].

In the TF-G regime, collective excitation frequencies have been calculated numerically by solving the equations of collisionless hydrodynamics [6]. Moreover, in this regime, an analytic expression of the ground state density is obtained [4]. Within the sum-rule approach, collective excitation frequencies of a gravity-like self-bound Bose gas has been discussed in Ref. [7]. There has been no systematic and detailed study on the collective excitation frequencies and vortices of a gravitationally self-bound Bose gas by using the time-dependent variational approach. The purpose of this chapter is to give analytic expressions for collective excitation frequencies, superfluid coherence length and critical angular frequencies required to create a vortex of a rotating Bose condensed state and to compare qualitatively the results of the TF-G regime with the results obtained in the TF regime of an ordinary atomic BEC.

In section [5.2], by using the time-dependent variational method, we obtain the excitation spectrum of a gravity-like self-bound Bose gas. We also calculate the lower bound of the ground state energy, monopole and quadrupole mode frequencies of the TF-G and the G regimes. In section [5.3], we consider a rotating Bose condensed state with a single vortex along the z axis. We estimate the superfluid coherence length and the critical angular frequencies required to create a vortex along the z -axis. We find that the TF-G regime of a gravitationally self-bound Bose condensed state should exhibit superfluid properties more prominently than the G regime. We find that the monopole mode frequency of the condensate decreases due to the presence of the vortex. We present a summary and conclusions of our work in section [5.4].

5.2 Collective excitation of Bose condensed state with gravity-like interatomic attractive interaction

The equation of motion of the condensate wave function is described by the generalized Gross-Pitaevskii equation [8],

$$i\hbar \frac{\partial \psi(\mathbf{r}, t)}{\partial t} = \left[-\frac{\hbar^2}{2m} \nabla^2 + \frac{m\omega_0^2 r^2}{2} + V_H(r) \right] \psi(\mathbf{r}, t), \quad (5.1)$$

where $V_H(\mathbf{r})$ is the self-consistent Hartree potential,

$$V_H(\mathbf{r}) = \frac{4\pi a\hbar^2}{m} |\psi(\mathbf{r}, t)|^2 - u \int d^3r' \frac{|\psi(\mathbf{r}', t)|^2}{|\mathbf{r} - \mathbf{r}'|}. \quad (5.2)$$

The normalization condition for ψ is $\int |\psi(\mathbf{r}, t)|^2 d^3r = N$, where N is the total number of particles in the condensed state. The original Gross-Pitaevskii equation can be obtained by setting $u = 0$.

One can write down the Lagrangian density corresponding to this system as follows,

$$\mathcal{L} = \frac{i\hbar}{2} \left(\psi \frac{\partial \psi^*}{\partial t} - \psi^* \frac{\partial \psi}{\partial t} \right) + \frac{\hbar^2}{2m} |\nabla \psi|^2 + \left(\frac{m\omega^2 r^2}{2} + \frac{V_H(\mathbf{r})}{2} \right) |\psi|^2, \quad (5.3)$$

where the asterisk denotes the complex conjugation. The nonlinear Schroedinger equation can be obtained from a minimization of the action, $I = \int \mathcal{L} d^3r dt$. The BEC of charged bosons [9] confined in an ion trap can be described by the above mentioned Lagrangian if we set $-u = e^2$, where e is the electronic charge.

To calculate the excitations spectrum of an atomic BEC with gravity-like interaction, we will use the time-dependent variational method. This technique has been first used to calculate the low-lying excitations spectrum of a harmonically trapped atomic BEC in Ref. [10]. The result obtained from the variational method matches with Stringari's [11] result within the sum-rule approach.

In Ref. [7] it is shown that the oscillation frequencies obtained from the exact ground state and a Gaussian ansatz are in good agreement. In this system, a Gaussian ansatz is also a good variational wave function. In order to obtain the evolution of the condensate we assume the following variational wave function:

$$\psi(\rho, z, t) = C(t) e^{-\frac{1}{2}[\alpha(t)\rho^2 + \beta(t)z^2]}, \quad (5.4)$$

where $C(t)$ is the normalization constant which can be determined from the normalization condition. ρ and z are the variables in units of Λ , where $\Lambda = \sqrt{\frac{\hbar}{m\omega_g}} = \frac{\hbar^2}{muN}$ is the length scale in this system (similar to the harmonic-oscillator length) when the harmonic trap is absent and $\omega_g = \frac{mu^2N^2}{\hbar^3}$ is the gravitational frequency. ρ is the two-dimensional vector. $\alpha(t) = \frac{1}{\alpha_1^2} + i\alpha_2$ and $\beta(t) = \frac{1}{\beta_1^2} + i\beta_2$ are the dimensionless time-dependent parameters. α_1 and β_1 are the condensate widths in the $x - y$ plane and along the z direction, respectively. The Gaussian variational wave function is in exact ground state when the two two-body interatomic interactions are absent.

Substituting (5.4) into (5.3) and integrating the Lagrangian density over the space coordinates, we get the following Lagrangian:

$$L = \frac{SNu}{2a} \left[\left(\alpha_1^2 \dot{\alpha}_2 + \frac{1}{2} \beta_1^2 \dot{\beta}_2 \right) - \left(\frac{1}{\alpha_1^2} + \alpha_1^2 \alpha_2^2 \right) - \frac{1}{2} \left(\frac{1}{\beta_1^2} + \beta_1^2 \beta_2^2 \right) - \sqrt{\frac{2}{\pi}} \left(\frac{S}{\alpha_1^2 \beta_1} - \frac{F\left[\frac{1}{2}, 1; \frac{3}{2}; \left(1 - \frac{\alpha_1^2}{\beta_1^2}\right)\right]}{\beta_1} \right) \right], \quad (5.5)$$

where $S = \frac{Na}{\Lambda} = \frac{umaN^2}{\hbar^2}$ is a dimensionless scattering parameter similar to the scattering parameter $P = \frac{Na}{a_0}$ [10] for an ordinary atomic BEC. Here, a_0 is the harmonic-oscillator length. This S can be positive or negative, depending on the sign of the scattering length a . The scattering parameter S can also be written as $S = (528\pi^2/105)\bar{I}(Na/\lambda_L)^2$, where $\bar{I} = I/I_0$ and $I_0 = (48\pi/7)(\hbar^2 \epsilon_0^2/m\alpha_0^2)a$ is the threshold laser intensity to create a self-bound condensate [5]. For a given intensity $\bar{I} = 1.5$, the realistic, stable and self-trapped system (for sodium atoms) contains 40 to 400 atoms [5] and the corresponding range of S is 1 to 100. This range can be altered by changing the scattering length a [12]. $F\left[\frac{1}{2}, 1; \frac{3}{2}; \left(1 - \frac{\alpha_1^2}{\beta_1^2}\right)\right]$ is the hypergeometric function. The last term in Eq. (5.5) is the mean-field energy of the gravity-like potential which is shown in the Appendix A5. We are interested to find out the excitation spectrum of a self-bound Bose gas as well as in the TF-G and G regimes. We have set $V_{ext} = 0$ because the system is stable even in the absence of an external trap potential [5].

The energy functional in terms of the variational parameter α in an isotropic system is

$$E = \frac{NuS}{2a} \left[\frac{3}{2\alpha^2} + \sqrt{\frac{2}{\pi}} \left(\frac{S}{\alpha^3} - \frac{1}{\alpha} \right) \right], \quad (5.6)$$

By minimizing the energy functional with respect to α , one can get the equilibrium point w which is given by

$$w = \frac{3}{2} \sqrt{\frac{\pi}{2}} \left[1 + \sqrt{\left(1 + \frac{8S}{3\pi}\right)} \right]. \quad (5.7)$$

The chemical potential is

$$\mu = \frac{uS}{2a} \left[\frac{3}{2w^2} + 2\sqrt{\frac{2}{\pi}} \left(\frac{S}{w^3} - \frac{1}{w} \right) \right]. \quad (5.8)$$

The sound velocity $c_s^2 = \mu/m$ vs the dimensional scattering parameter S is shown in Fig. 5.1.

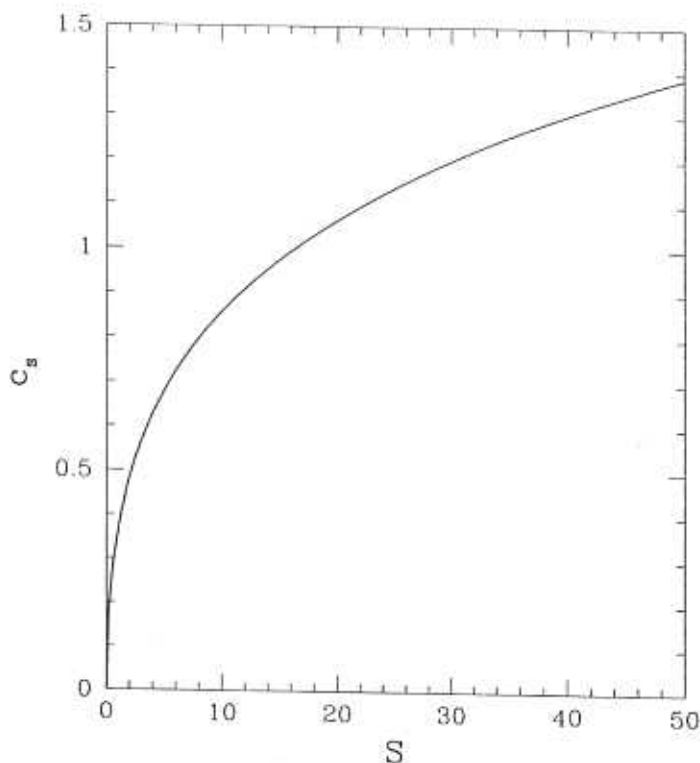


Figure 5.1: Sound velocity c_s as a function of the dimensionless scattering parameter S .

Using the Euler-Lagrange equation, the time evolution of the widths are

$$\ddot{\alpha}_1 = \frac{1}{\alpha_1^3} + \sqrt{\frac{2}{\pi}} \left(\frac{S}{\alpha_1^3 \beta_1} + \frac{F_{\alpha_1}[\alpha_1, \beta_1]}{2} \right), \quad (5.9)$$

$$\ddot{\beta}_1 = \frac{1}{\beta_1^3} + \sqrt{\frac{2}{\pi}} \left(\frac{S}{\alpha_1^2 \beta_1^2} + F_{\beta_1}[\alpha_1, \beta_1] \right). \quad (5.10)$$

$F_{\alpha_1}[\alpha_1, \beta_1]$ is the derivative of $F \left[\frac{1}{2}, 1; \frac{3}{2}, \left(1 - \frac{\alpha_1^2}{\beta_1^2} \right) \right] / \beta_1$ with respect to α_1 . Similarly, $F_{\beta_1}[\alpha_1, \beta_1]$ is the derivative of $F \left[\frac{1}{2}, 1; \frac{3}{2}, \left(1 - \frac{\alpha_1^2}{\beta_1^2} \right) \right] / \beta_1$ with respect to β_1 . The exact form of $F_{\alpha_1}[\alpha_1, \beta_1]$ and $F_{\beta_1}[\alpha_1, \beta_1]$ are given in the Appendix B5.

We are interested in the low-energy excitations of a gravity-like self-bound Bose condensate. The low-energy excitations of the condensate corresponds to the small oscillations of the state around the equilibrium widths α_{10} and β_{10} . Therefore, we expand around the time dependent variational parameters around the equilibrium widths in the following way: $\alpha_1 = \alpha_{10} + \delta\alpha_1$ and $\beta_1 = \beta_{10} + \delta\beta_1$.

The time evolution of the widths around the equilibrium points are

$$\delta\ddot{\alpha}_1 = - \left(\frac{3}{\alpha_{10}^4} + 3\sqrt{\frac{2}{\pi}} \frac{S}{\alpha_{10}^4 \beta_{10}} \right) \delta\alpha_1 - \sqrt{\frac{2}{\pi}} \frac{S}{\alpha_{10}^3 \beta_{10}^2} \delta\beta_1 + \frac{1}{2} \sqrt{\frac{2}{\pi}} F_{\alpha_1}[\alpha_{10}, \beta_{10}, \delta\alpha_1, \delta\beta_1], \quad (5.11)$$

$$\delta\ddot{\beta}_1 = -2\sqrt{\frac{2}{\pi}} \frac{S}{\alpha_{10}^3 \beta_{10}^2} \delta\alpha_1 - \left(\frac{3}{\beta_{10}^4} + 2\sqrt{\frac{2}{\pi}} \frac{S}{\alpha_{10}^2 \beta_{10}^3} \right) \delta\beta_1 + \sqrt{\frac{2}{\pi}} F_{\beta_1}[\alpha_{10}, \beta_{10}, \delta\alpha_1, \delta\beta_1]. \quad (5.12)$$

$F_{\alpha_1}[\alpha_{10}, \beta_{10}, \delta\alpha_1, \delta\beta_1]$ is the first-order fluctuations around the equilibrium points of $F_{\alpha_1}[\alpha_1, \beta_1]$. Similarly, $F_{\beta_1}[\alpha_{10}, \beta_{10}, \delta\alpha_1, \delta\beta_1]$ is the first-order fluctuations around the equilibrium points of $F_{\beta_1}[\alpha_1, \beta_1]$. The exact forms of $F_{\alpha_1}[\alpha_{10}, \beta_{10}, \delta\alpha_1, \delta\beta_1]$ and $F_{\beta_1}[\alpha_{10}, \beta_{10}, \delta\alpha_1, \delta\beta_1]$ are given in the Appendix B5.

We are looking for the solutions of $e^{i\omega t}$ type. First we solve for these two equations in terms of α_{10}, β_{10} and later we set $\alpha_{10} = \beta_{10} = w$. For isotropic system, the excitations spectrum are

$$\frac{\omega_+^2}{\omega_g^2} = \frac{3}{w^4} + \sqrt{\frac{2}{\pi}} \left(\frac{4S}{w^5} - \frac{2}{3w^3} \right), \quad (5.13)$$

$$\frac{\omega_-^2}{\omega_g^2} = \frac{3}{w^4} + \sqrt{\frac{2}{\pi}} \left(\frac{S}{w^5} - \frac{1}{15w^3} \right), \quad (5.14)$$

where $\omega_g = \frac{mu^2 N^2}{\hbar^3}$ is the gravitational frequency. The ω_+ and ω_- vs the dimensionless scattering parameter S are shown in Fig.5.2.

When S is small, the gravity-like $\frac{1}{r}$ attractive interaction dominates over the repulsive pseudopotential. In this limit, the system becomes more compressible. In other words the system becomes less resistant to density changes. So one would expect that monopole mode lies below quadrupole mode. From Fig. 5.2 we identify that the upper branch of the excitation spectrum is quadrupole mode ($\omega_- = \omega_Q$) and the lower branch is monopole mode ($\omega_+ = \omega_M$). The monopole and quadrupole modes shown in Fig. 5.2 matches very well with the spectrum obtained within the sum-rule approach [7]. When $S = -1.169$, ω_M starts decreasing as shown in Fig. 5.2. At $S_c = -1.179$, the system collapses. The value of S_c can also be obtained from Eq. (5.7). For large value of S , the monopole mode lies above the quadrupole mode because the repulsive pseudopotential start dominates over the attractive long-range interaction.

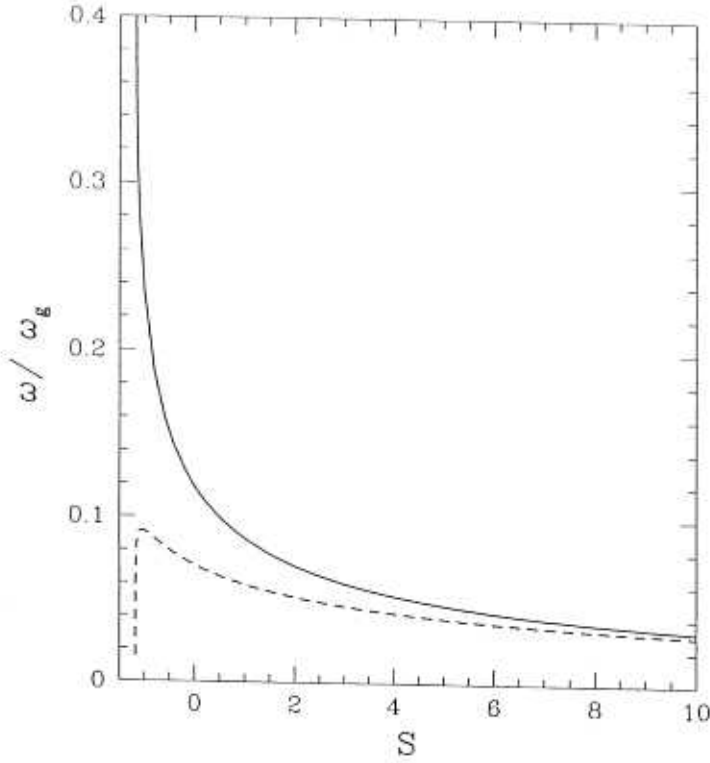


Figure 5.2: Monopole and quadrupole mode frequencies vs the scattering parameter S . The solid and dashed lines corresponds to the quadrupole and monopole mode frequencies, respectively.

At $S = 17.5$, there is a crossing between these two modes which is shown in the Fig. 5.3. Interestingly, this crossing of these two modes is also obtained from the time-dependent variational method.

5.2.1 TF-G regime

For large s -wave scattering length, the kinetic and the trap potential energy can be neglected. The gravity-like potential is balanced by the s -wave interaction strength. The total ground state energy is $E_0 = -0.9648N^2 \frac{\mu}{\Lambda_J}$, where $\Lambda_J = 2\pi\sqrt{\frac{\hbar^2}{m\mu}}$ is the Jeans wavelength which is the shortest wavelength to keep stable condensed state. The ground state energy per particle varies as N . The sound velocity is $c_s^2 = \frac{\mu}{m} = 0.307106 \frac{\mu\sqrt{S}}{m}$. So the sound velocity c_s varies as $N^{1/2}$ whereas $c_s \sim N^{1/5}$ for an ordinary atomic BEC in the TF approximation [13]. In this regime we neglect the contribution of the kinetic energy term in Eqs. (5.9) and (5.10) and we find that the monopole and quadrupole frequencies are $\omega_M = 0.319951\omega_g S^{-3/4}$ and $\omega_Q =$

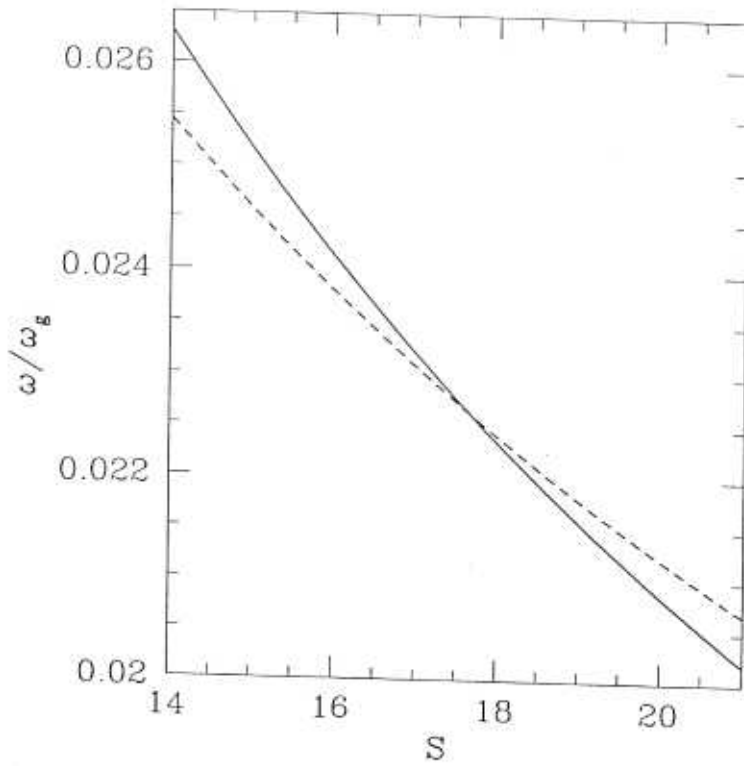


Figure 5.3: Crossing between monopole (dashed line) and quadrupole (solid line) modes

$0.202355\omega_g S^{-3/4}$. In this regime, the monopole and quadrupole frequencies are obtained by solving the hydrodynamic equations numerically in [7]. The monopole and quadrupole frequencies obtained from the variational approach are similar to the exact numerical values. For an ordinary atomic BEC in the TF regime, the ω_M and ω_Q are independent of the scattering length a [10, 11]. But, in this system, it still depends on the scattering length a . Here, the ratio $\frac{\omega_M}{\omega_Q}$ is $\sqrt{\frac{5}{2}} = 1.58114$. Remarkably, this ratio is identical to the result of [7] which is obtained within the sum-rule approach. This is also true for trapped atomic BEC without gravity-like interaction in the large- N limit. It was first pointed out in [7, 11].

5.2.2 G regime

In this regime gravity-like potential is balanced by the kinetic energy. The trap potential and s -wave interaction can be neglected. This is analog of boson star (non-relativistic) [14]. The total ground state energy is $E_0 = -\frac{N}{19}\hbar\omega_g$. Using the uncertainty relation, we estimate the total ground state energy is $E_0 = -\frac{N}{16}\hbar\omega_g$.

which is very close to the energy obtained from the variational approach. So our variational ansatz for wave function is good in this regime also. The ground state energy per particle varies as N^2 . The sound velocity is $c_s^2 = 0.159155 \frac{uS}{m}$. So the sound velocity c_s varies as N . In this regime, neglecting the contribution of the s -wave interaction potential in Eqs. (5.9) and (5.10), we get the monopole and quadrupole modes are $\omega_M = 0.0707355\omega_g$ and $\omega_Q = 0.118363\omega_g$. These frequencies are very close to the frequencies obtained within the sum-rule approach [7]. Here, $\frac{\omega_M}{\omega_Q} = \sqrt{\frac{5}{14}} = 0.597615$. This ratio is also identical (up to five decimal) with that of [7], which is obtained within the sum-rule approach.

5.3 Vortex of a Bose condensed state with gravity-like interatomic interaction

We consider a gravitationally self-bound Bose condensate state with a vortex along the z axis. The experimental realization of a vortex state would be a direct signature of macroscopic phase coherence of this new atomic BEC with an attractive long-range interaction. Vortex filament in the condensate can be generated by rotating the condensate above the certain angular frequency, known as critical frequency. In this section we calculate the coherence length and critical angular frequency to create a vortex along the z axis. We also study the monopole mode frequency of the condensate state in presence of a vortex. One can use the time-dependent variational approach to describe the vortex state. In the previous section we have explicitly shown that the monopole and quadrupole mode frequencies obtained by using the Gaussian ansatz coincides with the numerical results. So it is a natural choice to assume that a variational wave function of a self-bound BEC state with a vortex along the z axis is

$$\psi_q(\mathbf{r}, t) = C_q(t) \rho^q e^{iq\phi} e^{-\frac{r^2}{2} \left[\frac{1}{\alpha^2(t)} + i\beta(t) \right]}, \quad (5.15)$$

where q is the vortex quantum number and $C_q(t)$ is the normalization constant. Also, $\rho^2 = x^2 + y^2$, $r^2 = x^2 + y^2 + z^2$ and $\phi = \tan^{-1}(\frac{y}{x})$. For simplicity, we consider only $q = 1$ and $q = 2$. By following the same procedure of the preceding section, one would obtain the effective Lagrangian which is given by

$$L = \frac{NuS}{2a} \left[\left(q + \frac{3}{2} \right) \alpha^2 \dot{\beta} - \left(q + \frac{3}{2} \right) \left(\frac{1}{\alpha^2} + \alpha^2 \beta^2 \right) - \sqrt{\frac{2}{\pi}} \left(\frac{g_q S}{\alpha^3} - \frac{c_q}{\alpha} \right) \right], \quad (5.16)$$

where $g_q = \frac{(2q)!}{2^{2q}(q!)^2}$, $c_1 = \frac{23}{30}$ and $c_2 = \frac{37}{56}$.

The energy functional of the vortex state in terms of the variational parameter α is

$$E_q = \frac{NuS}{2a} \left[\left(q + \frac{3}{2} \right) \frac{1}{\alpha^2} + \sqrt{\frac{2}{\pi}} \left(\frac{g_q S}{\alpha^3} - \frac{c_q}{\alpha} \right) \right]. \quad (5.17)$$

By minimizing the energy with respect to the variational parameter α , one could obtain the equilibrium width w_q which is given by

$$w_q = \frac{\sqrt{2\pi} \left(q + \frac{3}{2} \right) + \sqrt{2\pi \left(q + \frac{3}{2} \right)^2 + 12g_q S c_q}}{2c_q}, \quad (5.18)$$

where g_q and c_q are given above. The system collapses when $S_c = -8.53694$ for $q = 1$ and $S_c = -25.8875$ for $q = 2$. This critical value S_c is increasing with an increasing of the number of vorticity. The expectation value of the square of the system radius is $I_q = \sqrt{\langle r^2 \rangle} = \sqrt{N \left(q + \frac{3}{2} \right)} w_q$. The energy functional satisfies the stability condition, $\frac{\partial^2 E_q}{\partial \alpha^2} |_{\alpha=w_q} > 0$.

The superfluid coherence length ξ is a distance over which the condensate wave function can heal. In the case of a vortex, it corresponds to the distance over which the wave function increases from zero, on the vortex axis, to the bulk density. It can be calculated by equating the kinetic energy to the interaction energies. The kinetic energy term can not be neglected even for large S , since it determines the structure of the vortex core. The system exhibits superfluid properties if the coherence length is small compared to the size of the condensed state, otherwise it will be less prominent to observe the superfluid properties. Equating the kinetic energy to the interaction energies,

$$\frac{\hbar^2}{2m\xi^2} = \frac{4\pi a N \hbar^2}{mR^3} - \frac{uN}{\xi}, \quad (5.19)$$

where $R = aN\sqrt{\frac{F}{S}}$ is the radius of the condensed state at S and

$$F = \frac{3}{2w^2} + \sqrt{\frac{8}{\pi}} \left(\frac{S}{w^3} - \frac{1}{w} \right). \quad (5.20)$$

w is given in Eq. (5.7). After rescaling the above equation, we get a quadratic equation of ξ whose solution is

$$\frac{\xi}{R} = \frac{F + \sqrt{F^2 + 8S\sqrt{F}}}{8\pi S}. \quad (5.21)$$

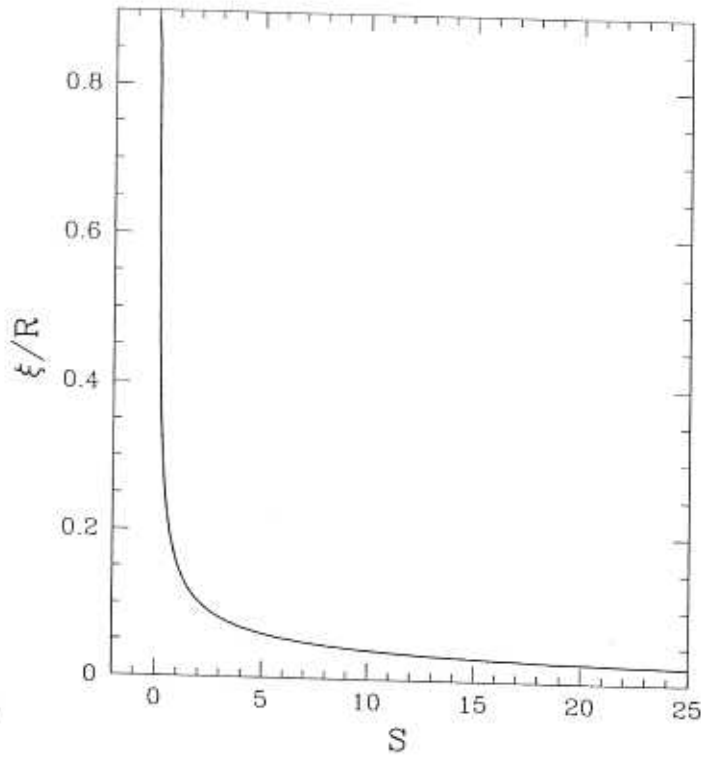


Figure 5.4: Superfluid coherence length ξ as a function of the dimensionless scattering parameter S .

The superfluid coherence length ξ/R vs S is shown in Fig. 5.4 for a wide range of S .

The vortex state play an important role in characterizing the superfluid properties of the Bose system. The critical angular frequency required to produce a vortex state is [15]

$$\Omega_q = \frac{(E_q - E_0)}{N\hbar q}, \quad (5.22)$$

where E_q is the energy of a vortex state with vortex quantum number q and E_0 is the energy with no vortex. The critical angular frequency Ω_1 vs the dimensionless scattering parameter S is shown in Fig.5.5.

The critical angular frequency decreases with increasing S (or N). For an attractive interaction, Ω_q increases with the increasing of S . This is also true for an ordinary BEC in the TF regime [15].

The monopole mode frequency of the condensate state in presence of the vortex state with a vortex number q is

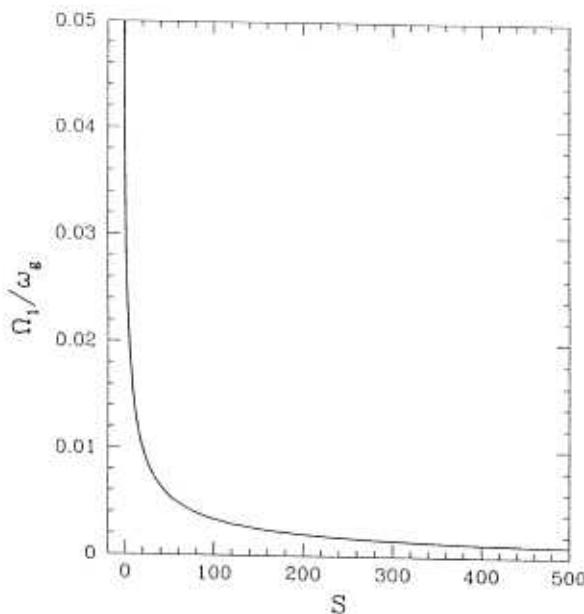


Figure 5.5: Critical angular frequency Ω_1 as a function of the dimensionless scattering parameter S .

$$\frac{\omega_q^2}{\omega_g^2} = \left[\frac{3}{w_q^4} + \sqrt{\frac{2}{\pi}} \frac{1}{\left(q + \frac{3}{2}\right)} \left(6 \frac{S g_q}{w_q^5} - \frac{c_q}{w_q^3} \right) \right], \quad (5.23)$$

where w_q is given in Eq. (5.18).

5.3.1 TF-G regime

For large s -wave scattering length, the kinetic energy can be neglected. The superfluid coherence length can be obtained from Eq. (5.21). When S is large, one gets $F = 0.6142S^{-1/2}$ from Eq. (5.20). Then, $\xi/R = 0.1765S^{-5/8}$. When S is very large, the coherence length is very small compared to the size of the system. The TF-G regime should exhibit the superfluid properties. The mean size of the condensate with $q = 1$ and $q = 2$ are $I_1 = 2.21163\sqrt{S}$ and $I_2 = 2.4412\sqrt{S}$ respectively. The size of a condensate state with vortices increases with the number of vorticity. The critical angular frequencies for $q = 1$ and $q = 2$ are $\Omega_1 = \omega_g 0.0077S^{-1/2}$ and $\Omega_2 = \omega_g 0.0094S^{-1/2}$, respectively. The monopole mode frequencies for one and two vortices are $\omega_1 = 0.299\omega_g S^{-3/4}$ and $\omega_2 = 0.26\omega_g S^{-3/4}$, respectively. These two monopole mode frequencies are less than the monopole mode frequency of the vortex-free condensate. So, in the TF-G limit, monopole mode frequency of the con-

densate decreases due to the presence of the vortex. The monopole mode frequency of an ordinary atomic BEC in the TF regime is independent of the vortex [16].

5.3.2 G regime

In this regime we neglect the contribution from the s -wave interaction energy. The superfluid coherence length ξ can be obtained by equating the kinetic energy to the gravity-like interaction energy, $\frac{\hbar^2}{2m\xi^2} = \frac{uN}{\xi}$, which gives $\xi = 0.8862R_g$ which is almost equal to the radius (R_g) of the condensed state in this regime. As we know that if the coherence length is comparable to the radius of the condensate, it is difficult to exhibit the superfluid properties. In this regime, $I_1 = 12.92$ and $I_2 = 24.84$. Here, $I_2 \gg I_1$. The size of a condensate state (with vortices) expands abruptly with an increase in the number of the vorticity. For example, $I_1/I_0 \sim 2.8$ and $I_2/I_0 \sim 5.39$, where $I_0 = 4.604$ is the mean size of the vortex-free condensate. The critical angular frequencies for $q = 1$ and $q = 2$ are $\Omega_1 = 0.0343\omega_g$ and $\Omega_2 = 0.0215\omega_g$, respectively. Here, $\Omega_2 < \Omega_1$. In this regime, the condensate state with vortex of $q = 2$ is unbounded because $|\mu_2|/\hbar < 2\Omega_2$, where $\mu_2 = -0.0297uS/a$ is the chemical potential in the rotating frame. So the vortex of $q \geq 2$ can not be created in this regime unless there is an additional repulsive potential. Note that although there is an indication of instability of vortex with $q = 2$, this may be just an artifact of the variational approach. The monopole mode frequency for $q = 1$ is $\omega_1 = 0.0149\omega_g$. The ω_1 is also less than the monopole mode frequency ω_M in the vortex-free condensate.

It should be noted that the vortex has two different length scales, the condensate radius and the core radius, whereas the trial wave function (5.15) has only one variational length scale (α). In this variational approach the various numerical values computed for the energies of the two regimes and for the collapse are just indicative, but more accurate values can be obtained by other rigorous methods.

5.4 Summary and conclusions

In this chapter we have derived an analytic expression for the monopole and quadrupole excitation frequencies of a self-bound Bose gas induced by the electromagnetic wave for a wide range of the dimensionless scattering parameter S . Later, we consider two new regimes, namely, TF-G and G regimes. In these regimes we have calculated the lower bound of the ground state energy, the sound velocity, monopole and quadrupole mode frequencies. Our results are in excellent agreement with the results [7] obtained by using the sum-rule approach. Interestingly, the ratio ω_M/ω_Q is

identical (in both the regimes) with that of [7], which is obtained within the sum-rule approach. In the TF regime of an ordinary atomic BEC, the monopole and quadrupole mode frequencies are independent of the scattering length a . On the other hand, in the TF-G regime, the monopole and quadrupole mode frequencies depend on the scattering length a . The local sound velocity c_s varies as $N^{1/2}$ in the TF-G regime, whereas $c_s \sim N^{1/5}$ for an ordinary atomic BEC in the TF regime. For a harmonic trapped Bose system, the excitation frequencies are determined by the oscillator frequency of the trap potential. But, in this system, the monopole and quadrupole mode frequencies are fixed by the gravitational frequency ω_g .

In the section 5.3, based on the time-dependent variational method and simple ansatz for the wave function (Eq. 5.15), we have studied a rotating gravity-like self-bound BEC states with vortices along the z axis. We derived an analytic expression for the coherence length and the critical angular frequency to create a vortex in the condensed state. We found that the coherence length in the TF-G regime is very very small compared to the radius of the system. On the other hand, the coherence length in the G regime is comparable to the radius of the system. We could say that the TF-G regime should exhibit the superfluid properties more prominently than the G regime. In the TF regime of an ordinary atomic BEC, the monopole mode frequency of the condensate does not change due to the presence of the vortex. But, the monopole mode frequency in the TF-G regime as well as in the G regime of this new BEC decreases due to the presence of the vortex. The change in the monopole mode frequency due to the presence of a vortex can be used to detect the vortex in the condensate since the measurements of collective excitation frequencies can be carried out with high precision. It would be interesting to study the frequency shift in the quadrupolar excitation frequencies due to the presence of the vortex in BEC with gravity-like attractive interaction.

A5 Appendix: Mean-field energy of the gravity-like potential

The mean-field energy of the gravity-like potential is

$$E_g = \frac{u}{2} \int d^3r d^3r' \frac{n(\mathbf{r})n(\mathbf{r}')}{|\mathbf{r} - \mathbf{r}'|}, \quad (\text{A5.1})$$

where $n(\mathbf{r}) = |\psi(\mathbf{r})|^2$ is the condensate density. In momentum space it can be written as

$$E_g = \frac{u}{4\pi^2} \int d^3k \frac{n(\mathbf{k})n(-\mathbf{k})}{k^2}, \quad (\text{A5.2})$$

where $n(\mathbf{k}) = \int d^3r e^{i\mathbf{k}\cdot\mathbf{r}} n(\mathbf{r})$ is the condensate density in the k space and $n(\mathbf{k}) = n(-\mathbf{k})$. In the cylindrical co-ordinate system, the above equation is

$$E_g = \frac{uN^2}{2\pi\Lambda} \int dk_\rho dz k_\rho \frac{e^{-\frac{1}{2}(\alpha_1^2 k_\rho^2 + \beta_1^2 k_z^2)}}{k_\rho^2 + k_z^2}. \quad (\text{A5.3})$$

Here, k_ρ and k_z are the dimensionless variables. Using the standard integral [17], we obtain

$$E_g = \frac{NuS}{2a} \sqrt{\frac{2}{\pi}} \frac{F\left[\frac{1}{2}, 1; \frac{3}{2}; \left(1 - \frac{\alpha_1^2}{\beta_1^2}\right)\right]}{\beta_1}. \quad (\text{A5.4})$$

B5 Appendix: Exact forms of $F_{\alpha_1}[\alpha_{10}, \beta_{10}, \delta\alpha_1, \delta\beta_1]$ and $F_{\beta_1}[\alpha_{10}, \beta_{10}, \delta\alpha_1, \delta\beta_1]$

Here, we shall give the exact form of $F[\alpha_1, \beta_1] = F\left[\frac{1}{2}, 1; \frac{3}{2}; \left(1 - \frac{\alpha_1^2}{\beta_1^2}\right)\right] / \beta_1$, its derivative with respect to α_1 , β_1 and the first order deviation from the equilibrium functions $F_{\alpha_1}[\alpha_{10}, \beta_{10}]$ and $F_{\beta_1}[\alpha_{10}, \beta_{10}]$.

$$F[\alpha_1, \beta_1] = \frac{1}{\beta_1} \left[1 + \frac{1}{3} \left(1 - \frac{\alpha_1^2}{\beta_1^2}\right) + \frac{1}{5} \left(1 - 2\frac{\alpha_1^2}{\beta_1^2} + \frac{\alpha_1^4}{\beta_1^4}\right) + \frac{1}{7} \left(1 - 3\frac{\alpha_1^2}{\beta_1^2} + 3\frac{\alpha_1^4}{\beta_1^4} - \frac{\alpha_1^6}{\beta_1^6}\right) + \dots \right]. \quad (\text{B5.1})$$

The derivative of $F[\alpha_1, \beta_1]$ with respect α_1 is given by

$$F_{\alpha_1}[\alpha_1, \beta_1] = \frac{1}{\beta_1} \left[-\frac{2}{3} \frac{\alpha_1}{\beta_1^2} + \frac{4}{5} \left(-\frac{\alpha_1}{\beta_1^2} + \frac{\alpha_1^3}{\beta_1^4}\right) + \frac{6}{7} \left(-\frac{\alpha_1}{\beta_1^2} + 2\frac{\alpha_1^3}{\beta_1^4} - \frac{\alpha_1^5}{\beta_1^6}\right) + \dots \right]. \quad (\text{B5.2})$$

Expanding $F_{\alpha_1}[\alpha_1, \beta_1]$ around the equilibrium widths α_{10} and β_{10} . The first order deviation from the equilibrium function $F_{\alpha_1}[\alpha_{10}, \beta_{10}]$ is

$$\begin{aligned} F_{\alpha_1}[\alpha_{10}, \beta_{10}, \delta\alpha_1, \delta\beta_1] &= \frac{1}{\beta_{10}} \left[-\frac{2}{3} \frac{1}{\beta_{10}^2} + \frac{4}{5} \left(-\frac{1}{\beta_{10}^2} + 3\frac{\alpha_{10}^2}{\beta_{10}^4}\right) + \frac{6}{7} \left(-\frac{1}{\beta_{10}^2} + 6\frac{\alpha_{10}^2}{\beta_{10}^4} - 5\frac{\alpha_{10}^4}{\beta_{10}^6}\right) + \dots \right] \delta\alpha_1 \\ &+ \frac{1}{\beta_{10}^2} \left[-\frac{2}{3} \frac{\alpha_{10}}{\beta_{10}^2} + \frac{4}{5} \left(-\frac{\alpha_{10}}{\beta_{10}^2} + \frac{\alpha_{10}^3}{\beta_{10}^4}\right) + \frac{6}{7} \left(-\frac{\alpha_{10}}{\beta_{10}^2} + 2\frac{\alpha_{10}^3}{\beta_{10}^4} - \frac{\alpha_{10}^5}{\beta_{10}^6}\right) + \dots \right] \delta\beta_1 \\ &+ \frac{1}{\beta_{10}} \left[\frac{4}{3} \frac{\alpha_{10}}{\beta_{10}^3} + \frac{8}{5} \left(\frac{\alpha_{10}}{\beta_{10}^3} - 2\frac{\alpha_{10}^3}{\beta_{10}^5}\right) \right] \delta\alpha_1 \delta\beta_1 \end{aligned} \quad (\text{B5.3})$$

$$+ \frac{12}{7} \left(\frac{\alpha_{10}}{\beta_{10}^3} - 4 \frac{\alpha_{10}^3}{\beta_{10}^5} + 3 \frac{\alpha_{10}^5}{\beta_{10}^7} \right) + \dots \right] \delta \beta_1. \quad (\text{B5.4})$$

The derivative of $F[\alpha_1, \beta_1]$ with respect to β_1 is given by

$$\begin{aligned} F_{\beta_1}[\alpha_1, \beta_1] = & -\frac{1}{\beta_1^2} \left[1 + \frac{1}{3} \left(1 - \frac{\alpha_1^2}{\beta_1^2} \right) + \frac{1}{5} \left(1 - 2 \frac{\alpha_1^2}{\beta_1^2} + \frac{\alpha_1^4}{\beta_1^4} \right) + \dots \right] \\ & + \frac{1}{\beta_1} \left[\frac{2}{3} \frac{\alpha_1^2}{\beta_1^3} + \frac{4}{5} \left(\frac{\alpha_1^2}{\beta_1^3} - \frac{\alpha_1^4}{\beta_1^5} \right) + \frac{6}{7} \left(\frac{\alpha_1^2}{\beta_1^3} - 2 \frac{\alpha_1^4}{\beta_1^5} + \frac{\alpha_1^6}{\beta_1^7} \right) + \dots \right] \end{aligned} \quad (\text{B5.5})$$

Expanding $F_{\beta_1}[\alpha_1, \beta_1]$ around the equilibrium widths α_{10} and β_{10} . The first order deviation from the equilibrium function $F_{\beta_1}[\alpha_{10}, \beta_{10}]$ is the following:

$$\begin{aligned} F_{\beta_1}[\alpha_{10}, \beta_{10}, \delta \alpha_1, \delta \beta_1] = & -\frac{1}{\beta_{10}^2} \left[-\frac{2}{3} \frac{\alpha_{10}}{\beta_{10}^2} + \frac{4}{5} \left(-\frac{\alpha_{10}}{\beta_{10}^2} + \frac{\alpha_{10}^3}{\beta_{10}^4} \right) + \dots \right] \delta \alpha_1 \\ & + \frac{1}{\beta_{10}} \left[\frac{4}{3} \frac{\alpha_{10}}{\beta_{10}^3} + \frac{8}{5} \left(\frac{\alpha_{10}}{\beta_{10}^3} - 2 \frac{\alpha_{10}^3}{\beta_{10}^5} \right) + \dots \right] \delta \alpha_1 \\ & + \frac{2}{\beta_{10}^3} \left[1 + \frac{1}{3} \left(1 - \frac{\alpha_{10}^2}{\beta_{10}^2} \right) + \frac{1}{5} \left(1 - 2 \frac{\alpha_{10}^2}{\beta_{10}^2} + \frac{\alpha_{10}^4}{\beta_{10}^4} \right) + \dots \right] \delta \beta_1 \\ & - \frac{2}{\beta_{10}^2} \left[\frac{2}{3} \frac{\alpha_{10}^2}{\beta_{10}^3} + \frac{4}{5} \left(\frac{\alpha_{10}^2}{\beta_{10}^3} - \frac{\alpha_{10}^4}{\beta_{10}^5} \right) + \dots \right] \delta \beta_1 \\ & + \frac{1}{\beta_{10}} \left[-2 \frac{\alpha_{10}^2}{\beta_{10}^4} + \frac{4}{5} \left(-3 \frac{\alpha_{10}^2}{\beta_{10}^4} + 5 \frac{\alpha_{10}^4}{\beta_{10}^6} \right) \right. \\ & \left. + \frac{6}{7} \left(-3 \frac{\alpha_{10}^2}{\beta_{10}^4} + 10 \frac{\alpha_{10}^4}{\beta_{10}^6} - 7 \frac{\alpha_{10}^6}{\beta_{10}^8} \right) + \dots \right] \delta \beta_1. \end{aligned} \quad (\text{B5.6})$$

Bibliography

- [1] M. H. Anderson, J. R. Ensher, M. R. Matthews, C. E. Wieman, and E. A. Cornell, *Science* **269**, 198 (1995);
C. C. Bradley, C. A. Sackett, J. J. Tollet, and R. G. Hulet, *Phys. Rev. Lett.* **75**, 1687 (1995);
K. B. Davis, M. O. Mewes, M. R. Andrews, N. J. van Druten, D. S. Durfee, D. M. Kurn, and W. Ketterle, *Phys. Rev. Lett.* **75** 3969 (1995).
- [2] Visit this web site: <http://amo.phy.gasou.edu/bec.html/>
- [3] F. Dalfovo, S. Giorgini, L. P. Pitaevskii, and S. Stringari, *Reviews of Modern Physics* **71**, 463 (1999);
A. S. Parkins and D. F. Walls, *Phys. Rep.* **303**, 1 (1998).
- [4] D. O'Dell, S. Giovanazzi, G. Kurizki and V. Akulin, *Phys. Rev. Lett.* **84**, 5687 (2000).
- [5] S. Giovanazzi, D. O'Dell, and G. Kurizki, *Phys. Rev. A* **63**, R031603 (2001).
- [6] I. E. Mazets, cond-mat/0007209.
- [7] S. Giovanazzi, G. Kurizki, I. E. Mazets, and S. Stringari, *Europhys. Lett.* **56**, 1 (2001).
- [8] E. P. Gross, *Nuovo Cimento A* **20**, 454 (1961);
L. P. Pitaevskii, *Pis'ma Zh. Eksp. Teor. Fiz.* **77**, 988 (1961) [*Sov. Phys. JETP* **13**, 451 (1961)].
- [9] Takeya Tsurumi, Hirofumi Morise, Miki Wadati. *Int. J. of Mod. Phys. B* **14**, 655 (2000).
- [10] Victor M. Perez-Garcia, H. Michinel, J. I. Cirac, M. Lewenstein, and P. Zoller, *Phys. Rev. Lett.* **77**, 5320 (1996).

- [11] S. Stringari, *Phy. Rev. Lett.* **77**, 2360 (1996).
- [12] S. Inouye, M. R. Andrews, J. Stenger, H.-J. Miesner, D. M. Stamper-Kurn, W. Ketterle, *Nature (London)* **392**, 151 (1998);
J. Stenger, S. Inouye, M.R. Andrews, H.-J. Miesner, D.M. Stamper-Kurn, W. Ketterle, *Phys. Rev. Lett.* **82**, 2422 (1999).
- [13] G. Baym and C. Pethick, *Phys. Rev. Lett.* **76**, 6 (1996).
- [14] R. Ruffini and S. Bonazzola, *Phys. Rev.* **187**, 1767 (1969), P. Jetzer, *Phys. Rep.* **220**, 163 (1992).
- [15] F. Dalfovo and S. Stringari, *Phys. Rev. A* **53**, 2477 (1996).
- [16] L. Salasnich, *Int. J. Mod. Phys. B* **14**, 1 (2000).
- [17] I. S. Gradshteyn and I. M. Ryzhik, *Table of Integrals, Series and Products* (Academic Press, New York, 1994).

Chapter 6

When the collective modes go unstable: Quantum melting of the vortex lattices in a rapidly rotating quasi-2D atomic Bose-Einstein condensate

6.1 Introduction

So far we have discussed various properties of collective excitations of non-rotating atomic Bose-Einstein condensates (BEC). What will happen if we rotate the atomic BEC? Many vortices will appear in the condensate by rotating the condensate with higher angular frequency. Recently, the ENS [1] and MIT group [2] have observed the formation of triangular vortex lattices in rapidly-rotating atomic Bose-Einstein condensate. The vortices are highly excited collective states of BEC's. These triangular lattices contained more than 130 vortices [2] with lifetimes of several seconds. The creation and observation of the triangular vortex lattices in a rapidly-rotating atomic BEC has opened a new direction for the study of quantum vortex matter. Theoretical predictions[3] for the existence of fractional quantum Hall like states at even higher rotational speeds in quasi two dimensional atomic BEC has given a further impetus to this fascinating field. The quantum melting of an ordered vortex lattice to an exotic quantum fluid of atoms at very low temperatures is a quantum phase transition, where one would like to understand the mechanism of melting and nature of phase transition.

Melting of classical solids with short range inter atomic potential in 2D

is a well studied subject, where topological defects play a fundamental role. In the presence of long range interaction, such as one component coulomb plasma in 2D, melting is dominated by ring exchanges [4] rather than topological defects. From this point of view the logarithmic repulsion among the imposed vortices in a rotating BEC provides an opportunity to study quantum melting of a 'pristine' Wigner solid with long range forces, that is free from the complications of solid state systems.

In this chapter we write down an effective Hamiltonian for the vortex degrees of freedom, motivated by an analogy [5, 6] between the Magnus force acting on a vortex moving on a two dimensional neutral superfluid and the Lorenz force acting on a charged particle in a magnetic field. We develop a theoretical approach, borrowing heavily from pioneering ideas of Kivelson, Kallin, Arovas and Schrieffer (KKAS) [7], developed in the context of fractional quantized Hall effect (FQHE), and suggest a cooperative ring exchange (CRE) mechanism for quantum melting of vortex lattices in quasi 2D atomic BEC and indicate a possible direction for a microscopic understanding of the quantum liquid of molten vortices.

In contrast to many recent theoretical works on atomic BEC which exploits an analogy between the Hamiltonian of a rotating neutral boson atoms and charge particle in an external magnetic field in two dimensions, our work uses the vortex (collective) coordinates directly and provides another microscopic approach to understand quantum melting and the quantum Hall-like state that may be formed in these atomic system. Existing theoretical works focus on exact diagonalization [8] of small number of atoms to get some idea about quantum melting and the possible quantum Hall like melted states. A recent interesting work [9] that studies melting of vortex lattices in a rapidly-rotating 2D BEC, also shows that BEC is destroyed by the vortex lattices.

Experimentally, at the present moment it is a challenging task to produce vortex liquid state in a rapidly-rotating atomic BEC, in contrast to the formation of an incompressible liquid state of electrons in a high magnetic field at higher filling fractions. With the rapid advances in the field of laser cooled atomic gases one can anticipate to get 'snapshots' of the melted configurations of the vortex lattice, where CRE should leave its unique signatures as we mention in the section of summary and conclusions.

In the cooperative ring exchange approach to FQHE, KKAS view the Laughlin quantum Hall state as a Wigner solid of electrons in 2D in strong magnetic field, that has been quantum melted by cooperative ring exchange processes. Briefly, ring exchange, as the name suggests, is a cooperative shift of a ring of contiguous

particles in an ordered lattice (figure 1) resulting in a cyclic permutation within the ring. While the amplitude for a quantum tunneling event of a specific ring of size L sites is exponentially small $\sim \alpha^L$ (with α , the single particle tunneling amplitude being < 1), the number of rings of size L is exponentially large $\sim e^{bL}$. Thus the total amplitude $\sim \alpha^L e^{bL}$ may exponentially diverge, if $-\ln \alpha < b$, leading to a proliferation of ring exchanges and a consequent quantum melting.

This melting depends on the electronic filling fraction, the ratio between the density of conduction electrons and the density of flux quanta. For very low filling fraction, electrons are expected to form a Wigner crystal. At higher filling fraction, electrons form an incompressible liquid state and exhibit quantized Hall effect. Similarly, we could also expect the quantum melting of the vortex lattices depends on the vortex filling factor, the ratio of the total number of vortex to the total number of boson.

This chapter is organised as follows. In section [6.2] we write down an effective Hamiltonian for the vortex degrees of freedom. In section [6.3] we review the coherent state path integration and rederive the action for vortices in a pseudomagnetic field generated by the background neutral superfluid Bose particles. In section [6.4] we suggest cooperative ring exchange as a mechanism of quantum melting of the vortex lattices. We calculate the tunneling coefficient in section [6.5]. We present a summary and conclusions of this chapter in section [6.6].

6.2 Hamiltonian of the vortices in a rapidly rotating quasi-2D BEC

We consider a large number of vortices in a rapidly rotating quasi 2D BEC; rapid rotation in a quasi 2D condensate is defined as $\rho_0 g_2 < \hbar \omega_z$ and $\rho_0 g_2 < 2\hbar \Omega$. Here, ρ_0 is the boson density and $g_2 = 2\sqrt{2\pi}\hbar\omega_z a_z a$ is the effective interaction strength in quasi-2D Bose system [10]. Also, Ω is the trap rotational frequency and ω_z is the trap frequency in the axial (z) direction. Recently, the quasi-2D Bose condensate (non-rotating) has been realized at MIT [11]. A vortex in a fluid is an excitation in which each fluid particle is given an angular momentum m relative to the vortex center. Consequently, the velocity field $\mathbf{v}(\mathbf{r})$ of the fluid satisfies $\oint_C \mathbf{v} \cdot d\mathbf{l} = \frac{2\pi m}{m_0}$, where m_0 is the mass of the fluid particle and C is the curve that encloses the vortex center. Here, we treat a vortex as a point particle moving under the influence of the Magnus force. The Magnus force is an effective interaction between superfluid particles and

vortices in relative motion [5, 6]. The force acting on a single vortex is then

$$\mathbf{F} = \mathbf{v} \times \hat{z}(2\pi\hbar\rho_0), \quad (6.1)$$

where \mathbf{v} is the vortex velocity relative to the superfluid particles and ρ_0 is the superfluid particle density. The Magnus force is equivalent to the Lorentz force acting on a charge particle (e) in a magnetic field. Hence, $eB_{\text{eff}} = 2\pi\hbar\rho_0$ is the pseudo magnetic field.

The interaction potential between two vortices separated by a distance r is

$$V(r) = \frac{2\pi\hbar^2\rho_0}{m_0} \ln\left(\frac{r}{\xi}\right), \quad (6.2)$$

where $\xi \sim \sqrt{\frac{a_s}{\rho_0 a}}$ is the coherence length of the vortex core and m_0 is the mass of a superfluid particle. The above potential is valid only when the distance between two vortices is large compared to the coherence length. Notice that the interaction strength between two vortices depends on the superfluid density as well as the s -wave scattering length.

The Hamiltonian of a rotating BEC containing vortices can be written in terms of center of vortices (collective coordinate) as [5]

$$H_v = \sum_{i=1}^{N_v} \frac{(\mathbf{p}_i - \pi\hbar\rho_0\hat{z} \times \mathbf{r}_i)^2}{2m_v} + \frac{2\pi\hbar^2\rho_0}{m_0} \sum_{i<j} \ln\left[\frac{|\mathbf{r}_i - \mathbf{r}_j|}{\xi}\right], \quad (6.3)$$

where N_v is the total number of vortices and m_v is an effective mass of the vortex. The effective mass m_v can be in principle derived from a microscopic approach [5]. This Hamiltonian is similar to that of charged particles moving under the influence of the Lorentz force by a magnetic field B_{eff} . The pseudo vector potential due to the Magnus force is,

$$\mathbf{A}_{\text{eff}} = -\frac{1}{2}\mathbf{r} \times \mathbf{B}_{\text{eff}}. \quad (6.4)$$

For N_v number of vortices in an area A , one gets the vortex filling factor,

$$\nu_v = \frac{N_v}{A} \frac{h}{eB_{\text{eff}}} = \frac{N_v}{N}, \quad (6.5)$$

where N is the number of the superfluid particles. Notice that the vortex filling factor ν_v is just inverse of the bosonic filling factor $\nu_b = \frac{N}{N_v}$. For large N_v the vortex density is approximately uniform and $N_v = (2m\omega A)/(\hbar)$. The eigen spectrum of the single vortex Hamiltonian is uniformly spaced with energy gap $\hbar\omega_{\text{eff}}$, where $\omega_{\text{eff}} = \frac{2\pi\hbar\rho_0}{m_v}$ is the effective cyclotron frequency. It has been shown that the mass of the vortex is zero or finite but small [5]. The limit of $m_v \rightarrow 0$ and/or large

density (ρ_0) is equivalent to the vortices are in the lowest Landau level (LLL). We can project the Hamiltonian onto the LLL and the corresponding wave functions are degenerate eigenfunctions of the angular momentum m given by

$$\psi(z) = \frac{1}{\sqrt{(2l_0^2)^{m+1}\pi m!}} z^m e^{-\frac{|z|^2}{4l_0^2}}, \quad m = 0, 1, 2, \dots \quad (6.6)$$

where $z = x + iy$ and (x, y) are the position coordinate of a vortex. The effective magnetic length is $l_0 = \sqrt{\frac{\hbar}{eB_{\text{eff}}}} = \frac{1}{\sqrt{2\pi\rho_0}}$. This is the smallest length scale in this problem. When the vortices are confined to the lowest Landau level, the kinetic degrees of freedom of the vortices are frozen, since the spacing between Landau levels, $\hbar\omega_{\text{eff}}$, is large compared to all other energies in the problem. Hence the vortices in the LLL will remain localized about a given guiding center \mathbf{R} indefinitely. The guiding center coordinate \mathbf{R} specify the center of a Gaussian-localized probability amplitude of width l_0 .

6.3 Coherent state path integration

In symmetric gauge, the wave function of a vortex in the LLL with guiding-center position \mathbf{R} is

$$\phi_{\mathbf{R}}(\mathbf{r}) = \frac{1}{\sqrt{2\pi l_0^2}} \exp \left[-\frac{|\mathbf{r} - \mathbf{R}|^2}{4l_0^2} + \frac{i(\mathbf{r} \times \mathbf{R}) \cdot \hat{z}}{2l_0^2} \right]. \quad (6.7)$$

It has the same form as a coherent state in a two-dimensional phase space [12]. Here, the state label \mathbf{R} is a continuous variable. The coherent state overlap is given by,

$$\langle \mathbf{R}_1 | \mathbf{R}_2 \rangle = \exp \left[-\frac{|\mathbf{R}_1 - \mathbf{R}_2|^2}{4l_0^2} + \frac{i(\mathbf{R}_1 \times \mathbf{R}_2) \cdot \hat{z}}{2l_0^2} \right]. \quad (6.8)$$

This coherent state $|\mathbf{R}\rangle$ forms a nonorthogonal, overcomplete basis. Nevertheless, the projection operator P onto the LLL is given by,

$$P = \int \frac{d^2 R}{2\pi l_0^2} |\mathbf{R}\rangle \langle \mathbf{R}| \quad (6.9)$$

which is unity within the LLL since $\langle \mathbf{R}_1 | P | \mathbf{R}_2 \rangle = \langle \mathbf{R}_1 | \mathbf{R}_2 \rangle$.

We use the coherent state path integral [12, 13] expression for the partition function to calculate the tunneling coefficient of a vortex. The partition function for 2D interacting vortices in a pseudomagnetic field due to the Magnus force is

$$Z(\nu_v) = \text{Tr} e^{-\beta H_v}. \quad (6.10)$$

Here, we discuss the main features of this formalism for a single vortex in the LLL in the complex plane. This can be generalized for many vortex system very easily. The coherent state in the complex plane is

$$|R\rangle = \frac{1}{\sqrt{2\pi l_0^2}} \exp\left[\frac{zR^* - z^*R}{4l_0^2}\right] \exp\left[-\frac{|z - R|^2}{2l_0^2}\right], \quad (6.11)$$

where $R = X + iY$ is the guiding center coordinate of a vortex in the complex plane and the asterisk denotes the complex conjugation. The coherent state overlap in the complex plane is

$$\langle R_j | R_k \rangle = \exp\left[\frac{R_j R_k^* - R_j^* R_k}{4l_0^2}\right] \exp\left[-\frac{|R_j - R_k|^2}{2l_0^2}\right] \quad (6.12)$$

$$= \exp\left[-\frac{1}{4l_0^2} [R_j^* (R_j - R_k) - (R_j^* - R_k^*) R_k]\right]. \quad (6.13)$$

Now the path integral representation of the partition function $Z(\nu_v)$ can be obtained in the usual way. First, we split the inverse temperature β into a large number of equal intervals $\epsilon = \beta/n$, i.e., $e^{-\beta V}$ is written as $[e^{-\epsilon V}]^n$, and then insert the projection operator P at each infinitesimally small interval. Then,

$$\langle R_f | e^{-\beta V} | R_i \rangle = \int \prod_{k=1}^n \frac{d^2 R_j}{(2\pi l_0^2)^n} \prod_{j=0}^n \langle R_{j+1} | e^{-\epsilon V} | R_j \rangle, \quad (6.14)$$

where $R_0 = R_i, R_{n+1} = R_f$. In general, the Hamiltonian can be written

$$V(R_j^*, R_k) = \frac{\langle R_j | V | R_k \rangle}{\langle R_j | R_k \rangle}. \quad (6.15)$$

The matrix element can be written as,

$$\begin{aligned} \langle R_f | e^{-\beta H} | R_i \rangle &= \int \prod_{k=1}^n \frac{d^2 R_j}{(2\pi l_0^2)^n} \prod_{j=0}^n \langle R_{j+1} | R_j \rangle \\ &\times [1 - i\epsilon V(R_{j+1}^*, R_j) + O(\epsilon^2)] \end{aligned} \quad (6.16)$$

We are neglecting terms of $O(\epsilon^2)$ and higher order terms by standard procedure. Using Eq.(6.12), and

$$\frac{dR_j}{dt} = \frac{R_{j+1} - R_j}{\epsilon} \quad (6.17)$$

we obtain

$$Z(\nu_v) = \int \prod_{k=1}^n \frac{d^2 R_j}{(2\pi l_0^2)^n} \exp\left[i\epsilon \left\{ \sum_{j=0}^n \frac{i}{4l_0^2} \left(R_j^* \frac{dR_j}{dt} - \frac{dR_j^*}{dt} R_{j+1} \right) - V(R_j^*, R_{j+1}) \right\}\right]. \quad (6.18)$$

The path integral is

$$\begin{aligned} Z &= \int \prod_{k=1}^n \frac{d^2 R_k}{(2\pi l_0^2)^n} \times \exp \left\{ -i \int_0^\beta dt \left[\frac{1}{4l_0^2} \left(R^* \frac{dR}{dt} - \frac{dR^*}{dt} R \right) + V(R^*, R) \right] \right\} \\ &= \int D[\mathbf{R}] e^{iS[\mathbf{R}]} \end{aligned} \quad (6.19)$$

This action is linear in time derivatives and hence discontinuous paths have finite action. It implies that the coherent state path integral is dominated by discontinuous paths and the limits is ill defined. Despite these difficulties, the continuum version of the path integral can be used to develop a saddle-point approximation for the partition function [7]. We are interested in the semiclassical limit when $V(R)$ is a slowly varying function of its argument over the length scale l_0 and we can use the saddle point approximation to evaluate the path integral.

The single vortex path integral generalized to many vortex path integral directly parallels that of the single vortex problem. The action for many vortex is

$$S(\mathbf{R}) = \int_0^\beta dt \left[\frac{1}{2} \sum_{j=1}^{N_v} (\dot{\mathbf{R}}_j \times \mathbf{R}_j) \cdot \hat{z} + \sum_{j < k} V(\mathbf{R}_j - \mathbf{R}_k) \right] \quad (6.20)$$

$V(R) = \langle \phi_{\mathbf{R}}(\mathbf{r}) | V(\mathbf{r}) | \phi_{\mathbf{R}}(\mathbf{r}) \rangle$ is two-body interaction potential in coherent states representation. In the saddle point-approximation, the classical path is obtained by minimizing the action, $\frac{\delta S}{\delta \mathbf{R}_j(\tau)}|_{R=R_c} = 0$. The classical paths satisfy the following equations of motion,

$$\dot{\mathbf{R}}_j = \frac{l_0^2}{\hbar} (\nabla_j V_j) \times \hat{z}, \quad (6.21)$$

where $V_j = \sum_{k \neq j} V(\mathbf{R}_j - \mathbf{R}_k)$. The guiding center dynamics in presence of a potential $V(\mathbf{R})$ is equivalent to the quantum dynamics of a particle in a two-dimensional phase space such that X plays the role of the spatial coordinate, Y that of the momentum of the particle, and l_0^2 plays the role of \hbar since $[X, Y] = i l_0^2$.

The path integral can be expressed as a sum over saddle point contribution in which the contribution of paths in the neighborhood of each classical path is evaluated by expanding the action to quadratic order in $R - R_c$. The partition function Z is calculated within the semiclassical approximation. The partition function can be expressed as a sum over classical paths, assuming the vortices to be bosons,

$$Z = \sum_c D[R_c] e^{-S[R_c]}, \quad (6.22)$$

where $D[R_c]$ is the fluctuation determinant. There are interesting issues [14] about the statistics of vortices in a compressible superfluid such as ours, and we will not

worry about it in this Thesis. The partition function Z can be written by considering only the leading order contribution as [7]

$$Z = Z_0 \sum_c \tilde{D}[R_c] e^{-S_0[R_c]} \quad (6.23)$$

where $S = S_0 + \tilde{S}$. Let us consider the contribution of a single large exchange ring to Z . The real part of the action would be $\alpha_0 L$, where L is the number of vortices in the ring and α_0 is independent of path. The fluctuation determinant [7] is $\tilde{D}[R_c] = -\tau_0^{-1} d\tau \exp[-\delta\alpha L + O(\ln L)]$, where τ_0 is the cooperative tunneling time. We expect that the contribution from the fluctuation determinant is very small, which renormalized α_0 . The imaginary part, the phase change as a cooperative motion along a ring is

$$\theta = \oint e \mathbf{A}_{\text{eff}} \cdot d\mathbf{l} = 2\pi N, \quad (6.24)$$

where N is the number of the superfluid particles enclosed by the ring [14]. This is the analog of the corresponding result for a charged particle moving in a magnetic field.

6.4 Cooperative ring exchange mechanism

How do the collective modes go unstable? To understand the melting of the vortex lattices, the Lindemann criteria can not be used here since it is used in the melting of classical solids. The vortices are not executing almost independent thermal motions as in a classical solid. The dynamics of the present problem is governed by a Hamiltonian with only first-order time derivatives, which give rise to its own peculiar properties. We give an argument how Wigner crystal can melt at $T = 0$. If we consider a rigid Wigner solid and allow one ring of vortices to tunnel coherently they see a periodic potential with the periodicity of the lattice (figure 6.1). If we observe the coherent motion of one chain over a long time compared to τ_0 , the potential that it sees will not be periodic. The physically important rings being one-dimensional and long, this can result in the destruction of the long-range order along the chain rather easily. This in turn will feed back and affect the rest of the neighborhood, resulting possibly in a molten state. This will also result in the path of the wave packets of vortices being displaced away from the edges of the triangle of the lattice. This means that the self-consistent potential seen by an vortex no longer has a component which has long-range order.

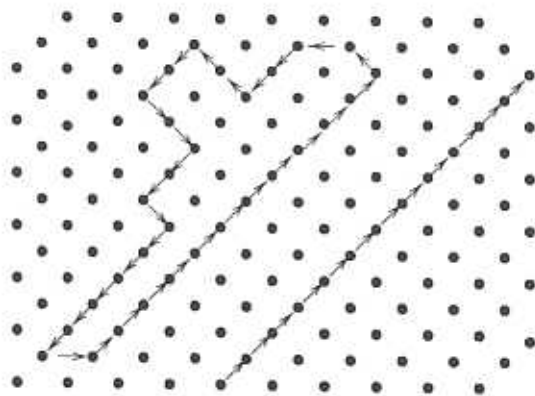


Figure 6.1: A schematic diagram of cooperative ring exchange events on a ring and line

6.5 Calculation of the tunneling coefficient

The numerical value of the tunneling coefficient $\alpha(\nu_v)$ determines whether the vortices form the liquid state or Wigner crystal. To estimate this tunneling coefficient we consider the following simple exchange path which is shown in Fig.6.1. Consider the path in which one row of vortices exchanges one step in the X direction in the background of the static potential of all other vortices, $X_i(\beta) = X_i(0) + d$ and $Y_i(\beta) = Y_i(0)$, where $d = \sqrt{\frac{4\pi}{3\nu_v}} l_0$ is the lattice constant of the Wigner crystal for a given density ν_v . There is no net phase change since this straight path does not enclose any area. We are imposing the periodic boundary conditions in the X direction, $X_i(\tau) = X_{i+L}(\tau)$.

For $|Y_j| \ll d$, the actual potential can be approximated by,

$$\begin{aligned} \frac{V}{\hbar\Omega} = & \frac{4\pi}{\sqrt{3\nu_v}} \left\{ \sum_{j=1}^L \left[\frac{Q_y}{2} Y_j^2 + \frac{Q_x}{(2\pi)^2} (1 - \cos(2\pi X_j)) \right] \right. \\ & \left. + \frac{1}{2} \sum_{j>k} [K_x(j-k)(X_j - X_k)^2 + K_y(j-k)(Y_j - Y_k)^2] \right\}, \quad (6.25) \end{aligned}$$

where X_j 's and Y_j 's are in units of the lattice constant d . Here, $K_x(j-k) = \frac{\partial^2 V_{jk}}{\partial X_j \partial X_k} |_{R_C}$ and $K_y(j-k) = \frac{\partial^2 V_{jk}}{\partial Y_j \partial Y_k} |_{R_C}$ are evaluated along the classical paths. For example, the best fit to the actual potential is obtained with $\frac{Q_x}{Q_y} \sim 0.6$ for $\nu_v \sim \frac{1}{2}$. Notice that $Q_x/Q_y < 1$ implies that when the one-dimensional chain moves coherently in the

X direction, the potential barrier is much less than in the Y direction compared to that of the Y direction.

The dimensionless Euclidian action is given by,

$$S = \frac{4\pi}{\sqrt{3}\nu_v} \left\{ \sum_j \left[\frac{i}{2} \dot{X}_j Y_j + \frac{Q_y}{2} Y_j^2 + \frac{Q_x}{(2\pi)^2} (1 - \cos(2\pi X_j)) \right] \right. \quad (6.26)$$

$$\left. + \frac{1}{2} \sum_{j>k} \left[K_x(j-k) (X_j - X_k)^2 + K_y(j-k) (Y_j - Y_k)^2 \right] \right\}. \quad (6.27)$$

Since S is a quadratic form in Y_j , the motion in the Y direction can be integrated out exactly. After doing the Y_j integration, we get an effective action S_{eff} for the X motion with a quadratic kinetic energy,

$$S_{\text{eff}} = \frac{1}{\sqrt{3\pi}\nu_v} \int_0^\beta d\tau \left\{ \sum_{j<k} \left[\frac{1}{2} \dot{\phi}_j M(j-k) \dot{\phi}_k + \frac{1}{2} K_x(j-k) (\phi_j - \phi_k)^2 \right] \right. \quad (6.28)$$

$$\left. + \sum_j \frac{Q_x}{(2\pi)^2} (1 - \cos(\phi_j)) \right\}, \quad (6.29)$$

where τ is the imaginary time variable, $\phi_j = 2\pi X_j$ and

$$(M(j-k))^{-1} = \frac{1}{8} \left[\left(\frac{Q_y}{2} + \sum_j K_y(j) \delta_{jk} \right) - \sum_{j<k} K_y(j-k) \right]. \quad (6.30)$$

S_{eff} is the action for a one-dimensional sine-Gordon chain. The classical path satisfying the boundary conditions $\phi_j(0) = 0$ and $\phi_j(\beta) = 2\pi$, correspond to the simultaneous coherent motion of all the vortices, i.e. $\phi_j(\tau) = \phi_0(\tau)$. Hence, $S[R_c] = \alpha_0 L$, where $\alpha_0(\nu_v) = \frac{4}{\sqrt{3\pi}\nu_v} \sqrt{\frac{Q_x}{Q_y}}$. The α_0 is independent of K 's. To evaluate the fluctuation determinant we have to take the continuum limit of the effective action S_{eff} . To take a continuum limit of equation (6.28), $(\phi_j - \phi_k)$ is replaced by $(j-k)\partial_x \phi$, but $\sum_j j^2 K_x(j)$ is diverging linearly. This procedure does not work and the continuum model must be constructed with care. Here, we do not calculate the $\delta\alpha$ which will be very small and it does not change the result drastically.

All the contributions from ring exchanges happening in a time interval τ_0 are summed by modeling the change in the action by a discrete Gaussian model in an imaginary field

$$H_{DG} = \alpha(\nu_v) \sum (S_\lambda - S_\gamma)^2 + ih(\nu_v) \sum S_\lambda, \quad (6.31)$$

where S_λ is an integer variable associated with every triangle in the lattice. S_λ counts the number of clockwise minus counterclockwise ring exchanges that surround

a plaquette λ . The function $\alpha(\nu_v) = \alpha_0(\nu_v) + \delta\alpha(\nu_v)$ is a measure of the tunneling barrier. The function $h(\nu_v)$ is the phase factor which arises as a result of the pseudo magnetic flux enclosed by the exchange rings. This model is known to have a phase transition [15] at a critical value of $\alpha = \alpha_c(\nu_v) \sim 1.1$ [7]. For $\alpha(\nu_v) > \alpha_c(\nu_v)$, the ground state is a vortex Wigner crystal and for $\alpha(\nu_v) < \alpha_c(\nu_v)$, the ground state is a quantum mechanical vortex liquid state. In our calculation we find the tunneling coefficient is $\alpha_0 \sim 1.1$ when $\nu_v \sim \frac{1}{2}$. So the quantum melting will occur at $\nu_v \sim \frac{1}{2}$. When $\nu_v > \frac{1}{2}$, the vortices form the liquid state where as for $\nu_v < \frac{1}{2}$, the vortices form the Wigner crystal. Current experiments [1, 2] with $\nu_v \ll \frac{1}{2}$ are in the regimes of vortex lattice ground state. Based on the exact diagonalization, Cooper *et al.* [8] have calculated the vortex filling factor ν_v , at which melting instability occurs to be $\frac{1}{6}$. Based on the Lindemann criteria, Sinova *et al.* [9] have shown that the melting instability occurs when the vortex filling factor is $\frac{1}{8}$. Our result is consistent with the experimental result [8, 9], but does not match very well with the results based on the exact diagonalization [8] and the Lindemann criteria [9].

6.6 Summary and conclusions

In this chapter, we treated the vortices as new degrees of freedom and considered a model Hamiltonian of these interacting vortices produced in a rapidly-rotating atomic BEC. Later, we assumed that the vortices are in the lowest Landau level due to the low mass of the vortices and the high densities of the Bose superfluid particles. We rederived the action for many vortices by using the coherent state path integral method. The cooperative ring exchange is suggested as a mechanism of the quantum melting of the vortex lattices in atomic Bose condensed state. Finally, we estimated the tunneling coefficient by considering the contribution of large-correlated ring exchanges to the energy of a vortex Wigner crystal in a strong pseudomagnetic field generated by the superfluid Bose particles. We find that the vortices form the Wigner crystal when $\nu_v < \frac{1}{2}$. Latest experiments [1] with $N \sim 10^5$, $N_v \sim 10$ ($\nu_v \sim 10^{-4}$) and [2] with $N \sim 10^5$, $N_v \sim 100$ ($\nu_v \sim 10^{-3}$) are in the regime in which the ground state is a vortex lattice. Our result is consistent with the experimental observation, but our result does not match very well with other results [8, 9]. It is challenging for experimentalists to produce a vortex liquid state in a rotating Bose condensed state.

Our work, resulting in a discrete Gaussian model (6.31) predicts Laughlin like even denominator hierarchy (bosonic vortex filling factor $\nu_v = \frac{1}{2p}$, where p is an

integer) to emerge on quantum melting. We can also determine the asymptotic form of the wave functions [16]. Along with a rich phase structure the discrete Gaussian model also determines the nature of the quantum melting transition. To the extent the vortex degrees of freedom retain their identity, the results of CRE approach may remain valid in the quantum melted region. This needs to be investigated further.

As mentioned in the introduction, CRE processes should leave its finger print as specific fluctuation patterns (figure 1) that preempts quantum melting. It should be interesting to look for snapshots of such displaced large rings in the actual vortex lattice imaging.

A6 Appendix: Calculation of the parameters Q_x and Q_y

Here, we show how to calculate the parameters Q_x and Q_y . We consider the simplest possible exchange path, namely one line of vortices shifting coherently within the Wigner crystal. When the line \mathcal{L} is displaced, we have $\mathbf{R}_i = \mathbf{T}_i + \mathbf{d}\delta_{i \in \mathcal{L}}$, with $\delta_{i \in \mathcal{L}}$ unity if and only if lattice site i lies on the line in question. The matrix element of the potential between two vortices in coherent basis state is

$$V(\mathbf{R}) = \langle \phi_{\mathbf{R}}(\mathbf{r}) | V(\mathbf{r}) | \phi_{\mathbf{R}}(\mathbf{r}) \rangle \quad (\text{A6.1})$$

Accordingly, the energy of the displaced line configuration relative to that of the perfect Wigner crystal is

$$\Delta E = \sum_{\langle i, j \rangle} [V(\mathbf{R}_i - \mathbf{R}_j) - V(\mathbf{T}_i - \mathbf{T}_j)]. \quad (\text{A6.2})$$

This sum is broken up into three terms. The first term includes all pairs (i, j) in which both sites i and j lie off the line. This contribution to ΔE is zero. The second term involves all pairs (i, j) where one of the sites, say i , is on the line and the other, j , is off:

$$\Delta E_2 = \sum_{i \in \mathcal{L}, j \notin \mathcal{L}} [V(\mathbf{T}_i + \mathbf{d} - \mathbf{T}_j) - V(\mathbf{T}_i - \mathbf{T}_j)]. \quad (\text{A6.3})$$

Clearly the line energy is extensive, hence the energy per tunneling of the vortex can be written

$$U(\mathbf{d}) = \Delta E_2 / L = \sum_{j \notin \mathcal{L}} [V(\mathbf{T}_j - \mathbf{a}) - V(\mathbf{T}_j)], \quad (\text{A6.4})$$

where we have chosen the origin to lie on the line. The third and final term is that arising from both i and j on the line. Since the tunneling is cooperative, this contribution to the classical action vanishes.

By allowing one line of vortices to tunnel coherently along the line, one can fit the change in energy into a periodic potential with the appropriate choice of the parameter Q_x . On the other hand, by allowing one line of vortices to tunnel coherently perpendicular to the line, one can fit the change in energy into a quadratic potential with appropriate choice of the parameter Q_y .

Bibliography

- [1] K. W. Madison, F. Chevy, W. Wohleben, and J. Dalibard, Phys. Rev. Lett. **84**, 806 (2000).
- [2] J. R. Abo-Shaeer, C. Raman, J. M. Vogels, and W. Ketterle, Science **292**, 476 (2001).
- [3] N. K. Wilkin and J. M. F. Gunn, Phys. Rev. Lett. **84**, 6 (2000); S. Viefers, T. H. Hansson and S. M. Reimann, Phys. Rev. A **62**, 053604 (2000); Tin-Lun Ho, Phys. Rev. Lett. **87**, 060403 (2001).
- [4] Ph. Choquard, and J. Clerouin, Phys. Rev. Lett. **50**, 2086 (1983).
- [5] Q. Niu, P. Ao, and D. J. Thouless, Phys. Rev. Lett. **72**, 1706 (1994).
- [6] R. J. Donnelly, *Quantized Vortices in Helium II*, (Cambridge, 1991).
- [7] S. Kivelson, C. Kallin, D. P. Arovas, and J. R. Schrieffer, Phys. Rev. Lett. **56**, 873 (1986);
S. Kivelson, C. Kallin, D. P. Arovas, and J. R. Schrieffer, Phys. Rev. B **36**, 1620 (1987).
- [8] N. R. Cooper, N. K. Wilkin, J. M. F. Gunn, Phys. Rev. Lett. **87**, 120405 (2001).
- [9] Jairo Sinova, C.B. Hanna, and A. H. MacDonald, Phys. Rev. Lett. **89**, 030403 (2002).
- [10] Tin-Lun Ho and Michael Ma, J. Low Temp. Phys. **115**, 61 (1999).
- [11] A. Gorlitz *et al*, Phys. Rev. Lett. **87**, 130402 (2001).
- [12] L. Schulman, *Techniques and Applications of Path Integration*, (Wiley New York, 1981).
- [13] S. M. Girvin and T. Jach, Phys. Rev. B **29**, 5617 (1984).

- [14] R. Y. Chiao, A. Hansen and A. A. Moultrop, Phys. Rev. Lett. **54**, 1339 (1985);
F. D. M. Haldane, and Y. S. Wu, Phys. Rev. Lett. **55**, 2887 (1985).
- [15] S. T. Chui and J. D. Weeks, Phys. Rev. B **14**, 4978 (1976).
- [16] Dung-Hai Lee, G. Baskaran and S. A. Kivelson, Phys. Rev. Lett. **59**, 2467 (1987).

Chapter 7

Inner structure of collective modes: Modeling two-magnetoroton bound state formation in fractional quantum Hall systems

7.1 Introduction

In this chapter we consider fractional quantum Hall system at $\nu = \frac{1}{3}$ filling fraction [1]. This $\nu = \frac{1}{3}$ state was explained successfully by Laughlin's pioneering work [2]. Using the single mode approximation, Girvin, Macdonald and Platzman (GMP) [3] analyzed the collective excitation spectrum of fractional quantum Hall states. In the single mode approximation a neutral excitation is defined by (unnormalized) wave function $\psi_q = P_{LLL}\rho_q\psi_L$, where $\rho_q = \sum_i e^{iq\cdot r_i}$ and P_{LLL} is the projection operator onto the lowest Landau level. This dispersion curve has finite gap at $k = 0$, quite different from the case of superfluid helium and trapped Bose gas in which mode is gapless. The minimum of energy ($E_{\min} = E_{\text{rot}}$) occurred at $k = k_0$ and this excitation was called magnetoroton, by analogy with roton of liquid ^4He [4]. The pioneering work of GMP brought out non-trivial inner structure of neutral excitations of the fractional quantum Hall effect (FQHE) systems. This inner structure is very transparent for the magnetoroton, the minimum energy neutral excitations at a finite wave vector $k_0 l_0 \sim 1.4$ for the $\nu = \frac{1}{3}$ quantum Hall state. They are well approximated by a Laughlin quasi-hole ($\frac{\epsilon}{3}$) - quasi-particle ($-\frac{\epsilon}{3}$) bound

state, as shown in Fig. 7.1a. The composite fermion (CF) [5] approach, that goes beyond Laughlin hierarchy of $\frac{1}{m}$ filling, views the neutral excitations as a *composite fermion interband excitons* of the ‘pseudo’ Landau bands. The CF approach has also suggested variational schemes that is amenable to numerical studies. Theoretical studies of neutral excitations have become meaningful in the light of the Raman scattering experiments [6, 7].

It was observed by GMP [3] that the zero momentum neutral excitation, as observed by numerical experiment [8] was in disagreement with their result at $E(k=0)$. Since the numerically observed results was slightly less than $2E_{\text{rot}}(k=k_0)$, they speculated that the minimum energy excitation could be a two-magnetoroton bound state, as shown in Fig. 7.1b. Within the Landau-Ginzburg theory, Lee and Zang [9] also proposed that the $k=0$ excitation consists of two dipoles (two magnetorotons), arranged in such a way that it has quadrupole moment but the net dipole moment is zero. Two-roton bound states are suspected to occur in liquid ^4He [10].

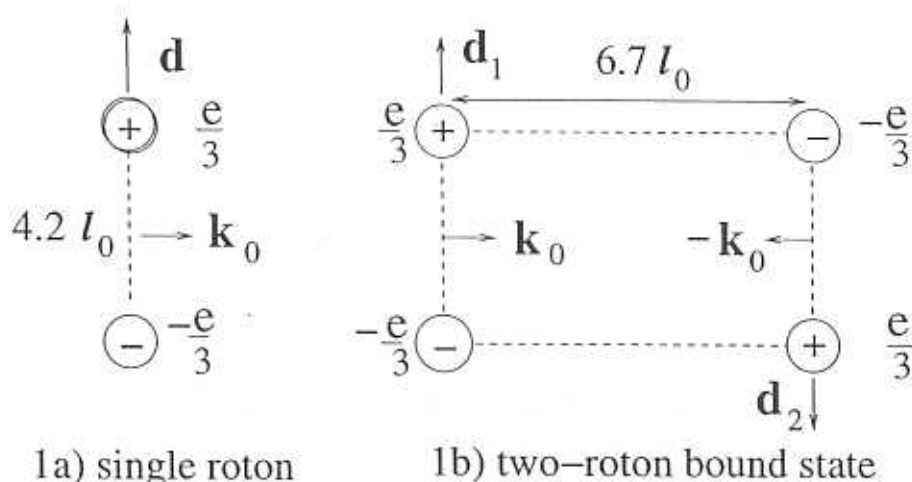


Figure 7.1: Schematic diagrams for (a) a single magnetoroton with momentum \mathbf{k}_0 and (b) a two-magnetoroton bound state with total momentum $\mathbf{K} = 0$.

Park and Jain [11] have extended their CF exciton theory of magnetoroton to two-magnetoroton bound state problem. Using parallel computing technique, they have handled upto 30 particle systems. They have shown very convincingly that the zero momentum lowest energy excitations is a two-magnetoroton bound

state.

The aim of this chapter is to provide an effective microscopic model that uses the essential structure of magnetoroton. In our parameter free theory we get the binding energy of a two-magnetoroton bound state which is in good agreement with the extensive finite particle system study result in the CF approach.

This chapter is organised as follows. In section [7.2] we discuss dynamics of a magnetoroton and show that the magnetoroton is an *oriented dipole* analogous to the description of a magnetic exciton [12, 13, 14] as well as Read's [15] dipole description of the neutral composite fermion at $\nu = \frac{1}{2}$. In section [7.3] we write down the kinetic energy operator for magnetorotons. We also derive velocity dependent effective interaction between two magnetorotons by using the oriented character of the dipole moment, analogous to the velocity dependent interaction found by G. Baskaran [16], in the context of BCS instability of composite Fermi liquid. In section [7.4] we propose a variational wave function for two-magnetoroton bound state. In section [7.5], the resulting two body problem is solved variationally to find a bound state. We present a summary and conclusions of this chapter in section [7.6].

7.2 Dynamics of a magnetoroton

According to Laughlin [2], the elementary charged excitations, at the filling fraction $\nu = \frac{1}{m}$ (m is an odd integer), are quasiparticles (qp) and quasiholes (qh) with fractional charge $\pm \frac{e}{m}$. The effective magnetic length for a particle with fractional charge $\frac{e}{m}$ is $l_0 \sqrt{m}$, where $l_0 = \sqrt{\frac{\hbar c}{eB}}$ is the magnetic length for a particle with charge e . A magnetoroton with wave vector $|\mathbf{k}|$ is a bound state of a qp and qh separated by a large distances $mk l_0^2$. A qp and qh have an attractive Coulomb interaction $V(\mathbf{r}) = -\frac{e^2}{m^2 \epsilon r}$. In lowest Landau level at filling fraction $\nu = \frac{1}{m}$, they obey the following guiding center dynamics [15, 16]

$$\frac{d\mathbf{r}_e}{dt} = \frac{m l_0^2}{\hbar} \nabla_e V(\mathbf{r}_e - \mathbf{r}_h) \times \hat{z}, \quad (7.1)$$

$$\frac{d\mathbf{r}_h}{dt} = -\frac{m l_0^2}{\hbar} \nabla_h V(\mathbf{r}_e - \mathbf{r}_h) \times \hat{z}, \quad (7.2)$$

where \mathbf{r}_e and \mathbf{r}_h are the coordinates of the qp and the qh. These equations lead to a drift velocity $\mathbf{v}_d = \frac{d}{dt} \mathbf{R}$ of the center of mass of the pair:

$$\mathbf{v}_d = \frac{m l_0^2}{\hbar} [\nabla_{\mathbf{r}} V(\mathbf{r}) \times \hat{z}], \quad (7.3)$$

where $\mathbf{r} = \mathbf{r}_e - \mathbf{r}_h$ is the relative distance between the qp and qh and $\mathbf{R} = \frac{(\mathbf{r}_e + \mathbf{r}_h)}{2}$ is the center of mass coordinate. Since the qp and qh carry opposite charges, they both drift in a direction perpendicular to their separation vector \mathbf{r} direction.

$$\mathbf{r} \cdot \mathbf{v}_d = \frac{ml_0^2}{\hbar} \mathbf{r} \cdot [\nabla_{\mathbf{r}} V(\mathbf{r}) \times \hat{z}] = \frac{ml_0^2}{\hbar} [\mathbf{r} \times \nabla_{\mathbf{r}} V(\mathbf{r})] \cdot \hat{z} = 0, \quad (7.4)$$

since $\mathbf{r} \times \nabla_{\mathbf{r}} V(\mathbf{r})$ is zero. Hence $\mathbf{r} \cdot \mathbf{v}_d = 0$. Laughlin's quasiexciton wave function (see Eq. (8) of Ref. [13]) can be rewritten in terms of the center of mass and the relative coordinates as

$$|z_0\rangle = \frac{1}{\sqrt{2mL}} \iint e^{i\mathbf{R} \cdot \left(\mathbf{k} + \frac{\mathbf{r} \times \hat{z}}{2ml_0^2}\right)} e^{-\frac{|\mathbf{r} - ml_0^2 \hat{z} \times \mathbf{k}|^2}{4ml_0^2}} S_{z_e}^\dagger S_{z_h} |m\rangle d^2 z_e d^2 z_h. \quad (7.5)$$

The amplitude of this wave function is maximum when $\mathbf{r} = ml_0^2 \mathbf{k} \times \hat{z}$. So Laughlin's quasiexciton wave function strongly suggests the oriented nature of our dipole. This dipole dynamics is very similar to the dynamics of a vortex antivortex in fluid dynamics. The distance between the constituent particles of a magnetoroton (*oriented dipole*) is $\mathbf{r} = ml_0^2 (\hat{z} \times \mathbf{k})$. The dipole moment of this magnetoroton is $\mathbf{d} = \frac{e}{m} ml_0^2 (\hat{z} \times \mathbf{k})$ or $\mathbf{d} = el_0^2 (\hat{z} \times \mathbf{k})$. The dipole moment vector (\mathbf{d}), the momentum of the magnetoroton (\mathbf{p}) and the external magnetic field (\hat{z}) form a triad ($\hat{z} = \frac{\mathbf{d} \times \mathbf{p}}{|\mathbf{d}| |\mathbf{p}|}$). The dipole moment is the same for $\nu = \frac{1}{3}$ and $\nu = \frac{1}{2}$ for a given \mathbf{k} .

7.3 Hamiltonian of two magnetorotons

7.3.1 Kinetic energy operator

At filling fraction $\nu = \frac{1}{m}$, there is a parabolic dispersion around the minimum energy at finite $k = k_0$. The energy spectrum can be written around the minimum energy at $k = k_0$ as

$$E(k) = E_{\text{rot}} + \frac{\hbar^2}{2m_r} (|k| - k_0)^2, \quad (7.6)$$

where E_{rot} is the minimum magnetoroton energy at $k = k_0$ and m_r is the magnetoroton mass. The minimum magnetoroton energy E_{rot} and the corresponding k_0 are different for different filling fractions. So the kinetic energy of a magnetoroton is different for different filling fractions through m_r and k_0 . For $\nu = \frac{1}{3}$, $E_{\text{rot}} = 0.075 \frac{e^2}{\epsilon l_0}$ is the minimum magnetoroton energy at $k_0 l_0 \sim 1.4$. $m_r \sim \frac{2e\hbar^2}{e^2 l_0}$ is the magnetoroton mass. The mass of a magnetoroton is calculated from the curvature of the excitation spectrum at $\nu = \frac{1}{3}$ given in Ref. [3] by using the relation $m_r = \frac{\hbar^2}{\frac{\partial^2 E(k)}{\partial k^2}}$ at $k = k_0$.

The kinetic energy for two magnetorotons with momenta \mathbf{k}_1 and \mathbf{k}_2 is

$$T = \frac{\hbar^2}{2m_r} \left[(|\mathbf{k}_1| - k_0)^2 + (|\mathbf{k}_2| - k_0)^2 \right]. \quad (7.7)$$

7.3.2 Two-body potential energy operator

Since each magnetoroton is an *oriented dipole*, it is a natural choice to consider the interaction between two magnetorotons as a dipole-dipole interaction. This momentum dependent dipole-dipole interaction was first suggested by G. Baskaran [16] for $\nu = \frac{1}{2}$ composite Fermi liquid. The classical dipole-dipole interaction energy with two dipoles \mathbf{d}_1 and \mathbf{d}_2 is

$$U = \frac{\mathbf{d}_1 \cdot \mathbf{d}_2}{\epsilon r^3} - 3 \frac{(\mathbf{d}_1 \cdot \mathbf{r})(\mathbf{d}_2 \cdot \mathbf{r})}{\epsilon r^5}, \quad (7.8)$$

where \mathbf{r}_1 and \mathbf{r}_2 are the position vectors of the two dipoles and $\mathbf{r} = \mathbf{r}_1 - \mathbf{r}_2$ is the relative distance between two dipoles. ϵ is the dielectric constant of the background material.

$\mathbf{d}_1 = el_0^2(\hat{z} \times \mathbf{k}_1)$ and $\mathbf{d}_2 = el_0^2(\hat{z} \times \mathbf{k}_2)$ are the dipole moments of the two magnetorotons with wave vector \mathbf{k}_1 and \mathbf{k}_2 , respectively. Using the dipole moments \mathbf{d}_1 and \mathbf{d}_2 for the two magnetorotons, this interaction energy can be rewritten in terms of the total momentum $\mathbf{K} = \mathbf{k}_1 + \mathbf{k}_2$ and relative momentum $\mathbf{k} = \mathbf{k}_1 - \mathbf{k}_2$ as

$$U = \frac{e^2 l_0^4}{4\epsilon} \left[\frac{(\mathbf{K}^2 - \mathbf{k}^2)}{r^3} - 3 \frac{(\hat{z} \times (\mathbf{K} + \mathbf{k}) \cdot \mathbf{r})(\hat{z} \times (\mathbf{K} - \mathbf{k}) \cdot \mathbf{r})}{r^5} \right]. \quad (7.9)$$

This is a semi classical expression for the potential energy of two interacting *oriented dipoles*. Since an *oriented dipole* is a quantum mechanical particle, we pass on to quantum dynamics by symmetrizing the above classical energy expression and replacing the total momentum \mathbf{K} and the relative momentum \mathbf{k} by an operator $-i\nabla_{\mathbf{R}}$ and $-i\nabla_{\mathbf{r}}$, respectively. After symmetrization, interaction energy reduces to

$$U = \frac{e^2 l_0^4}{4\epsilon} \left[\frac{\mathbf{K}^2}{r^3} - \left(\frac{1}{r^3} \right) \mathbf{k}^2 - \mathbf{k}^2 \left(\frac{1}{r^3} \right) - 3 \frac{(\hat{z} \times \mathbf{K}) \cdot \mathbf{r} (\hat{z} \times \mathbf{K}) \cdot \mathbf{r} - (\hat{z} \times \mathbf{k}) \cdot \mathbf{r} (\hat{z} \times \mathbf{k}) \cdot \mathbf{r}}{r^5} \right]. \quad (7.10)$$

In operator form, it becomes

$$U = \frac{e^2 l_0^4}{4\epsilon} \left[\frac{-\nabla_{\mathbf{R}}^2}{r^3} + \frac{1}{2} \left(\frac{1}{r^3} \nabla_{\mathbf{r}}^2 + \nabla_{\mathbf{r}}^2 \left(\frac{1}{r^3} \right) \right) - \frac{3}{r^5} \frac{\partial^2}{\partial \phi^2} + \frac{3}{r^3} \left(\sin^2(\theta + \phi) \frac{\partial^2}{\partial R^2} + \cos^2(\theta + \phi) \frac{1}{R^2} \frac{\partial^2}{\partial \theta^2} + \cos^2(\phi - \theta) \frac{1}{R} \frac{\partial}{\partial R} + \sin 2(\phi - \theta) \frac{1}{R^2} \frac{\partial}{\partial \theta} \right) \right], \quad (7.11)$$

where ϕ is the angle between \mathbf{r} and x axis and θ is the angle between \mathbf{R} and X axis. The term $\frac{1}{2} \left(\frac{1}{r^3} \nabla_{\mathbf{r}}^2 + \nabla_{\mathbf{r}}^2 \left(\frac{1}{r^3} \right) \right)$ in the above expression is due to symmetrization of $\frac{\nabla_{\mathbf{r}}^2}{r^3}$ term. Without symmetrization of this term $\frac{\nabla_{\mathbf{r}}^2}{r^3}$, the interaction does not give the correct binding energy. So quantum mechanics play a crucial role in the interaction between two magnetorotons. This is a *momentum dependent*, non-central potential between two *oriented dipoles* of nonzero total momentum. This *momentum dependent* interaction energy is same for all $\nu = \frac{p}{(2mp+1)}$ filling fractions, where m and p are integers.

Since we are interested in pair formation, we concentrate on only two magnetorotons with opposite momenta ($\mathbf{k}_1 = -\mathbf{k}_2$), as done in BCS theory. Hence the total momentum is zero. The interaction energy can be written as

$$U = \frac{e^2 l_0^4}{4\epsilon} \left[\frac{1}{2} \left(\frac{1}{r^3} \nabla_{\mathbf{r}}^2 + \nabla_{\mathbf{r}}^2 \left(\frac{1}{r^3} \right) \right) - \frac{3}{r^5} \frac{\partial^2}{\partial \phi^2} \right]. \quad (7.12)$$

7.3.3 Total Hamiltonian

The Hamiltonian for this two body problem with the total momentum $\mathbf{K} = 0$ becomes

$$H = \frac{\hbar^2}{4m_r} (|\mathbf{i}\nabla_{\mathbf{r}}| - 2k_0)^2 + \frac{e^2 l_0^4}{4\epsilon} \left[\frac{1}{2} \left(\frac{1}{r^3} \nabla_{\mathbf{r}}^2 + \nabla_{\mathbf{r}}^2 \left(\frac{1}{r^3} \right) \right) - \frac{3}{r^5} \frac{\partial^2}{\partial \phi^2} \right]. \quad (7.13)$$

7.4 Variational wave function for two-magnetoroton bound state

We propose a variational wave function

$$\psi(r) = N r^2 e^{-\alpha r} J_0(2k_0 r), \quad (7.14)$$

where N is the normalization constant which is determined by the condition $\int d^2r |\psi(r)|^2 = 1$, $J_0(2k_0 r)$ is the zeroth order Bessel function. α is the variational parameter which can be determined by minimizing the energy expectation value.

In superconductivity, a Cooper pair forms at the Fermi surface between two electrons with opposite momenta. Similarly, a magnetoroton pair forms at and near $k = k_0$. The annular region in k space that contributes to the $\mathbf{K} = 0$ magnetoroton bound state is shown in Fig.7.2. Like Cooper pair wave function, we construct a wave function for the two-magnetoroton bound state with momenta $(\mathbf{k}_0, -\mathbf{k}_0)$ which gives $J_0(2k_0 r)$ for s state. $2k_0$ is the relative momentum of these

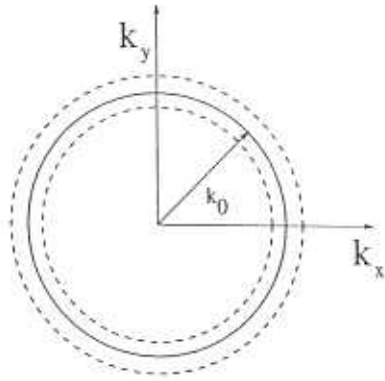


Figure 7.2: Annular region in k -space that contributes to $K = 0$ magnetoroton bound state.

two magnetorotons. Using the convolution theorem, we get the following variational wave function in momentum space:

$$\psi(k) = N' \frac{6}{\alpha^4} \int_0^{2\pi} d\theta F \left[2, 2.5; 1; -\frac{(k^2 + 4k_0^2 - 4kk_0 \cos \theta)}{\alpha^2} \right], \quad (7.15)$$

where N' is the normalization constant and $F[2, 2.5; 1; x]$ is the hypergeometric function. This wave function is shown in Fig. 7.3.

7.5 Binding energy of a two-magnetoroton bound state

To calculate the expectation value of the kinetic energy of this Hamiltonian, we go to the momentum space. In momentum space the kinetic energy operator is $T = \frac{\hbar^2}{4m}(k - 2k_0)^2$. The expectation value of the kinetic energy in momentum space is $E_1(\tilde{\alpha}) = 0.125E_c \int d^2\tilde{k} |\psi(\tilde{k})|^2 (\tilde{k} - 2.8)^2$, where $E_c = \frac{e^2}{\epsilon l_0}$ is the unit of Coulomb energy and $\tilde{\alpha} = \alpha l_0$ and $\tilde{k} = kl_0$ are the dimensionless variables.

The expectation value of the interaction potential energy is $E_2(\tilde{\alpha}) = \frac{0.125B}{A}E_c$, where A and B are the following integrals:

$$A = \int_0^\infty d\tilde{r} \tilde{r}^5 (J_0(2.8\tilde{r}))^2 e^{-2\tilde{\alpha}\tilde{r}}, \quad (7.16)$$

$$B = \int_0^\infty d\tilde{r} [4 - 2\tilde{r}^2\tilde{\alpha}^2 + 2\tilde{\alpha}\tilde{r} - 15.68\tilde{r}^2] J_0^2(2.8\tilde{r}) e^{-2\tilde{\alpha}\tilde{r}}. \quad (7.17)$$

We are numerically minimizing the energy functional $E(\tilde{\alpha}) = E_1(\tilde{\alpha}) + E_2(\tilde{\alpha})$ with respect to the variational parameter $\tilde{\alpha}$. The minimum energy for the

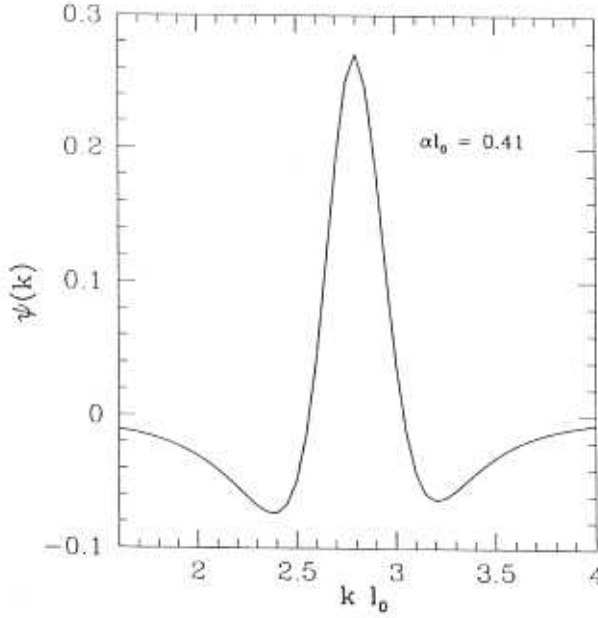


Figure 7.3: Two-magnetoroton bound state wave function in momentum space for $\alpha l_0 = 0.41$ at which the energy is minimized.

two-magnetoroton bound state is $0.138 E_c$ at $\tilde{\alpha} = 0.41$, whereas $2E_{\text{rot}} = 0.15E_c$ so that the binding energy is $0.012E_c$. Park and Jain have found a minimum energy of $0.135 E_c$, and hence the binding energy is $0.015 E_c$. Our binding energy is thus in good agreement with the extensive numerical results of Park and Jain [11]. So two magnetorotons with opposite momenta form a bound state.

The root mean square distance between these two magnetorotons or the effective size of the two-magnetoroton bound state is $\sqrt{\langle r^2 \rangle} \sim 6.7l_0$ where as the size of a single magnetoroton is approximately $4.2 l_0$. The structure of a two-magnetoroton bound state is shown in fig. 7.1b, which has a net quadrupole moment but total dipole moment is zero.

When the total momentum \mathbf{K} of a two-magnetoroton bound state is increased, the energy also increases. At $K \geq K_c$, the two-magnetoroton bound state breaks into two magnetorotons. To get a qualitative idea of how the excitation spectrum of a bound state goes with the total momentum, we use semiclassical approximation. We consider $\mathbf{k}_1 = \mathbf{k}_0 + \mathbf{q}$ and $\mathbf{k}_2 = -\mathbf{k}_0$, where $|\mathbf{q}| < |\mathbf{k}_0|$. One can easily get the semiclassical energy $E(K) = E_c [0.3125(Kl_0)^2 - 0.01(1 + 0.77(Kl_0)^2)]$. The critical momentum K_c can be determined from the condition, $E(K=0) + E(K) = 2E_{\text{rot}}$. Using this condition, we get $K_cl_0 = 0.22$. The two-magnetoroton bound state is not the lowest energy excitation when $K \geq K_c$. Expected excitation spectrum

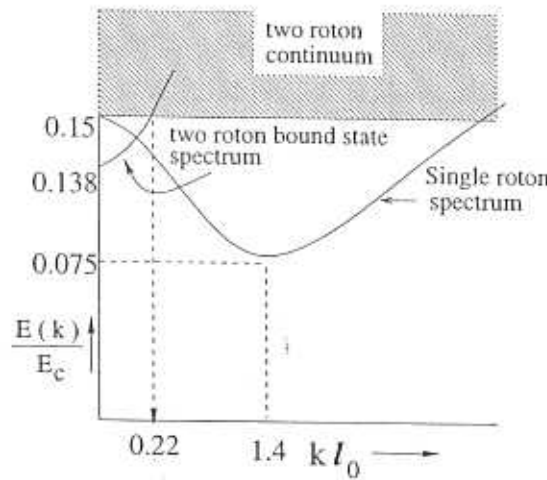


Figure 7.4: Expected qualitative excitation spectrum of two-magnetoroton bound state compared with excitation spectrum of a single magnetoroton.

of a two-magnetoroton bound state and the two magnetoroton continuum state is shown in Fig. 7.4. and compared with a single magnetoroton excitation spectrum which is given in Ref. [3]. The effective mass of a two-magnetoroton bound state is $M = 0.054m_e$ which is 75 percent less than the sum of the two magnetorotons masses.

7.6 Summary and conclusions

In conclusion, we have identified the magnetoroton as an *oriented dipole*. We derived the *momentum dependent*, non-central interaction energy form between two magnetorotons from a classical dipole-dipole interaction energy. Finally we proposed a wave function for two-magnetoroton bound state and showed analytically that at $\nu = \frac{1}{3}$ lowest energy excitation state is a two-magnetoroton bound state (with zero total momentum) instead of a single magnetoroton.

This analytical approach has the great advantage of being useful to analyze a more complex Hall system. For example, fractional quantum Hall effect is observed at $\nu = \frac{5}{2}$ state [17] whereas $\nu = \frac{1}{2}$ state [18] corresponds to metallic state. It has been shown numerically by Scarola *et al.* [19] that two composite fermion forms a *p*-wave bound state at $\nu = \frac{5}{2}$ but not at $\nu = \frac{1}{2}$. One can investigate this aspect in terms of the Read's dipole picture and using our above mentioned analytical

approach. The Read's dipole picture is equivalent to the Jain's composite fermion picture. By modifying this two-body potential and the variational wave function for higher Landau level, one can check whether two dipoles at $\nu = \frac{5}{2}$ can form a p -wave bound state.

Bibliography

- [1] D. C. Tsui, H. L. Stormer and Gossard, Phys. Rev. Lett. **48**, 1559 (1982).
- [2] R. B. Laughlin, Phys. Rev. Lett. **50**, 1395, (1983).
- [3] S. M. Girvin, A. H. Macdonald, and P. M. Platzman, Phys. Rev. Lett. **54**, 581 (1985); Phys. Rev. B **33**, 2481 (1986).
- [4] R. P. Feynman, *Statistical Mechanics* (Benjamin, reading, Mass, 1972);
R. P. Feynman, Phys. Rev. **91**, 1291, 1301 (1953); **94**, 262, (1954);
R. P. Feynman and M. Cohen, Phys. Rev. **102**, 1189 (1956).
- [5] J. K. Jain, Phys. Rev. Lett. **63**, 199 (1989); Phys. Rev. B **41**, 7653 (1990).
- [6] M. Kang, A. Pinczuk, B. S. Dennis, M. A. Eriksson, L. N. Pfeiffer, and K. W. West, Phys. Rev. Lett. **84**, 546 (2000).
- [7] H. D. M. Davies, J. C. Harris, J. F. Ryan, and A. J. Turberfield, Phys. Rev. Lett. **78**, 4095 (1997).
- [8] F. D. M. Haldane and E. H. Rezayi, Phys. Rev. Lett. **54**, 237 (1985).
- [9] D. H. Lee and S. C. Zang, Phys. Rev. Lett. **66**, 1220 (1991).
- [10] A. Zawadowski, J. Ruvalds, and J. Solana, Phys. Rev. A **5**, 399 (1972);
V. Celli, and J. Ruvalds, Phys. Rev. Lett. **28**, 539 (1972).
- [11] K. Park and J. K. Jain, Phys. Rev. Lett. **84**, 5576 (2000).
- [12] Yu. A. Bychkov, S. V. Iordanskii and G. M. Eliashberg, Sov. Phys. JETP Lett. **33**, 143 (1981).
- [13] R. B. Laughlin, Physica B **126**, 254 (1984).
- [14] C. Kallin and B. I. Halperin, Phys. Rev. B **30**, 5655 (1984).

- [15] N. Read, Semi. Sci. Tech. **9**, 1859 (1994); Surf. Sci. **361/362**, 7 (1996).
- [16] G. Baskaran, Physica B **212**, 320 (1995).
- [17] W. Pan *et al.* Phys. Rev. Lett. **83**, 3530 (1999).
- [18] R. L. Willet *et al.* Phys. Rev. Lett. **71**, 3846 (1993).
- [19] V. W. Scarola, K. Park and J. K. Jain, Nature **406**, 863 (2000).

Chapter 8

Conclusions

In this last chapter, we summarize our results which we have presented in this Thesis and indicate possible future work arising out of the approach presented here.

8.1 Summary of this Thesis

The study of collective excitations is of primary importance in quantum many body theories. It plays a crucial role in understanding the quantum nature of particles, two-body interactions and the effect of dimensionality. This Thesis was mainly devoted to theoretical study of various aspects of low-energy collective excitations in a trapped interacting alkali-metal atomic gases (Bose and Fermi) and of fractional quantum Hall systems. In the first chapter we have presented some of the basic properties of the Bose-Einstein condensation and the quantum Hall effect.

In the second chapter we have analyzed few low-lying excitation frequencies and damping rates of a two dimensional (2D) deformed trapped Bose gas above the critical temperature T_c . Using the conservation laws for number of particles, momentum and energy, we derived an equation of motion for the velocity fluctuations of a two-dimensional deformed trapped Bose gas just above T_c in the hydrodynamical regime. We recovered the sound velocity in an uniform system from the equation of motion of the velocity fluctuation. From this equation, we have calculated the eigenfrequencies and the corresponding density fluctuations for a few low-lying excitation modes. Using the method of averages, we also derived a dispersion relation in a deformed trap at very high temperature that interpolates between the collisionless and hydrodynamic regimes. We have made use of this dispersion relation to calculate the frequencies and the damping rates for monopole and quadrupole modes in

both the regimes. We found that there is no damping rate of the monopole mode of a 2D isotropic trapped Bose gas above T_c . We have first shown that the time evolution of the wave packet width of a Bose gas in a time-independent as well as time-dependent trap can be obtained from the method of averages. The time evolution of the wave packet width can be described by the non-linear singular Hill's equation.

In the third chapter we discussed the effect of two-body interaction on the low energy excitation frequencies of a 2D trapped Bose systems as well as Fermi systems at zero temperature, which is more meaningful in the context of current experimental scenario [1]. Using the time-dependent variational approach and the *most general Gaussian variational ansatz* for the order parameter of the condensed state, we calculated analytical spectra of the monopole and two quadrupole excitation frequencies of a two-dimensional anisotropic trapped Bose gas at zero temperature. Within the energy weighted sum-rule approach, we also derived a general dispersion relation of monopole and two quadrupole excitations of a two-dimensional deformed trapped interacting (contact interaction) quantum gas. This dispersion relation is valid for both statistics. Using this general dispersion relation, we also calculated analytical spectrums for the monopole and two quadrupole mode frequencies of a two-dimensional unpolarized Fermi gas in an anisotropic trap. The splitting between two quadrupole modes may be used to find the trap anisotropy. This splitting decreases with increasing interaction strength for both statistics. For a two-dimensional anisotropic Fermi gas, the two quadrupole frequencies are independent of the particle number within the Thomas-Fermi approach. Moreover, the monopole mode frequency for both statistics (in an isotropic trap) does not depend on the two-body interaction strength and it is a single particle excitation frequency. Recent experimental progress at MIT [1] on quasi-two-dimensional Bose condensed state shows the possibilities of verification of our results.

In the fourth chapter we considered a trapped interacting Bose gas in any dimensions d ($d \leq 3$) which can be described by the Gross-Pitaevskii equation. We obtained a general condition (see Eq. (4.10)) for the universality of the monopole mode frequency and dynamics of width of a class of Gross-Pitaevskii equation described the trapped interacting Bose gas, at varying spatial dimensionality, order of the nonlinearity and the scaling exponent of the interaction potential. We have also shown that the dynamics of the width of these class of Gross-Pitaevskii equation can be described *universally* by the same nonlinear singular Hill's equation. This monopole mode frequency and the dynamics of width are universal because it does not depend on the strength and nature (short-range, long-range, local, non-local) of

the interaction potential and the number of particles. We gave few examples which satisfy this particular condition and exhibit the universal nature of the monopole mode frequency and the dynamics of the width of the system. For example, we discussed the quasi-2D trapped interacting Bose gas, one-dimensional Tonk-Girardeau gas and the various other systems which satisfy that particular condition and exhibit the universal nature of the monopole mode frequency and the dynamics of the width of a system. Due to the current experimental progress in low dimensional Bose-Einstein condensate (BEC) state [1] it is quite possible to check the universal properties of the monopole mode frequency and the dynamics of the width of a trapped interacting Bose gas.

So far we have discussed about the low-energy excitations of a Bose condensed state with short-range interaction. In the fifth chapter we considered a Bose condensed state with gravity-like interatomic attractive interaction. There is a competition between the gravity-like potential either with the kinetic energy or the two-body short-range potential characterized by the s wave scattering length a , which gives gravity (G) and Thomas-Fermi-Gravity (TF-G) regimes, respectively. Using the time-dependent variational approach, we derived an analytical spectrum for monopole and quadrupole mode frequencies of a gravity-like self-bound Bose-Einstein condensate. We also analyzed the excitation frequencies of the TF-G and G regimes. Next, we have also considered a vortex at the center of the condensate state. We have estimated the superfluid coherence length and the critical angular frequencies to create a vortex around the z axis. We found that the TF-G regime should exhibit the superfluid properties more prominently than the G regime. We have also suggested that a vortex with $q \geq 2$ can not be created in the G regime, where q is the vortex quantum number. Interestingly, the monopole mode frequency of the condensate in presence of a vortex is less than the monopole mode frequency of the condensate without a vortex. This may be due to the long-range interaction. The change in the monopole mode excitation frequency due to the presence of a vortex can be used to detect the presence of a vortex in the condensate since the collective excitation frequency measurements can be carried out with high precision.

In the sixth chapter we considered the vortex lattice structure (highly excited collective state) produced in a rapidly-rotating quasi-2D atomic BEC. We treated the vortex as a particle degrees of freedom. Motivated by the analogy between the Magnus force acting on a vortex moving on a two-dimensional neutral Bose superfluid and the Lorentz force acting on a charge particle in a magnetic field, we considered a model Hamiltonian of a rotating BEC containing vortices

in terms of the center of the vortices (collective coordinate). We have suggested the cooperative ring exchange as a mechanism of quantum melting of the vortex lattices. We have estimated the condition for quantum melting of vortex lattices produced in a rapidly-rotating quasi-2D atomic BEC. A semiclassical path integral is used to estimate the condition for quantum melting instability by considering large-correlated ring exchanges in a two-dimensional Wigner crystal of vortices in a strong 'pseudomagnetic field' generated by the background superfluid Bose particles. We found that the quantum melting will occur at $\nu_v \sim \frac{1}{2}$. When $\nu_v > \frac{1}{2}$, the vortices form the liquid state whereas for $\nu_v < \frac{1}{2}$, the vortices form the Wigner crystal. The current experiments at ENS [2] with $\nu_v \sim 10^{-4}$ and at MIT [3] with $\nu_v \sim 10^{-3}$ are in the regimes of vortex lattice ground state. So our result is consistent with the experimental observations but does not match very well with the results based on the exact diagonalisation, and the harmonic analysis and Lindemann criteria.

In the seventh chapter we addressed the two-magnetoroton bound state formation in fractional quantum Hall systems at $\nu = \frac{1}{3}$ state. We modeled the two-magnetoroton bound state problem at one-third filling fraction of quantum Hall systems. We have shown that the inner structure of a magnetoroton is an oriented dipole analogous to the description of a magnetic exciton. We obtained the *momentum dependent*, non-central effective potential between two magnetorotons by using the oriented character of the dipole moment. We proposed a variational wave function for the two-magnetoroton bound state. We have calculated the total energy and found the minimum energy variationally (analytically) to find a two-magnetoroton bound state. Our result is in good agreement with extensive numerical results based on the composite fermion picture.

8.2 Outlook for future studies

Method of averages was used to calculate the low-energy excitation frequencies of a three dimensional Bose gas above the critical temperature T_c [4]. In the second chapter of this thesis we have used the method of averages to calculate the low energy excitation frequencies and dynamics of width of a 2D Bose gas above T_c . The two-body interaction among the atoms have not been considered in this method. Our future work would be to develop the method of averages by taking into account the effect of particle interactions. The contribution from the mean field interaction energy in Boltzmann transport equation is also known as the Vlasov contribution. Low-lying excitation frequencies and dynamics of the width of a two and three

dimensional trapped interacting Bose gas above the critical temperature can be obtained from the method of average by including the Vlasov contribution in the Boltzmann transport equation. We expect that the mean field interaction term does not affect on the monopole mode frequency of a two dimensional Bose gas above T_c and the dynamics of the width of a two dimensional Bose gas can be described by the same nonlinear singular Hill's equation.

The time-dependent variational method has been widely used in non-linear problems. This method with the Gaussian variational ansatz was first used by Victor M. Perez-Garcia *et al.* [5] in cylindrically trapped Bose condensed state to calculate analytically the low-energy excitation spectra. In the past few years, this method is being used extensively and successfully to explain many properties in trapped Bose condensed state. We have also used this method in this Thesis to calculate many properties of atomic Bose gas at zero temperature. For simplicity, we considered *most general Gaussian variational ansatz* (see Eq. (3.7)) for the order parameter of a 2D deformed trapped Bose condensed state to calculate monopole and quadrupole modes. The time-dependent variational method and the most general Gaussian ansatz for the order parameter can also be extended to three dimensional anisotropic Bose systems to study the various quadrupole modes and coupling between various scissors modes. It will be interesting to study the splitting between the quadrupole modes of an anisotropic quantum system in presence of terms having definite chirality, like magnetic field or rotation.

Low-energy excitation frequencies can also be obtained by using the sum-rule method. Using the sum-rule method, Sandro Stringari [6] derived the low-energy excitation frequencies of a 3D trapped BEC. Using the energy weighted sum-rule approach we also derived the general dispersion relation of the monopole and quadrupole modes of quasi-2D trapped interacting (contact interaction) quantum gas. The main advantage of the sum-rule method is that it can be applied to both trapped boson and fermion systems. This sum-rule method can be extended to a system with Coulomb interaction to study quadrupole excitations. For example, one can calculate the quadrupole excitation frequencies in an elliptic quantum dots. Moreover, we would like to study the frequency shift in the quadrupolar excitation frequencies ($m = \pm 1$ and $m = \pm 2$, m is the angular quantum number) due to presence of the vortex in BEC with gravity-like interaction, by using the sum-rule approach.

Cooperative ring exchange mechanism is suggested as a mechanism of quantum phase transition of a vortex Wigner lattices produced in a rapidly-rotating

quasi-2D atomic Bose condensed state. The cooperative ring exchange mechanism provides another microscopic approach to understand the quantum Hall-like state that may be formed in this atomic system. So our future work would be to investigate whether or not the vortex liquid state can exhibit the Hall-like state.

In the seventh chapter we obtained a two-body potential energy between two magnetorotons by using the oriented character of dipole moment of a magnetoroton. We also proposed a variational wave function for two-magnetoroton bound state. Our purely analytical approach has the great advantage of being useful in analysing more complex quantum Hall states. For example, fractional quantum Hall effect is observed at $\nu = \frac{5}{2}$ state [7] whereas $\nu = \frac{1}{2}$ state [8] corresponds to metallic state. It has been shown numerically by Scarola *et al.* [9] that two composite fermion forms a p -wave bound state at $\nu = \frac{5}{2}$ but not at $\nu = \frac{1}{2}$. This is the subject of considerable debate and controversy [10]. One can investigate this aspect by using the Read's dipole picture and our analytical approach given in the seventh chapter. The Read's dipole picture is equivalent to the Jain's composite fermion picture. We have the momentum dependent, non-central potential between two dipoles and their wave function in the lowest Landau level. By modifying this two-body potential and the variational wave function for higher Landau level, one can check whether or not the two dipoles at $\nu = \frac{5}{2}$ can form a p -wave bound state.

Bibliography

- [1] A. Gorlitz *et al.* Phys. Rev. Lett. **87**, 130402 (2001).
- [2] K. W. Madison, F. Chevy, W. Wohleben, and J. Dalibard, Phys. Rev. Lett. **84**, 806 (2000).
- [3] J. R. Abo-Shaeer, C. Raman, J. M. Vogels, and W. Ketterle, Science, **292**, 476 (2001).
- [4] David Guery-odolin, F. Zambelli, J. Dalibard, and S. Stringari, Phys. Rev. A **60**, 4851 (1999).
- [5] Victor M. Perez-garcia *et al.* Phys. Rev. Lett. **77**, 5320 (1996).
- [6] S. Stringari, Phys. Rev. Lett. **77**, 2360 (1996).
- [7] W. Pan *et al.* Phys. Rev. Lett. **83**, 3530 (1999).
- [8] R. L. Willett *et al.* Phys. Rev. Lett. **71**, 3846 (1993).
- [9] Vito W. Scarola, K. Park, and J. K. Jain, Nature **406**, 863 (2000).
- [10] N. Read, cond-mat/0010071